Enrichment of Anode Respiring Bacteria from Textile Effluent Contaminated Soil by Microbial Fuel Cell

By
Maham Khalid

(02052113015)

Department of Microbiology
Faculty of Biological Sciences
Quaid-I-Azam University
Islamabad, Pakistan
2023

Enrichment of Anode Respiring Bacteria from Textile Effluent Contaminated Soil by Microbial Fuel Cell

A thesis submitted in partial fulfillment of the requirements for the Degree of

Master of Philosophy

In

Microbiology

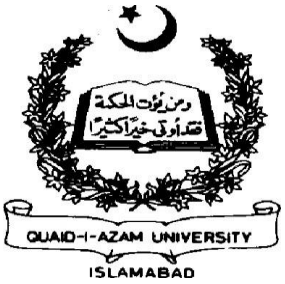

By

Maham Khalid

(02052113015)

Department of Microbiology
Faculty of Biological Sciences
Quaid-I-Azam University
Islamabad, Pakistan
2023


بسم الله الرحمن الرحيم

Dedication

For every demanding and difficult work, support, motivation, strength, and guidance is needed, along with prayers of loved ones close to our hearts.

My humble effort I dedicate to my affectionate

Father & Mother

and

Siblings

Whose constant efforts and encouragement have made me able to get such success

and acclaim.

And my constant source of guidance, strength, motivation

Prof. Dr. Naeem Ali

Declaration

The material and information contained in this thesis is my original work. I have not previously presented any part of this work elsewhere for any other degree.

Maham Khalid

ACKNOWLEDGMENTS

*All the praises and appreciations to the **Allah**, The Lord of Almighty, In the name of Allah, the Most Gracious and the Most Merciful. Alhamdulillah, all praises to be Allah for the strengths and His blessing in completing this thesis. The deepest respect and love for the **Holy Prophet, Hazrat Muhammad (P.B.U.H),** who enlightened our lives with Islam, saved us from the dark and helped us to recognize our only and true Creator.*

*It gives me immense pleasure to thank my mentor **Dr. Naeem Ali,** for his kindness and moral support during my work. His invaluable help, constructive comments and suggestions throughout the experimental and thesis work have contributed to the success of this research.*

*It gives me great pleasure in extending my sincere thanks and gratitude to **my lab mate, especially Shumaila Rafaqat** for her friendly attitude and facilitating my research here in the department.*

*I would like to express my appreciations and special thanks to my senior **Dr. Warda Imran, Saimoon,** and **Raqba** who were very supportive during my research work. I appreciate all my friends and fellows especially **Rafia and Faiqa** for their help and a lot of memories. Last but not the least special thanks to my parents, brothers, and sister for their prayers, love, and encouragement.*

MAHAM KHALID

Certificate

This thesis by **Maham Khalid** is accepted in its present form by the Department of Microbiology, Quaid-I-Azam University, Islamabad, for the requirement of the degree of Master of Philosophy in Microbiology.

Supervisor: Dr. Naeem Ali _____

Chairperson: Dr. Naeem Ali _____

Date: __/_____/2023

Table of Content

Dedication----------*i*

Declaration ----------*ii*

ACKNOWLEDGMENTS ----------*iii*

Certificate ---------- *iv*

Table of Content ---------- *v*

List of figures----------*viii*

List of Tables----------*x*

Abstract---------- *1*

1. Introduction ---------- *3*

1.2 Research Aims and Objectives ---------- *7*

1. Literature review ---------- *8*

2.1 Foreword----------**8**

2.2 Microbial Fuel Cells and their various layouts ---------- **10**

2.2.1 Two-component microbial fuel cell system ---------- 12

2.2.2 Single-component Microbial Fuel Cells---------- 12

2.2.3 Up-Flow mode MFC design ---------- 13

2.2.4 Stacked MFC setups ---------- 13

2.2.5 Paper MFC ---------- 14

2.3 Enrichment Strategies and Sources of EAB---------- **14**

2.3.1 Importance of Inoculum in Enrichment ---------- 16

2.3.2 Sources of Inoculum ---------- 18

2.3.3 Enrichment of electroactive microorganisms---------- 20

1.3.3.1 Altered anode potential Influence ---------- 21

1.3.3.2 Enrichment media---------- 23

2.4 Electricigens: Molecular Machinery of MFCs---------- **24**

2.5 Operational conditions affecting the microbial community in MFCs ---------- **27**

2.5.1 Temperature---------- 27

2.5.2 pH ---------- 28

2.6 Challenges ---------- **29**

- Enhancing Power Output ---------- 29
- Cost-effective Construction: ---------- 29
- Limited Understanding of Electron Transfer Mechanisms ---------- 30

2. Materials and Methods----------*31*

3.1. Collection of samples/inoculum ---------- **31**

3.2. Electrolyte preparation---------- **32**

3.3. MFC assembly and operation ---------- **32**

3.4. Electrochemical analysis ---------- **35**

3.4.1 Voltage measurement ---------- 36

3.4.2 Voltage analysis with different resisters ---- 36
3.4.3 Cyclic voltametric analysis ---- 37
3.5. Performance of MFCs ---- 37
3.5.1 TDS ---- 38
3.5.2 Electric conductivity (EC) ---- 38
3.5.3 Fourier-Transform Infrared) spectroscopy FTIR analysis ---- 38
3.6. Heterotrophic Plate Count and Bacterial Isolation from Anode ---- 39
3.7. Gram staining and light microscopy ---- 42
3.7.1 Gram Staining ---- 42
3.7.2 Light Microscopy ---- 43
3.8. Biochemical Testing ---- 44
3.8.1 Catalase Test ---- 44
3.8.2 Oxidase Test ---- 45
3.8.3 Urease Test ---- 45
3.8.4 Citrate Test ---- 45
3.8.5 TSI Test ---- 46
3.8.6 SIM Test ---- 47
3.9. DNA Isolation and Running Gel electrophoresis ---- 48
3.9.1 DNA extraction ---- 48
3.9.2 Gel Electrophoresis ---- 51
3.10. Molecular phylogeny of Anodic Biofilms ---- 52
4. Results ---- *54*
4.1 Electrochemical Performance In MFC ---- 54
4.1.1 Voltage ---- 55
4.1.2 Effect of External Resistance ---- 57
4.1.3 Cyclic voltammetry (CV) ---- 59
4.2 Performance of MFC ---- 65
4.2.1 TDS ---- 65
4.2.2 Electrical Conductivity ---- 67
4.2.3 FTIR analysis ---- 70
4.3 Culturable Electricigens anodic biofilms ---- 72
4.3.1 Plate count ---- 73
4.3.2 Purification ---- 74
4.3.3 Gram staining ---- 74
4.3.4 Biochemical testing ---- 75
Catalase Test: ---- 75
Oxidase Test: ---- 75
Urease Test ---- 75
Simmon Citrate Test: ---- 76
TSI (Triple Sugar Iron) Test: ---- 76
SIM (Sulfur Indole Motility) Test ---- 76
4.4. DNA extraction and Gel Electrophoresis ---- 80
4.4.1 DNA extraction ---- 80
4.4.2 Gel electrophoresis ---- 81
4.5 Molecular phylogeny of Anodic Biofilms (pyrosequencing) ---- 82
5. Discussion ---- *86*
6. Conclusion ---- *90*

7. References --- *91*

List of figures

Figure 1: Number of publications and citations on MFCs until 2020 10

Figure 2: Types of MFCs (Malik et al., 2023) 13

Figure 3: Mechanisms for bidirectional electron transfer between bacteria and electrodes. (A) Represents two mechanisms of direct electron transfer, one is mediated by nanowire, the other is mediated by outer membrane cytochromes with or without electron shuttles (Zheng et al., 2020) 26

Figure 4: Methodology Flowchart 31

Figure 5: Inoculum samples (A) Landfill soil (B) Activated sludgr (C) Textile contaminated soil 32

Figure 6: Microbial Fuel Cells (MFC) (A) Individual MFC with (T+L incoulum) and (B) Three MFCs 33

Figure 7: Schematic design of double chamber of double chamber MFC separated by Nafion ... 34

Figure 8: Recording voltage readings using a precision multimeter 36

Figure 9: Recording TDS (A) and EC (B) values using TDS & EC meter 38

Figure 10: General overview of what FTIR peak depicts 39

Figure 11: Bacterial colony isolation (A) from textile MFC (B) from T+S MFC (C) from T+L MFC 41

Figure 12: Purified bacterial isolates from the colonies obtained from Biofilm 42

Figure 13: Observation under 100x microscope after Gram staining 44

Figure 14: Urease test (A) depicting Negative results (B) depicting positive pinkish slant 45

Figure 15: Citrate test (A) indicating negative (B) positive results 46

Figure 16: TSI test showing (A) alkaline slant/acidic butt (B) Acidic slant and/acidic butt (C) Alkaline slant and butt 47

Figure 17: SIM test indicating indole, motility, and H2S production 48

Figure 18: Brief Overview of DNA extraction using extraction kit 50

Figure 19: Gel electrophoresis assembly (A) Gel tray with Gel inside (B) Gel tray attached to power supply for voltage 52

Figure 20: Voltage measurement for enrichment phase 1 55

Figure 21: Voltage measurement for enrichment phase 2 57

Figure 22: Polarization curve and power density of double chamber MFC at various resisters ... 59

Figure 23: Cyclic voltammograms representing the difference in redox electric current (I) at the scan rate of 20 mV/s in anodic chamber of MFC for enrichment phase-1 for T-cell 61

Figure 24Cyclic voltammograms representing the difference in redox electric current (I) at the scan rate of 20 mV/s in anodic chamber of MFC for enrichment phase-2 for T-cell 62

Figure 25: Cyclic voltammograms representing the difference in redox electric current (I) at the scan rate of 20 mV/s in anodic chamber of MFC for enrichment phase-1 for T+S-cell 63

Figure 26: Cyclic voltammograms representing the difference in redox electric current (I) at the scan rate of 20 mV/s in anodic chamber of MFC for enrichment phase-2 for T+S-cell. 64

Figure 27: Cyclic voltammograms representing the difference in redox electric current (I) at the scan rate of 20 mV/s in anodic chamber of MFC for enrichment phase-1 for T+L-cell.....65
Figure 28: Cyclic voltammograms representing the difference in redox electric current (I) at the scan rate of 20 mV/s in anodic chamber of MFC for enrichment phase-2 for T+L-cell.....65
Figure 29: TDS trends over period of time for enrichment phase 1.....66
Figure 30: TDS trends over period of time for enrichment phase 2.....67
Figure 31: Electrical conductivity trends over period of time for enrichment phase-1 68
Figure 32: Electrical conductivity trends over period of time for enrichment phase-2 69
Figure 33: FTIR peaks for T-cell control, phase-1 and phase-2 71
Figure 34: FTIR peaks for T+L-cell control, phase-1 and phase-2 71
Figure 35: FTIR peaks for T+S-cell control, phase-1 and phase-2 72
Figure 36: DNA fragment bands after successful DNA extraction and gel electrophoresis run 81
Figure 37: Taxonomic composition of RAW and Isolated bacteria strains using Pyrosequencing 83
Figure 38: Rank abundance plot 84
Figure 39: Venn diagram: Showing diverse distribution of species across samples 85

List of Tables

Table 1: Summary of basic components required in MFCs----------11

Table 2: Effect of substrate, MFC type and inoculum on enrichment of electricigens----------15

Table 3: Gram staining and colony characteristics----------75

Table 4: Identification of isolated bacterial strain through biochemical test. Here, MAC= MacConkey agar, EMB= Eosin methylene blue, TSI= Triple sugar iron, SIM= Sulfur indole motility, LF= Lactose fermenters, NLF= Non-lactose fermenters, Y/Y= yellow/yellow (slant & butt alkaline), R/R= Red/Red (slant & butt acidic), Y/R= Yellow/red (slant alkaline and butt acidic), M= Motility, I= Indole, (+) = Growth, (-) = No growth----------77

Abstract

In our increasingly polluted world, it is necessary to develop sustainable avenues for both energy generation and waste degradation has grown more urgent than ever. This thesis delves into the enrichment of Anode Respiring Bacteria (ARB) derived from soil contaminated with textile effluent (like dyes and other, employing the innovative platform of a Microbial Fuel Cell (MFC). By harnessing the inherent capability of microorganisms to respire on anode surfaces, this study seeks to address the dual challenge of energy scarcity and environmental contamination. The motivation behind this work lies in the pressing need to explore alternative energy sources that not only generate power but also actively participate in the breakdown of pollutants, thereby offering a synergistic approach to mitigating environmental impact.

A pivotal aspect of this investigation revolves around the employment of an H-shaped dual chamber MFC for two-stage enrichment, which exhibited remarkable voltage outputs. The dual chamber setup facilitated controlled microbial interactions, resulting in heightened electrochemical activity. This was validated through comprehensive voltammograms, which provided evidence of pronounced redox activity. To confirm the engagement of ARB in the electrochemical processes, enrichment cultures were subjected to cyclic voltammetry using a potentiostat. The subsequent analysis substantiated their involvement in facilitating electron transfer.

Furthermore, a multifaceted analytical approach was undertaken to unravel the complete impact of ARB enrichment. Through Total Dissolved Solids (TDS), Electrical Conductivity (EC), and Fourier Transform Infrared Spectroscopy (FTIR) analyses, evidence emerged of substantial carbon-based substrate consumption and biodegradation, leading to the formation of diverse byproducts. Complementary biochemical tests not only offered insights into the distinctive cellular characteristics and morphology of the enriched ARB but also hinted at potential species identification.

As we chart a course towards future outcomes, the findings of this study shed light on a promising avenue for sustainable energy generation intertwined with environmental remediation. The demonstrated potential of ARB enrichment within MFCs underscores the viability of coupling energy production with pollution control. Expanding this research could yield enhanced MFC configurations and broader applications, ranging from waste treatment to novel biotechnological solutions. By synergistically addressing

Abstract

energy and pollution challenges, this study underscores the potential of microbiological innovations to shape a more sustainable future.

1. Introduction

The rapid growth of industrialization and urbanization has resulted in the release of various pollutants into the environment, including textile effluents. Textile industry wastewater is characterized by high organic content, toxic compounds, and a range of recalcitrant contaminants, making it a significant environmental concern. Traditional treatment methods often fail to efficiently remediate these effluents, leading to the accumulation of pollutants in water bodies and soil. Therefore, there is an urgent need for innovative and sustainable technologies to address this environmental challenge (K. Obileke et al., 2021). Microbial fuel cells (MFCs) have emerged as promising systems for the treatment of wastewater, including textile effluents (Chaturvedi & Verma, 2016; Javed et al., 2018). MFCs employ the metabolic activities of electrochemically active microorganisms to convert organic matter into electricity through microbial respiration (Moqsud et al., 2013). Thes e devices offer several advantages over conventional treatment methods, such as the potential for simultaneous energy production and pollutant removal (Baicha et al., 2016). Harnessing the power of anode respiring bacteria (ARB) in MFCs presents a unique opportunity to enhance the treatment efficiency of textile effluent-contaminated soi (Chaturvedi & Verma, 2016; Katuri et al., 2020a) l.

Microbial Fuel Cells (MFCs) have been the subject of rigorous investigation in the realm of electricity generation for a span of approximately five decades (Naik & Jujjavarappu, 2020). In their fundamental configuration, MFCs bear semblance to conventional batteries and fuel cells, comprising a duo of distinct electrodes, namely, an anode and a cathode. These electrodes remain separated by electrolytic mediums. Nevertheless, their differentiating factor lies in their utilization of organic compounds as substrates for the primary incentive of electricity generation. Within the anodic compartment, microorganisms facilitate the oxidation of said organic compounds, thereby effecting the liberation of electrons and protons as consequential byproducts (Yaqoob, Ibrahim, et al., 2020). The emergent electrons resultant from this oxidation phenomenon navigates through an extraneous electric circuit, subsequently culminating at the cathode wherein they assist in generation of an electric current (Naik & Jujjavarappu, 2020). In the cathodic domain, the electrons are engaged in equal interaction with electron acceptors and protons, thereby causing the production of

compounds in a reduced state. The prevalent cathodic redox process, often encountered, involves the reduction of molecular oxygen. Current applications involving MFCs include, but are not limited to, electricity production, wastewater treatment, bioremediation, and hydrogen production(K. C. Obileke et al., 2021). Although practical applications will require mixed communities of microorganisms, understanding the building blocks of such complex systems helps to enhance the desired functions (Roy et al., 2023).

The microorganisms that facilitate the oxidation of organic compounds while transferring electrons to the anodes within MFCs are termed electricigens. This designation, "electricigen," was introduced to distinctly characterize the power generation mechanisms within MFCs (Katuri et al., 2020b). The way electricigens generate electricity stands apart from that of other microorganisms. Within the framework of an MFC setup, the electricigen utilized in the anodic chamber emerges as a fundamental determinant influencing the efficacy of electricity production. The process of electron transfer from the microbial cell to the extracellular environment encompasses a twofold progression: firstly, electrons migrate from the cytoplasmic membrane to the external cellular membrane; secondly, electrons are subsequently conveyed from the outer membrane to the extracellular electron receptor. Predominant electricigen examples like *Geobacter* display the ability to directly oxidize modest organic acid molecules via membrane-bound dehydrogenase, enabling the transfer of liberated electrons to the membrane-located electron receptor. Contrasting electricigens, such as *R. ferrireducen* and *Shewanella,* possess the capacity to oxidize organic compounds like sugars, generating reducing potential (NADH); following this, electrons shift from NADH to the metabolic respiratory chain's electron transport route, facilitated by NADH dehydrogenase (Miceli et al., 2012). Ultimately, these electrons are liberated externally from the cell through the respiratory chain. At present, pivotal components of the electron transport system on the cellular membrane encompass NADH dehydrogenase, quinones, flavin enzymes, and cytochrome C (Lahiri et al., 2022; Zheng et al., 2020). These constituents collectively play a significant role in directing the progression of electron transfer from the cell to the extracellular milieu.

Microbial fuel cell’s performance is directly linked with the enrichment of electricigens on anodic surface as biofilms. These electricigens are found in variety of habitats like waste and chemical contaminated soil, freshwater sediments, marine sediments, salt

marshes, anaerobic sludge from potato processing, wastewater treatment plants, and in mangrove swamp sediments, sewage sludge, composts, paddy and submerged soils, aquatic and marine sediments (Cao et al., 2019; Miceli et al., 2012; Yousaf et al., 2017). The presence of electrochemically active bacteria (EAB) on anode and their diversity are largely dependent on the enrichment methods, inoculum sources, inoculation techniques, MFC designs, electrode material, electron donor and acceptors on the enhanced outputs of MFCs. Substrates that are completely oxidized by the bacteria in MFCs are: 100% coulombic efficiency (CE) of *Geobacter sp*., to oxidize the acetate and 84% for benzoate oxidation, followed by *Geothrix fermentans* (94 % columbic efficiency for acetate oxidation) and 83% CE of glucose oxidation by *Rhodoferax ferrireducens* has been reported. It is studied that *Shewanella oneidensis* had a columbic efficiency of about 56.2% because it did not oxidize the lactate organic substrate completely in MFCs, leaving behind electrons unused as waste products like acetate (Miceli et al., 2012). These reported CEs can vary with environmental samples like wastewater maximum CE of 65–89 % after microbial enrichment

The biofilms establishment with identical inocula in MFCs depends on the type of electron donor being feed, so the community structure responds to and is highly dependent on the electron donor supply (Miceli et al., 2012). Relatively simple electron donors, such as acetate, have a more positive thermodynamic potential and provide the microbial community with a relatively small amount of free energy. More reduced compounds make more energy available to the community. In such cases, not all the members of the community are responsible for anode respiration, since fermentation and other respiratory processes allow different organisms to proliferate (Fan & Xue, 2016; Katuri et al., 2020a). Limiting the electron donor to acetate has previously resulted in enrichments containing 49% *Azospira* and 11% *Acidovorax;* almost entirely *Geobacter*; and 21% *Deltaproteobacteria*. With the objective to selectively enrich ARB, pressure was selectively increased the on microbial cultures by performing a biofilm transfer step and providing acetate as the electron donor. Biofilm transfers have proven effective previously and work by moving a portion of biofilm from a working MFC into a new MFC where natural selection should increase the population of ARB (Katuri et al., 2020b; Miceli et al., 2012; Torres et al., 2009a). Acetate was the only electron donor provided in abundance to control the available energy in the system (Khater et al., 2017a; Lee et al., 2003a).

Introduction

In the environment, ARB could be present in anaerobic sediments and soils where they have access to reduced compounds for use as electron donors and insoluble electron acceptors. Many locations around the world should easily fit these requirements while providing variations in other environmental parameters to which organisms will have adapted themselves (Cao et al., 2019). We, therefore, hypothesized that a greater variety of organisms capable of living as highly efficient ARB abound in the natural environment than previously discovered. To demonstrate their presence and find novel ARB, we used an ARB enrichment method. We obtained three samples, i.e., textile effluent contaminated soil, landfill-contaminated soil, and activated sludge obtained from an anaerobic reactor, placed them in MFCs with electrodes poised at −0.3 V vs Ag/AgCl as an electron acceptor and provided acetate as an electron donor (Miceli et al., 2012). The voltage output and decomposition of organic matter were traced. Further, to identify specific species of electricigens in anode-based biofilm, 16s rRNA sequencing was conducted, and FTIR analysis was done to assess the consumption of organic matter.

1.2 Research Aims and Objectives

The primary Aim of this study is to enrich and characterize anode-respiring electricigens from textile effluent-contaminated soil (with the capability to survive and degrade textile dyes), pure culture vs mixed communities using microbial fuel cell technology.

The specific research objectives are as follows:

- To construct and operate a double chamber mediator-less H-shaped MFC with Nafion membrane for growing biofilm of electrochemically active bacteria.
- To operationalize MFC under fed-batch conditions (under constant temperature 37°C in anaerobic incubator)
- To design and construct a microbial fuel cell system capable of efficiently harbouring microbial communities from textile effluent-contaminated soil, landfill soil, and sludge while producing electricity.
- To enrich anode-respiring bacteria from the contaminated soil and evaluate their electrochemical activity and performance in the microbial fuel cell system.
- To enrich the electricigens in two distinct stages i.e., phase-1 of enrichment help to grow anode respiring bacteria on electrode and phase-2 to help concentrate the presence of maximum electrochemically active bacteria.
- To compare the biofilm formation and metabolic activity of bacterial strains from pure inoculum and mixed communities in all three cells.
- To identify species of the microbial community in a biofilm through the application of biochemical tests for accurate characterization.
- To analyze the microbial community dynamics and diversity in the anodic biofilm of the microbial fuel cell and identify the essential microorganisms involved in pollutant degradation and electron transfer with the help of FTIR, SEM, and 16s rRNA sequencing.

1. Literature review

2.1 Foreword

The continuous rise in population, accompanied by industrial and economic growth, has led to a steady increase in environmental pollution. Environmental pollution and the depletion of non-renewable energy sources pose significant threats to the world in the present era. The global energy demand is steadily increasing, primarily relying on conventional energy generation technologies (Santoro et al., 2017). Approximately 85% of energy demand is met using fossil fuels such as petroleum, coal, and natural gas. However, exploiting these fossil fuels for energy and transportation has resulted in interconnected global warming and pollution issues (Bazina et al., 2023; Moqsud et al., 2013; Rajesh & Kumawat, 2023). As the depletion of natural resources becomes an increasingly unavoidable reality and environmental considerations gain more prominence, the need for producing fuels, energy, and chemicals through sustainable means, along with the effective recycling of essential nutrients and metals, is on the rise. This has led to a shift in the predominant industrial processes and business paradigms, moving away from a linear economy based on constant supply to a circular economy centered around resource recovery. In addressing these pressing issues, innovative technological remedies are being formulated to harness energy and materials from waste products and secondary sources (Javed et al., 2018).

In addition to the escalating energy demands, industrialization and urbanization have led to a rise in the need for clean resources and the associated challenges with treatment of waste contaminated lands and water bodies. Conventional waste treatment methods, such as those relying on activated sludge, necessitate substantial energy inputs and oxygen requirements(Bazina et al., 2023; K. Obileke et al., 2021; K. C. Obileke et al., 2021). As a result, there is a growing interest in alternative treatment technologies that require less energy while maintaining high sustainability and efficiency levels. One promising avenue of research is the application of Bioelectrochemical Systems (BES) employing microbial electrochemical technology (MET) (El-Khatib et al., 2015). This rapidly evolving approach employs microbial biocatalysts to convert organic or inorganic waste into valuable outputs, such as energy, nutrients, metals, or biochemicals. The adoption of such innovative approaches holds great promise in

addressing the pressing environmental and resource challenges we face today (Li et al., 2018).

Hence, there is a pressing need to opt for alternative approaches that enables simultaneous power and treatment of waste contaminated environments. One promising future energy source under consideration is biomass. However, the current utilization of biomass energy through combustion processes poses a persistent threat to ecological integrity and human well-being due to its contribution to air pollution. Consequently, a non-combustion-based method for harnessing the energy potential of biomass offers a viable solution to the energy crisis while mitigating local environmental pollution concerns. Extensive research has shown that bacterial communities have the capability to direct electrons derived from biomass, thereby generating power that humans can effectively utilize (Cao et al., 2019; K. Obileke et al., 2021).

Microbial-mediated techniques offer diverse opportunities for harnessing energy from biomass molecules, including but not limited to methanogenesis (associated with CH4 production), hydrogenesis (for hydrogen production), fermentation (enabling ethanol recovery), and the generation of electricity through Microbial Fuel Cells (MFCs). Consequently, to ensure sustainable power generation, it is imperative to integrate renewable energy resources with a wide range of carbon-neutral sources into the technological framework (Lee et al., 2003a; Samuel, n.d.).

In recent years, there has been a growing interest among researchers worldwide in utilizing enrichment technique with help of Microbial Fuel Cell (MFC) technology due to its inherent potential for simultaneous power generation and waste treatment. The increasing number of publications can substantiate this focus on MFC technology, as evidenced by a continuous upward trend till 2020 (see Figure 1) (Naseer et al., 2021). The present-day perception of MFC technology is highly favorable, owing to its unique capability to convert the chemical energy stored in both inorganic and organic waste into electrical energy. By linking electrogenic bacterial metabolism with electrochemical reactions, MFC technology offers a versatile platform for bioelectricity production, remediation of toxic compounds and heavy metals, wastewater treatment, and various other potential uses.

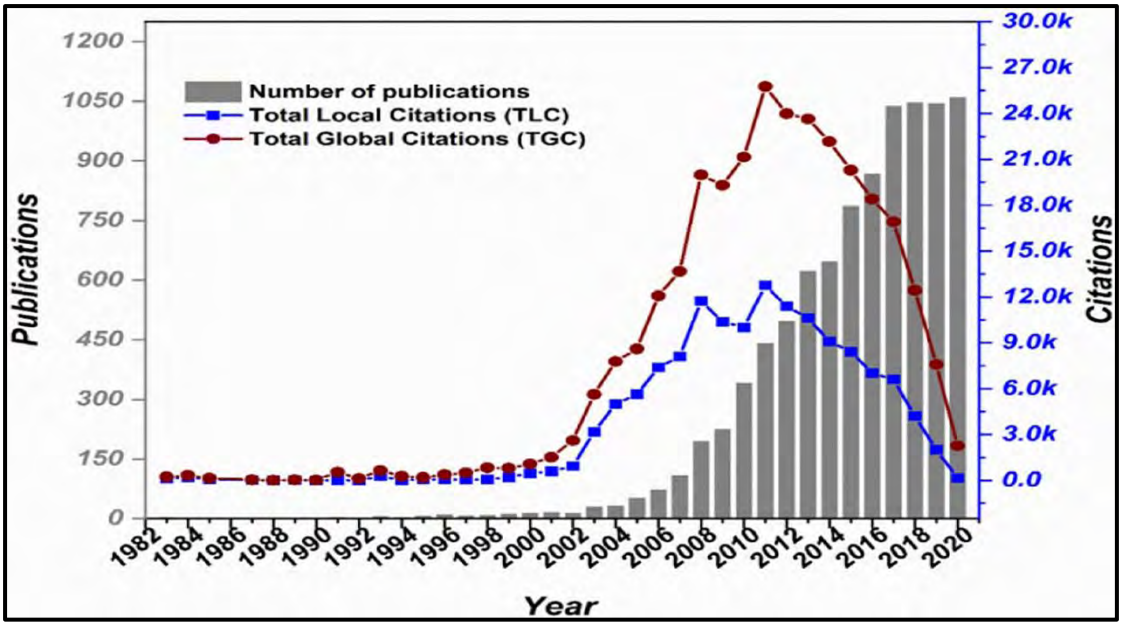

Figure 1: Number of publications and citations on MFCs until 2020

2.2 Microbial Fuel Cells and their various layouts

Microbial Fuel Cells (MFCs) can generate power by utilizing catalytically active bacteria to convert organic resources, including organic waste. The specific group of bacteria involved in this process is collectively referred to as electricigens, anode-respiring bacteria (ARB), or electrochemically active bacteria (EAB). These bacterial communities possess the remarkable ability to transfer electrons to the surfaces of anodes. As a result, MFC technology facilitates the conversion of stored chemical energy within organic matter into bioelectrical energy(Bhargavi et al., 2018; Flimban et al., 2019).

MFCs represent Bioelectrochemical systems that are typically composed of two distinct chambers: an anaerobic anode chamber comprising anode, anolyte, and electrochemically active bacterial communities, and a cathode chamber housing a cathode electrode and a catalyst, maintained either aerobically or under anaerobic conditions. A proton exchange membrane, such as the Nafion membrane separate the two chambers. Within this setup, the bacterial communities serve as biocatalysts that facilitate the oxidation of organic compounds present in the waste, resulting in the production of protons and electrons (Imran et al., 2019). These electrochemically active bacteria (EABs) essentially function as the powerhouses of MFC technology (Lahiri et al., 2022). The generated electrons traverse through the external circuit from the anode

surface to the cathode, while the protons migrate internally through the proton exchange membrane towards the cathode chamber. In the cathode chamber, the protons and electrons combine with oxygen, the electron acceptor, to form water (Uria et al., 2017; Zheng et al., 2020). While catalysts such as platinum and copper are traditionally employed for the reduction reaction at the cathode surface, bacteria can also serve as a cost-effective alternative to these expensive catalysts (Kumar et al., 2017; Oliveira et al., 2013; Vishwanathan, 2021). Table 1 provides an overview of the fundamental components of MFCs.

Table 1: Summary of basic components required in MFCs

MFC components	Material required	Remarks	References
Anodic chamber	Plexiglas, polycarbonate, Glass	Essential	(Toczyłowska-Mamińska et al., 2018; Zhou et al., 2019)
Cathodic chamber	Plexiglas, polycarbonate, Glass	Optional	(Zhou et al., 2019)
Anode material	Graphite felt, carbon-cloth, Graphite, RVC, carbon paper	Essential	(Singh et al., 2018; N. Yang et al., 2019)
Cathode material	Graphite felt, carbon paper, reticulated vitreous carbon (RVC), carbon cloth	Essential	(Y. Jiang et al., 2014; Singh et al., 2018)
Proton exchange filter	Proton exchange membrane: Ultrex, Nafion, porcelain septum, polyethylene, salt bridge or solely electrolyte	Essential	(Jana et al., 2018; Ramirez-Nava et al., 2021)
Catalysts used on cathode	Pt, polyaniline, MnO2, Pt black, Fe3+, microorganisms	Optional	(Santoro et al., 2018; Wu et al., 2018; Zafar et al., 2019)

MFCs can be designed in various configurations, some of which include:

1. Double chamber MFCs
2. Single chamber MFCs
3. Up-flow mode MFCs
4. Stacked MFCs

5. Paper MFC

2.2.1 Two-component microbial fuel cell system

Two-component MFC systems are commonly operated in batch mode using synthetic media, such as acetate or glucose, to facilitate electricity generation. Presently, these MFC configurations are predominantly utilized in laboratory settings. Typically, double chamber MFCs consist of an anodic chamber and a cathodic chamber that are internally connected by either a salt bridge or a proton exchange membrane (PEM) to enable proton exchange, while electron exchange from the anode to the cathode occurs externally via an external circuit (see Figure 2.) (Hidayat et al., 2022; Malik et al., 2023). Such MFC designs are commonly employed for wastewater treatment applications coupled with electricity generation, although the scalability of double chamber MFCs presents certain challenges. Furthermore, the regular aeration required for dual chamber MFCs restricts their practical implementation at an industrial level.

2.2.2 Single-component Microbial Fuel Cells

The complexity associated with the H-shaped design of MFCs has motivated the exploration of simpler and cost-effective single-component designs. Typically, these MFCs solely consist of an anode chamber without the requirement of a separate cathode chamber (see Figure 2). It was proposed a single-component fuel cell reactor featuring a rectangular anodic compartment along with a permeable air-cathode that is directly exposed to air. Proton exchange occurs directly from the anodic solution to the porous cathode in this design. Another variation of single-component MFC was developed by involving a plastic anodic cylindrical chamber with an embedded anode electrode, while the cathode is positioned externally (Sato et al., 2021).

In a study conducted by using a tubular MFC system was utilized, comprising an anode composed of graphite granules and an outer cathode. As there is no dedicated cathode chamber, the catholyte is introduced to the cathode by saturating the electrolyte above the graphite mat on the outer surface, thereby ensuring its continuous wetness and preventing drying (Malik et al., 2023).

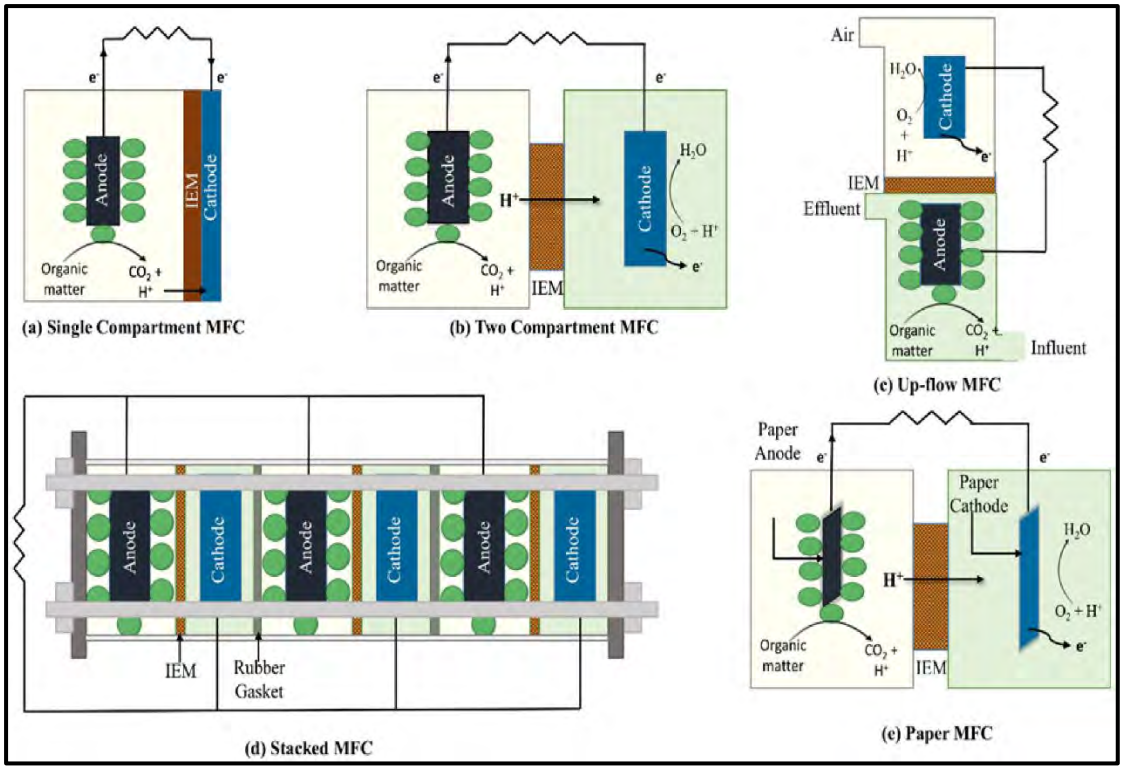

Figure 2: Types of MFCs (Malik et al., 2023)

2.2.3 Up-Flow mode MFC design

Jang et al. (2004) introduced an alternative MFC design that operates in continuous mode, employing a cylindrical structure constructed from plexiglass. The cylinder is divided into two chambers using glass bead and glass wool layers, thereby establishing separate anodic and cathodic compartments within the system (see Figure 2). To facilitate the electrochemical reactions, disk-shaped electrodes composed of graphite felt were positioned at the top and bottom of the reactors. This design was later adopted by Tartakovsky and Guiot (2006), who utilized a rectangular container without any physical separation between the anodic and cathodic compartments (Cabrera et al., 2022; Malik et al., 2023).

2.2.4 Stacked MFC setups

Aelterman et al. (2006) investigated the performance of combined MFC systems by linking multiple MFCs in parallel and series circuits. Such connections, whether in parallel or series, can yield improved current or voltage output. Stacked MFC systems were developed as an extension of Single Chamber MFCs (SCMFCs) with the aim of enhancing the power output of MFCs. These systems consist of multiple SCMFCs interconnected either in parallel or series. In the basic design, the stacked MFC

comprises an anode chamber separated from the cathode by a proton exchange membrane (PEM). Influent rich in organic compounds is introduced into the anode chamber, while a cathode mixture is evenly distributed throughout the cathode chamber (Malik et al., 2023; Nasrabadi & Moghimi, 2022).

One key advantage of the stacked MFC design is its ability to enhance current output and coulombic efficiency, particularly when the cells are connected in parallel. However, in series stacked MFCs, fuel starvation may occur, resulting in the loss of bacterial activity and polarity reversal within the stack. Consequently, the final voltage decreases. To mitigate this voltage loss, a continuous substrate supply to the stacked fuel cell is necessary. Since Single Chamber MFCs have inherent limitations on maximum power output, stacking multiple units together in series or parallel becomes crucial for achieving larger-scale power output and commercial viability (Nasrabadi & Moghimi, 2022).

2.2.5 Paper MFC

Paper-based MFCs offer numerous advantages, primarily encompassing cost efficiency, resistance to chemicals, and simple disposability. The MFC configuration comprises an anode and cathode hosting electrodes comprised of graphite particles. These graphite particles are applied onto the paper substrate using four distinct pencil applications. Proton exchange membranes (PEMs) crafted from parchment paper are employed, and crayons can be additionally employed to significantly enhance hydrophobic properties. In the anode chamber, microorganisms such as *Shewanella oneidensis* can be introduced along with suitable growth media (Y. J. Jiang et al., 2022) (Malik et al., 2023).

2.3 Enrichment Strategies and Sources of EAB

MFC technology primarily focuses on power production applications, prompting researchers to continually seek ways to enhance power density by improving MFC designs, modifying electrodes, and introducing various catalysts in both the anode and cathode compartments (G. T. Kim et al., 2006a). Previous studies have reported impressive outputs even from small reactors (14L), which serve as encouraging results driving scientists to further optimize MFC performance. However, the applicability of MFCs in real-world scenarios presents challenges such as high material costs (e.g., proton exchange membrane and electrodes), expensive catalysts (e.g., Pt) used for

oxygen reduction in the cathode, high internal resistance, and the enrichment of electrochemically active bacteria (EAB) from environmental samples (Lee et al., 2003b).

Nonetheless, researchers worldwide are dedicated to advancing the feasibility of MFC technology by focusing on enriching EAB populations in the anode compartment and promoting biofilm formation on the anode surface. The thickness of the biofilm can vary, ranging from a few tens of micrometers, such as approximately 50µm or 30µm. The development of biofilm by electrochemically active bacteria exhibits distinct characteristics compared to other bacterial species. It relies on the assembly of extracellular matrix and adhesin components to stimulate biofilm formation on the electrode surface. Notably, certain proteins play a crucial role in enhancing biofilm formation, including OMC c-Cyts, pili, OmcS, and OmcZ. Studies have demonstrated that the absence of OMC c-Cyts and pili inhibits biofilm development in *Geobacter sulfurreducens* (Inoue et al., 2011a; Sun et al., 2021). Achieving an optimal biofilm thickness is essential for efficient MFC performance, as excessively thick biofilms can increase resistance and restrict electron transport within the system.

Table 2: Effect of substrate, MFC type and inoculum on enrichment of electricigens

Fuel Cell type	Inoculum	Substrate	Predominant taxonomic groups	References
Two-chamber	River sediment	River water	β-Proteobacteria (46.2%	(Phung et al., 2004)
Two-chamber	Rice paddy soil	Cellulose	Firmicutes (39.5%) Proteobacteria (21%)	(De Schamphelaire et al., 2008)
sMFC planted	Rice root exudates	Potting soil	δ-Proteobacteria (75%)	(De Schamphelaire et al., 2008)
sMFC	Estuary sediment	Estuary sediment	δ-Proteobacteria (62.5%)	(Holmes et al., 2004)
Two-chamber	Activated sludge	Glucose, glutamate	Bacteroidetes (29.5%) β-Proteobacteria (29.5%) γ-Proteobacteria (19.2%)	(Ali et al., 2017; G. T. Kim et al., 2006b)
Two-chamber	Activated sludge	Ethanol	β-Proteobacteria (83%) δ-Proteobacteria (17%)	(J. R. Kim et al., 2007)

Two-chamber	Activated sludge	Acetate	δ-Proteobacteria (21%)	(Lee et al., 2003b)
Two-chamber	Activated sludge	Starch WW	β-Proteobacteria (25.0%) α-Proteobacteria (20.1%)	(Chen et al., 2018)
Single chamber	Anaerobic sludge	Glucose	Actinobacteria (34.4%) γ-Proteobacteria (37.5%)	(Chae et al., 2009a)
Single chamber	Anaerobic sludge	Wastewater	ε-Proteobacteria (57.8%)	(Bazina et al., 2023)
Two-chamber	Anaerobic sludge	Propionate	Firmicutes (59.3%) β-Proteobacteria (18.5)	(Li et al., 2018)

2.3.1 Importance of Inoculum in Enrichment

In addition to controlling biofilm thickness, the selection of an appropriate inoculum (mixed or pure cultures) and suitable substrate plays a crucial role in maximizing energy extraction for power production in MFCs. Studies have shown that *Geobacter sulfurreducens*, for instance, has the remarkable ability to fully utilize acetate, achieving nearly 100% electron recovery for bioenergy production(Yousaf et al., 2017). Once a well-established biofilm is formed, electrochemically active bacteria (EAB) facilitate the transport of metabolically generated electrons from their cell membrane surface to the anode (Torres et al., 2009a). These electrons are subsequently transferred from the anodic surface to the cathodic surface through an external circuit connection.

On the cathode surface, electrons engage in reactions with electron acceptors, including oxygen. When oxygen serves as the electron acceptor, the resulting end product is water, contributing to the generation of a maximum open-circuit voltage of approximately 0.805 V at the cathode. Typically, the cathode surface is coated with a catalyst, often platinum (Pt), to enhance the rate of oxygen reduction. Alternatively, in an effort to reduce the cost associated with MFCs, biocathode MFCs have also been introduced as an alternative approach. Furthermore, other electron acceptors such as potassium permanganate and ferricyanide have demonstrated potential as viable alternatives (Hassan et al., 2012).

Hence, the careful selection of appropriate electron acceptors, electron donors (substrates), and electricigens or electrochemically active bacteria (EAB) plays a pivotal role in Microbial Fuel Cells (MFCs) (Haddadi et al., 2014; Y. Liu et al., 2008).

Numerous studies have been conducted to evaluate the performance of mixed and pure cultures in terms of bioelectrical outputs within MFCs. Some investigations have reported higher current densities from MFCs operated with mixed cultures, while others have demonstrated that pure cultures can also achieve significant power outputs (Cao et al., 2019).

For instance, Nevin et al. conducted a study where *Geobacter sulfurreducens* produced higher current density in ministack continuous-flow MFCs, supplied with acetate and employing carbon cloth as the electrode material, compared to mixed cultures under similar operational and reactor conditions. The study achieved a maximum power density of 1900 m W/m^2, approximately 21% higher than sewage sludge-fed MFCs using mixed cultures (Nevin et al., 2008).

Inoculum selection during the exponential growth phase is crucial for achieving enhanced efficiency in fuel cells. Investigations have revealed that electricigens form thin biofilms during the lag phase, containing lower levels of c-type cytochromes. Conversely, EAB form thicker biofilms during the exponential growth phase, characterized by a higher concentration of cytochromes, resulting in increased bioelectricity generation. Moreover, the utilization of a selective mixed culture inoculum, comprising organisms such as *Azospira oryzae, Pseudomonas aeruginosa, Solimonas variicoloris,* and *Acetobacter peroxydans*, has been found to generate higher current density compared to unknown bacterial consortia. A comparative analysis study demonstrated that a selective mixed culture inoculum can produce 100% more electricity than a sludge inoculum in H-shaped MFCs (Jothinathan & Wilson, 2017). Additionally, various inoculum pretreatment methods are employed to enhance the efficacy of MFC technology, further improving performance (Anam et al., 2017).

In general, the enrichment of electrochemically active bacteria (EAB) within electroactive biofilms is typically achieved through the utilization of complex substrates to foster their development. Two main strategies are commonly employed for EAB enrichment: inoculum acclimation and optimization. In the case of inoculum acclimation, the primary objective is to enhance the growth of EAB initially present in the substrate. Among various enrichment acclimation methods, the most widely accepted approaches for promoting and optimizing the selection of electroactive bacterial species include: (1) the addition of essential substrates, nutrients, vitamins,

and other growth-promoting factors; (2) maintaining anaerobic environmental conditions; (3) selectively eliminating specific microbial groups through chemical means, such as the addition of fungicides, antibiotics, or employing physical methods such as temperature changes or ultrasound treatment; and (4) chemically modifying the substrate by adjusting factors such as pH, conductivity, and other relevant parameters (Fakhirruddin et al., 2018a; Jothinathan & Wilson, 2017). These acclimation methods serve to create favorable conditions for the proliferation of electrochemically active bacteria, thereby facilitating their enrichment within the biofilm.

The second strategy involves the successive transplantation of electroactive biofilms over multiple generations. In this technique, biofilms are cultivated for several generations on conductive porous or solid supports, such as metallic particles or electrodes. The biofilms used in this approach can either originate from mature bacterial populations obtained from environmental samples (e.g., soils, sediments, wastewater) or be previously colonized electrochemically active (EA) electrodes. This transplantation technique allows for a reduction in bacterial diversity within the EA biofilms by removing non-attached or non-electricigens from the electrode surfaces (Rabaey et al., 2004a).

The concept of transplanting EA biofilms was first explored by Rabaey et al. in 2004 (Rabaey et al., 2004a). They scraped the biofilm from the anode of one Microbial Fuel Cell (MFC) and inoculated it into a new MFC. As a result, the power density increased from 0.6 Wm^{-2} to 4.3 Wm^{-2}, accompanied by a significant improvement in coulombic efficiency from 4% to 81%. Another study conducted involved collecting biofilm from a floating metallic dock. Acetate was used as the fuel carbon source, graphite electrodes were employed, and the system was tested at -0.1V vs SCE using chronoamperometry. This study achieved a higher power density of approximately 2.5 Am^{-2}, whereas the use of inoculum from nearby sediments resulted in current densities of $\leq$ 1.0 Am^{-2} (Rabaey et al., 2004a). These findings confirm that transplanting EA biofilms from previous electrodes to a new anode surface can significantly improve the power output.

2.3.2 Sources of Inoculum

In the realm of Bioelectrochemical Systems (BES), both pure and mixed microbial cultures present valuable options for anode inoculation. When investigating the fundamental aspects of Microbial Electrochemical Technology (MET), such as

understanding electron transfer mechanisms or the metabolism of a specific electroactive microorganism, pure cultures prove to be particularly well-suited (Kumar et al., 2017). Additionally, the effective removal of certain specific compounds, for instance phenols, VOCs, and pharmaceuticals, may necessitate the selection of microorganisms possessing specialized metabolic capacities.

On the other hand, mixed cultures demonstrate greater suitability for a wide range of industrial and municipal applications. The advantage of employing mixed cultures lies in their ability to forego the requirement for sterilization, making them more practical for treating complex substrates (Mohd Yusoff et al., 2013a). Moreover, they exhibit higher resilience to changes in environmental conditions. In various scenarios, mixed cultures have been observed to generate higher and more stable current densities compared to their pure culture counterparts. Consequently, the selection of either pure or mixed microbial cultures is dependent on the specific objectives and environmental demands of the given BES application (Madjarov et al., 2016).

The phenomenon of microorganisms participating in extracellular electron transfer, wherein they contribute electrons to the anode electrode located outside their cell, is a widely observed natural process. Common sources of microorganisms introduced to the anode electrode are derived from human-made environments, including aerobic sludge, anaerobic sludge, and digestates. Similarly, microorganisms from natural settings like soil and sediments are used for this purpose (Mohd Yusoff et al., 2013b)(see Table 1). Furthermore, extensively developed electroactive microbial communities that have been previously employed in operated anodes are also commonly utilized. It's worth highlighting that wastewater holds potential as a reservoir of exoelectrogenic microorganisms. Notably, experiments involving the continuous operation of a Microbial Fuel Cell (MFC) with real wastewater at Hydraulic Retention Times (HRTs) ranging from 3 to 4 hours have shown that introducing an external inoculum alongside the existing microorganisms present in the wastewater does not significantly impact the production of electrical current.

The microbial composition of the inoculum, especially the abundance of electroactive microorganisms, significantly impacts the bioanode start-up period. Aerobic inocula may harbor a lower quantity of electroactive microorganisms but lack methanogenic communities that could compete with current production—a characteristic more

prevalent in most anaerobic inocula (Y. Liu et al., 2008). Within 5 days from start-up, aerobic inocula have demonstrated electron transfer initiation to MFC (Microbial Fuel Cell) anodes, whereas anaerobic microorganisms achieve this in just one day. On the other hand, enhanced starter cultures that combine biofilms and outflow from previously operated Bioelectrochemical Systems (BES) have the opposite effect, expediting the initial phases. This acceleration is due to the presence of electroactive microorganisms and potentially mediators (Haddadi et al., 2014). The time required for the starting phase was significantly slashed from 400 hours to 48 hours. Simultaneously, the power density doubled. This notable improvement was achieved by employing an enriched biofilm as the starter, deviating from the conventional use of household wastewater. To further augment the variety of electroactive microbial communities, a viable approach involves amalgamating starter cultures from diverse sources. These sources could include such as anodic effluent or biofilm with aerobic or anaerobic (Dessì et al., 2018).

Furthermore, it is important to highlight that existing biofilms can be utilized to restore BES (Bioelectrochemical System) performance in the event of a failure. Once a foundational electroactive biofilm has developed, the microorganisms within it demonstrate the ability to rapidly migrate and establish themselves on new surfaces during system initiation (Haavisto et al., 2019). Nevertheless, when not promptly utilized, these electroactive communities need to be properly preserved at a temperature of 4 °C. It's crucial to be mindful of prolonged storage periods, as exceeding one month could potentially have adverse effects on their biochemical and electroactive properties.

2.3.3 Enrichment of electroactive microorganisms

Within the realm of Microbial Fuel Cells (MFCs), the anode plays a pivotal role necessitating the involvement of electroactive microorganisms with the capability to facilitate electron transfer from the cell to the solid anode electrode. To achieve this, numerous research endeavors have been dedicated to formulating an effective strategy for the successful enrichment of electroactive microorganisms during both the start-up and operational phases of Microbial Electrochemical Technology (MET). These efforts and corresponding findings will be elucidated in the subsequent subsections.

1.3.3.1 Altered anode potential Influence

The configuration of the microbial consortium and, specifically, the pathways responsible for extracellular electron transfer can be impacted by the electrode potential. Microorganisms with electroactive properties obtain the necessary energy for their growth by transferring electrons to the anode electrode. This energy acquisition can be enhanced by employing an anode potential that surpasses the potential of the electron donor, as illustrated in Equation 1.

$$\Delta G\ 0' = -nF(E0'_{substrate} - E_{anode})$$

Where $\Delta G0'$ denotes the change in Gibbs free energy at pH 7, n is the number of electrons involved in the reaction, F is the Faraday constant (9.64853 × 104 C/mol), $Esubstrate0'$ (V) is the standard biological potential of the substrate, and $Eanode$ (V) is the anode potential.

However, it is important to note that the metabolic energy gain is not directly correlated to the applied anode potential, as microorganisms can only obtain the energy liberated through electron transfer outside the cell via the outer membrane proteins (Carmona-Martínez et al., 2013a). This is illustrated by Equation 2:

$$\Delta Gmic\ 0' = -nF(E0'_{substrate} - E_{TED})$$

Where $\Delta Gmic0'$ represents the energy gain by the microbial cell, and E_{TED} (V) is the standard biological potential of the terminal electron donor, which could be either the outer membrane protein for direct electron transfer or the mediator for mediated electron transfer. The interplay of these factors impacts the energy dynamics and electron transfer mechanisms within the microbial community associated with the anode potential in the context of Microbial Electrochemical Systems (Busalmen et al., 2008).

The upper threshold of the membrane proteins' potential in various bacterial strains typically hovers around 0 V vs. the standard hydrogen electrode (SHE). Consequently, elevating the anodic potential beyond 0 V vs. SHE may not yield additional energy gain for the microorganisms. Scholars have proposed that employing a negative anode potential favors the selection of electroactive microorganism's adept at respiratory activities at lower potentials. Remarkably, certain microorganisms, such as *Geobacter spp.* exhibit the capacity to optimize their energy efficiency by adapting their electron

transfer mechanisms in response to the anode potential, often involving the utilization of distinct outer membrane proteins (Wei et al., 2010). This ability to modulate their electron transfer strategies enables these microorganisms to adapt and thrive in varying electrochemical environments (Fakhirruddin et al., 2018b; Rabaey et al., 2004b).

In the majority of scenarios, both direct and mediated electron transfer display a Nernst-Monod potential. This indicates the anodic potential at which approximately half of the maximum current density is attained, typically around -0.2 V vs. SHE. However, there exist certain exceptions. One such exception is pyocyanin, a recognized mediator generated and utilized by *Pseudomonas sp*. for electron transfer. Pyocyanin possesses a redox potential of -0.03 V vs. SHE. As a result, it can be predicted that *Pseudomonas* sp. will flourish at elevated anodic potentials. In cases of mediated electron transfer, the necessary anode potential and the resultant current generation depend on the oxidation potential of the mediator. Microorganisms that are electroactive and employ mediators encounter challenges in achieving substantial current densities due to limitations in mediator diffusion. Consequently, it might be imperative to employ more positive anodic potentials to counterbalance the losses stemming from diffusion. This stands in contrast to microorganisms that employ direct electron transfer (Fakhirruddin et al., 2018b; Jeremiasse et al., 2012).

In spite of the favorable energy implications associated with utilizing higher positive anode potentials, there exists a lack of unanimous agreement concerning the superior choice between a positive or negative anodic potential. This choice aims to facilitate the expansion of an electroactive anodic biofilm and to optimize power density. Initially, a positive anode potential proves advantageous as it bolsters the formation of the biofilm, leading to increased thickness and subsequently greater resistance against disruptive shear forces. Nevertheless, as the process advances, opting for a lower anode potential becomes viable to enhance the prevalence of electroactive microorganisms. While this approach is advisable during the start-up phase, the prolonged application of potential may outweigh the benefits in power output, making it suitable only for shorter durations (Torres et al., 2009b). As such, the selection of anode potential requires careful consideration of the specific stage of biofilm development and the trade-offs between enhanced biofilm growth and sustained power output (Fakhirruddin et al., 2018b).

1.3.3.2 Enrichment media

In the realm of Bioelectrochemical Systems (BES), where mixed cultures play a pivotal role in the inoculation process, a significant challenge arises from the competition among a variety of microorganisms for the available substrate. To address this obstacle, proactive strategies can be employed. For instance, the preliminary enrichment of electroactive microorganisms on substrates that aren't fermentable can be undertaken. This approach fosters the preferential development of electroactive species within the biofilm of the anodic compartment. Notably, the makeup of the microbial community in the anodic region is markedly influenced by the nature of the electron donor that is supplied. While a multitude of substrates can sustain the proliferation of electroactive microorganisms, it's worth noting that growth mediums containing fermentable substrates like glucose or sucrose tend to yield a more diverse microbial community, encompassing both electroactive and non-electroactive microorganisms (Chae et al., 2009b; Jeremiasse et al., 2012; Michie et al., 2013).

On the other hand, when employing non-fermentable substances like acetate, and in the absence of methanogens, a more pronounced preference arises for electroactive microorganisms in comparison to more intricate substrates. It's important to note that fermentable or other intricate substrates might demand symbiotic interactions between electroactive and non-electroactive microorganisms to facilitate the exchange of energy and metabolic collaboration. In contrast, acetate can be directly converted into electric current by the electroactive microorganisms themselves. This exclusive reliance on acetate by electroactive microorganisms underscores its significance as the preferred substrate in (BES) for fostering the proliferation of electroactive species and enhancing electron transfer processes (Khater et al., 2017b).

Unlike synthetic anolytes, actual wastewater demonstrates reduced conductivity and possesses a multifaceted and variable composition. It may potentially include substances harmful to microorganisms. Moreover, the native microorganisms existing in the wastewater might impact the electrogenic population within the BES (Bioelectrochemical System). Elevated concentrations of Chemical Oxygen Demand (COD) could also result in decreased BES efficiency. To address these issues, an adjustment phase involving the gradual introduction of wastewater, coupled with incremental increases in the organic loading rate (OLR), can effectively avert inhibition of the microbial community (G. Liu et al., 2011).

In contrast to synthetic anolytes, real wastewater exhibits lower conductivity and possess a complex and fluctuating composition, potentially containing compounds that could be toxic to microorganisms. Additionally, the indigenous microorganisms present in the wastewater may influence the electrogenic community within the BES, and higher concentrations of Chemical Oxygen Demand (COD) may lead to diminished BES performance. To mitigate these challenges, an adaptation period involving gradual addition of wastewater while incrementally increasing the organic loading rate (OLR) can help prevent inhibition of the microbial community (G. Liu et al., 2011).

In order to advance the development of a tough electrogenic community and amplify sustained power generation, it is a prevalent strategy to introduce uncomplicated substrates and electron acceptors to the anode during the initiation of small-scale microbial electrochemical systems (BES) that receive actual waste streams as feedstock. This method has demonstrated its efficacy in fostering the creation of a robust electrogenic community, thereby guaranteeing the continued optimal operation of the BES in the long run (Chae et al., 2009b).

2.4 Electricigens: Molecular Machinery of MFCs

Understanding the unique characteristics of microbial fuel cells (MFCs) is of utmost importance, as this technology has garnered significant attention within the realm of renewable energy solutions. The intriguing nature of MFCs and their wide-ranging applications stems from the molecular machinery possessed by electrochemically active bacteria, which enables the transfer of electrons to the surface of the anode. This bacterial molecular machinery encompasses various proteins, biomolecules, and genes that facilitate the electron transfer process at the electrode interfaces. These molecular components are predominantly located between the outer and inner membranes of the bacteria. To date, a few bacteria, notably *Shewanella sp. and Geobacter sp*., have been extensively studied to elucidate the mechanisms underlying exogenous electron transfer (EET). Among the various mechanisms identified, two prominent pathways for extracellular electron transfer by bacteria are direct and mediated electron transfer mechanisms (Kumar et al., 2018).

Electrogenic bacteria, also known as exoelectrogenic bacteria, possess unique electron transporters within their membranes, enabling efficient electron transfer to external electron acceptors such as insoluble metals, fumarate, or nitrate. These specialized

electron transporters enable electrogenic bacteria to effectively participate in the electron transfer process and enhance MFC performance.

Geobacter sulfurreducens has emerged as a prominent and extensively studied exoelectrogen within the realm of microbial fuel cells. When cultivated on electrodes, *Geobacter* sp. forms robust biofilms and utilizes various carbon substrates to drive energy production. During the initial stages of biofilm formation, *Geobacter sulfurreducens* relies on a mediated electron transport mechanism for electron transfer (Inoue et al., 2011b).

Exoelectrogenic bacteria, including *Geobacter sulfurreducens*, secrete flavins such as riboflavin (RF) molecules to initiate biofilm development. These riboflavin molecules form complexes with outer membrane c-type cytochromes, facilitating the transfer of electrons to the anode surface. As the biofilm matures, *Geobacter sulfurreducens* undergoes a transition in its electron transport mechanism, shifting from mediated to direct electron transport for exogenous electron transfer. Within fully developed multi-layered biofilms, the active *G. sulfurreducens* cells in close proximity to the anode surface utilize outer membrane c-type cytochromes, particularly OmcZ, for efficient electron transport (Inoue et al., 2011a; Uria et al., 2017). Additionally, electrogenic bacteria situated further away from the anode produce conductive nanowires, such as type IV pili, that facilitate electron transport within the biofilm layers and ultimately reach the anode surface (Inoue et al., 2011b).

Shewanella oneidensis has emerged as the second most extensively investigated exoelectrogen in the context of microbial fuel cell (MFC) applications (Carmona-Martínez et al., 2013b). This bacterium, *S. oneidensis*, exhibits remarkable versatility as it possesses the ability to reduce various electron acceptors. Initially, there was speculation that *S. oneidensis* displayed nanowires similar to *Geobacter sulfurreducens*. However, subsequent research has confirmed that these structures are not nanowires per se but rather nanowire-like assemblies that extend from the outer membrane and periplasmic regions, often associated with outer-membrane vesicles.

Shewanella oneidensis secretes two types of Flavin molecules: riboflavin (RF) and flavin mononucleotide (FMN) (Carmona-Martínez et al., 2013b). These molecules serve as cofactors for MtrC and OmcA cytochromes. FMN is known to interact with MtrC, while RF functions as a cofactor for OmcA (Lahiri et al., 2022). The formation

of complexes between flavins and cytochromes (FMN-MtrC and RF-OmcA) facilitates the efficient transfer of electrons to the anode (Zheng et al., 2020). Although several genes and proteins have been identified to contribute to extracellular electron transport (EET) through specific pathways, the functional roles of other genes and proteins in EET remain not fully understood and subject to debate (Cao et al., 2019). Therefore, a comprehensive investigation is necessary to authenticate their capacity to mediate electron transfer to anode surfaces. Every bacterium behaves different in electrochemical behaviors; hence they follow different electron transfer mechanisms between cells and electrodes (Lahiri et al., 2022). There are three major mechanisms followed by electrochemically active bacteria which is depicted in following figure.

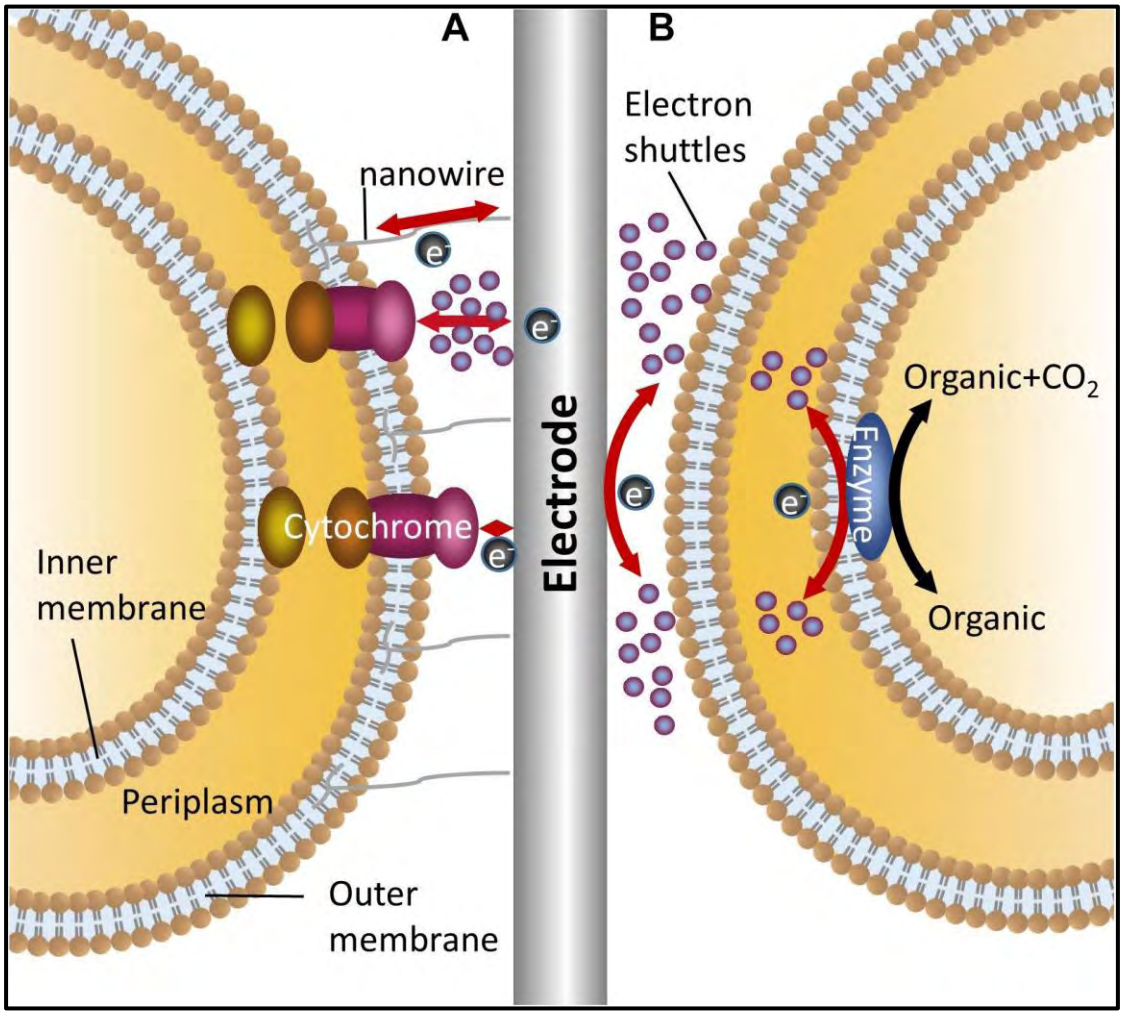

Figure 3: Mechanisms for bidirectional electron transfer between bacteria and electrodes. (A) Represents two mechanisms of direct electron transfer, one is mediated by nanowire, the other is mediated by outer membrane cytochromes with or without electron shuttles (Zheng et al., 2020)

2.5 Operational conditions affecting the microbial community in MFCs

The composition and performance of the electroactive biofilm in a Bioelectrochemical System (BES) are intricately dependent on the operational conditions. The subsequent sections explore the operational parameters that influence the start-up phase.

2.5.1 Temperature

Temperature is a critical parameter during BES operation, exerting an influence on both the microbial community composition and metabolic pathways. The start-up time is affected by kinetic constraints at low temperatures (L. Liu et al., 2013). Nevertheless, noteworthy research has revealed that the operation temperature does not impact the final power density achieved (L. Liu et al., 2012). Specifically, electroactive microorganisms forming an anodic biofilm at 30°C demonstrated the ability to adapt to lower temperatures (ranging from 4°C to 15°C) (S. Cheng et al., 2011) without any discernible decline in power density. Likewise, studies involving Microbial Fuel Cells (MFCs) initiated at 15°C exhibited stable performance even when the temperature was subsequently raised to 25°C. In contrast, Min et al. (Min O & Benito Román Irini Angelidaki, 2008) observed a reduction in start-up time and an increase in power production upon elevating the operation temperature from 22°C to 30°C (Heidrich et al., 2018).

In general, biofilms cultivated at lower temperatures exhibit greater resilience to fluctuations in temperature compared to those grown at higher temperatures. This has particular relevance for treating wastewaters that experience seasonal variations in temperature (L. Liu et al., 2012). It is advisable to commence the start-up of such BES systems during colder periods, even if it entails a longer start-up time, as it can lead to a more robust and stable performance over time (Heidrich et al., 2018).

Thermophilic Microbial Electrochemical Technology (MET) holds promise as a potential solution for treating high-temperature or pathogenic waste streams. Theoretical considerations suggest that the rapid microbial growth and enhanced reaction kinetics of thermophilic (>50°C) electroactive microorganisms could lead to high power densities (Shrestha et al., 2018). However, our current knowledge about thermophilic electroactive microbes remains limited. Despite their kinetic and thermodynamic advantages, studies have reported lower power densities in thermophilic BES compared to mesophilic conditions. This discrepancy may partly

arise from the fact that most investigations on thermophilic BES have focused on fundamental aspects, utilizing basic reactor configurations like H-type MFCs (L. Liu et al., 2013; Min O & Benito Román Irini Angelidaki, 2008). In contrast, more advanced reactor designs and electrode materials have been extensively tested under mesophilic conditions to maximize power production. Thus, the potential adaptation of mesophilic electroactive microorganisms to thermophilic conditions remains largely unexplored and demands further investigation (Heidrich et al., 2018).

It is crucial to determine the optimal temperature for a specific MET application, taking into account both the electroactive microbial community and economic feasibility (Chatterjee et al., 2019). The temperature selection involves a delicate trade-off among several factors: (i) the start-up time, which increases with decreasing temperature; (ii) the anodic electrocatalytic activity, which increases with rising temperature; and (iii) methanogenic growth, which peaks at temperatures up to approximately 37°C (Heidrich et al., 2018). Consequently, BESs acclimated and operated at lower temperatures (<30°C), despite requiring a longer start-up phase, may offer advantages in terms of selectively developing electroactive microbial communities while concurrently inhibiting competing organisms (Patil et al., 2010). This strategic temperature control could enhance the overall performance and efficiency of thermophilic MET systems (Chatterjee et al., 2019).

2.5.2 pH

The pH exerts a significant influence on the development of electroactive biofilms, regulating the metabolic pathways of electroactive microorganisms. While bioelectricity production has been demonstrated at extreme pH values (< 3 [105,106] and > 12) (Weerasinghe Mohottige et al., 2017), establishing an electroactive biofilm from mixed cultures, especially when dealing with complex organic substrates, typically necessitates a neutral or weakly alkaline pH (Chatterjee et al., 2019). This preference arises because hydrolysis processes are optimal at neutral pH levels. Additionally, if the inoculum is collected from environments with neutral pH, this requirement becomes even more pronounced (Ren et al., 2017). However, it is essential to consider that a neutral pH also favors the growth of methanogenic archaea.

Ren et al. have proposed that adjusting the pH to 9 during the start-up phase could potentially enhance the long-term performance of Microbial Fuel Cells (MFCs) (Ren

et al., 2018). This adjustment may serve to optimize the metabolic dynamics of the electroactive microbial community. In specific applications of Microbial Electrochemical Technology (MET), such as oxalate removal from aluminum refinery wastewater, which features a high pH of 10, initiating the start-up phase at a similarly elevated pH becomes imperative (Ren et al., 2017) . Such an approach allows for the necessary adaptation of the microbial community to function efficiently under alkaline conditions, thereby maximizing the effectiveness of the MET process in targeted industrial contexts.

2.6 Challenges

Despite the numerous applications of microbial fuel cells (MFCs), there are significant challenges that need to be addressed for their practical implementation at a commercial scale. Several key challenges include:

- *Enhancing Power Output*: The power potential output of MFCs needs to be significantly improved, as it is currently quite low for most commercial applications. One major obstacle is the high electron transfer resistance within bacterial biofilms formed on the anode. Further research and exploration, including mutagenesis techniques, are necessary to overcome this challenge. For instance, identifying and utilizing microbes that possess a large number of conductive pili per cell and/or secrete extracellular electron mediators at high concentrations could enhance power generation in MFCs. The synergistic interactions among microbial species within a biofilm consortium may hold the key to achieving this goal (Santoro et al., 2017).
- *Cost-effective Construction:* The construction of MFCs must be cost-effective to enable their widespread adoption. Currently, expensive proton exchange membranes (PEMs) and costly metals, such as platinum, are commonly used in laboratory setups. However, if these expensive materials are employed at the pilot scale, the overall cost of MFC systems will become prohibitive compared to other conventional wastewater treatment technologies. Therefore, it is crucial to explore the use of cost-effective materials. For instance, anion exchange membranes could be replaced with more affordable ion exchange membranes, and certain microbial fuel cells, such as sediment microbial fuel cells (SMFCs), may not require membranes at all. Moreover, biocathodes do not necessitate precious metal catalysts, opening up the possibility of using cost-effective

metals or their complexes in MFCs instead of expensive platinum (Santoro et al., 2017). Adopting these approaches would significantly improve the cost-effectiveness of MFCs.

- *Limited Understanding of Electron Transfer Mechanisms*: There is still a lack of comprehensive understanding regarding the intricate electron transfer mechanisms employed by electrogenic bacteria. It is possible that undiscovered electrochemical reactions occurring within biofilm communities could hold the potential to enhance MFC performance. In-depth research and exploration are needed to unravel these mechanisms and exploit their benefits in advancing MFC technology(Y. J. Jiang et al., 2022; Santoro et al., 2017) .

Addressing these challenges will contribute to the practical implementation of MFCs on a larger scale, promoting their commercialization and further utilization in diverse applications.

2. Materials and Methods

The experiment was designed in steps/series to keep the process error-free. Following is a general flowchart of procedural strategy:

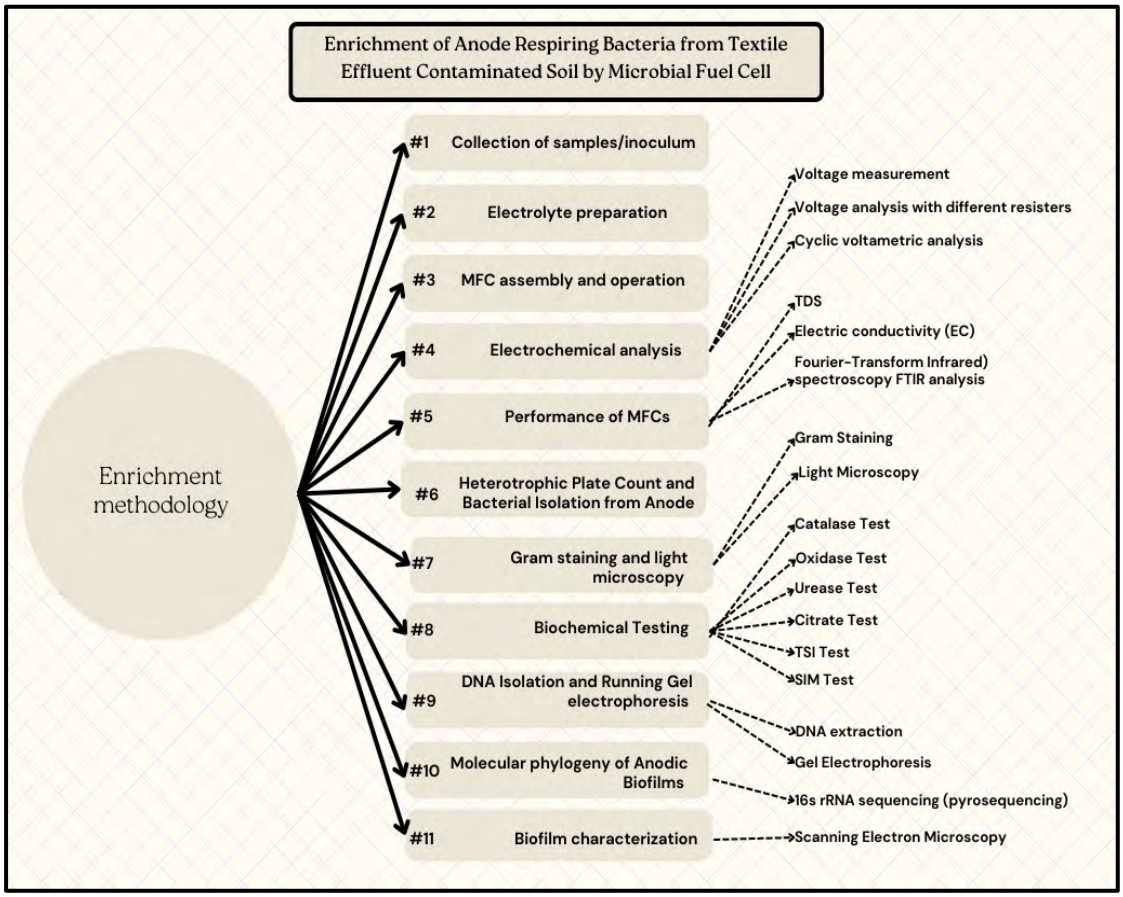

Figure 4: Methodology Flowchart

3.1. Collection of samples/inoculum

Three sites were chosen in Islamabad, Pakistan to collect soil and sludge samples i.e., a textile (Koh-e-Noor industry, Islamabad) effluent contaminated location, landfill (Rawat), and anaerobic sludge chamber (Qaid-I-Azam university). The soil samples were obtained from textile and landfill locations from depth of around 2-20cm to ensure the presence of ARBs. Then carefully samples were sealed away in a zip lock bags to avoid exposure to air (oxygen) and contamination. The sludge samples were packed into an air-tight container and brought back to the laboratory. All the samples were carefully sieved and strained for stones and other hard decaying objects. After that samples were stored away in an air-tight bags and containers at 4°C in refrigerator. The

experiment was performed at Microbial BioTech and BioEng Lab, Department of Microbiology, Quaid-i-Azam University, Islamabad, Pakistan.

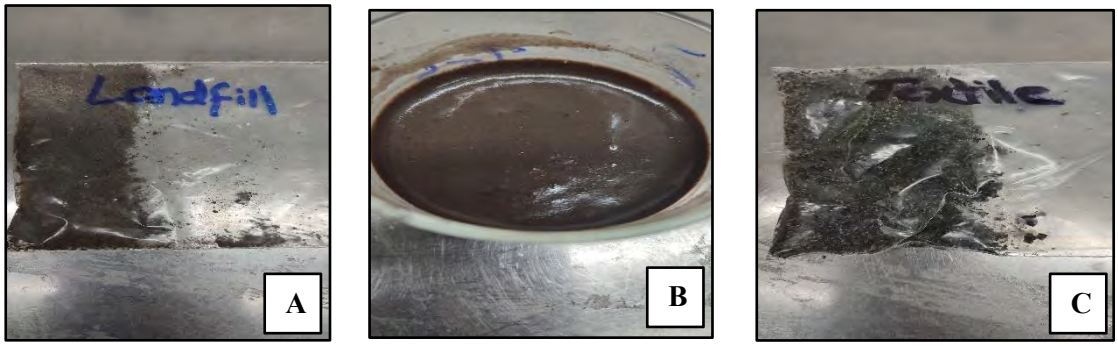

Figure 5: Inoculum samples (A) Landfill soil (B) Activated sludgr (C) Textile contaminated soil

3.2. Electrolyte preparation

The electrolyte solution for anode was prepared with the following components per liter: 450 mg of sucrose and potassium acetate, 480 mg of $NaHCO_3$, 95.5 mg of NH_4Cl, 10.5 mg of K_2HPO_4, 5.25 mg of KH_2PO_4, 63.1 mg of $CaCl_2.2H_2O$, and 19.2 mg of $MgSO_4.7H_2O$. Additionally, trace metals were included in the media, comprising 10 mg/L of $FeSO_4.7H_2O$, 0.526 mg/L of $MnSO_4.H_2O$, 0.526 mg/L of $NiSO_4.6H_2O$, 0.106 mg/L of H_3BO_3, 0.106 mg/L of $ZnSO_4.7H_2O$, 52.6 µg/L of $CoCl_2.6H_2O$, 52.6 µg/L of $(NH_4)_6Mo_7O_{24}.4H_2O$, and 4.5 µg/L of $CuSO_4.5H_2O$ (El-Khatib et al., 2015). The sucrose was used as the sole carbon provider in this case. A phosphate buffer solution containing of 2.27g of KH_2PO_4 and 5.8g K_2HPO_4 in a liter of distilled water was prepared for cathode chamber. The pH was maintained neutral 7 for cathode chamber.

3.3. MFC assembly and operation

A microbial electrochemical cell (MFC) with dual chamber was constructed/assembled using a two 350ml bottles, constructing a H-shape in an assembled form (Figure) (Yi & Harper, 2012). Both left and right sides have a protrusion towards each other that were then used to hold a connection between anode and cathode. The connection is a proton exchange membrane called Nafion (3.0 inch×3.0 inch, Nafion 115, Gas Hub Pte Ltd, Du Pont Company, USA) which allows the free movement of proton between chambers and avoids the fluids mixing. The structure of the MFC is held together with the help of a sealant (a sticky material like super glue used to hold objects together) to avoid leakage from the cell chambers. In this way the central joint has a thick circular rubber

(known as gaskit) and a circular cut Nafion, glued together and with the cell protrusions using sealant. Subsequently, both the chambers were held together for approximately 3hours with the help of clippers to allow sealant to become dry.

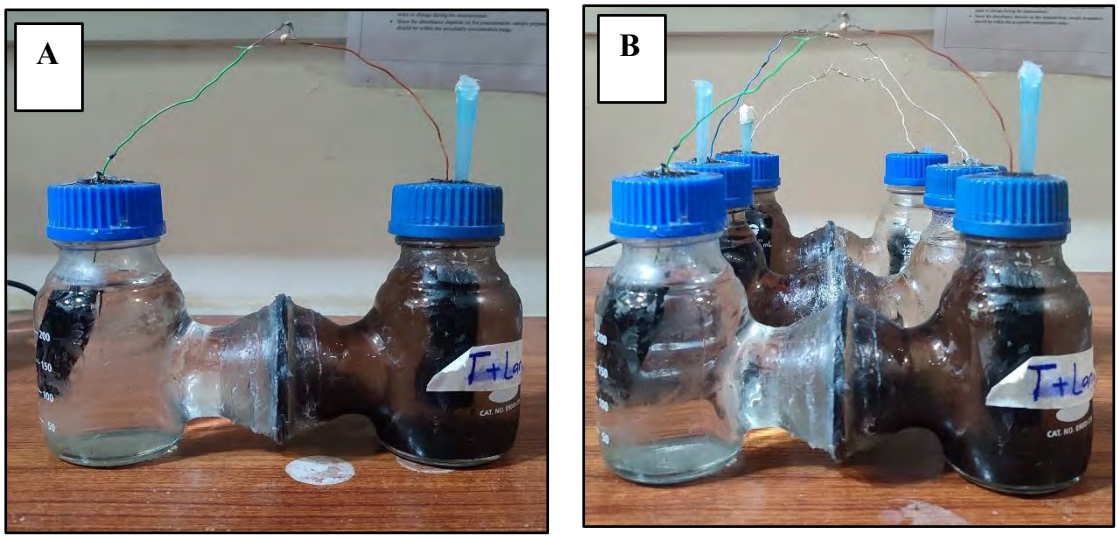

Figure 6: Microbial Fuel Cells (MFC) (A) Individual MFC with (T+L incoulum) and (B) Three MFCs

After 3 hours, the caps of the anode and cathode chambers were drilled to poke two holes. The purpose of one of the holes is to hold an electrode and other to occasionally act as a nitrogen inlet. The electrodes are carbon felt with an absorbent nature allowing a 3-D surface area for the biofilm formation (Yu et al., 2020). These electrodes were cut 3cm in width and 6cm in height and then dipped in distilled water for approximately an hour. After one hour the treatment of the electrodes was done with 40% nitric acid to remove any commercial residue and for its activation. They were dipped in nitric acid solution (40% acid and 60% distilled water) in a beaker containing a magnetic stirrer and left on the siring pate for approximately 30 minutes. Then they were washed with distilled water twice and placed on a petri plate to be left in an oven at 50°C for 3 hours for drying. When the electrodes were dried, they were connected to copper wires and fixed using a magic depoxy glue. The copper wires were stabbed along the length of electrode and fixed at top to avoid movement and the rest of the wire of approximately 6-8inches protrudes outside. After the depoxy dries out, the electrodes are fixed by passing wires through the hole and fixed the position using depoxy. In this way three cells were ready to receive media and inoculum.

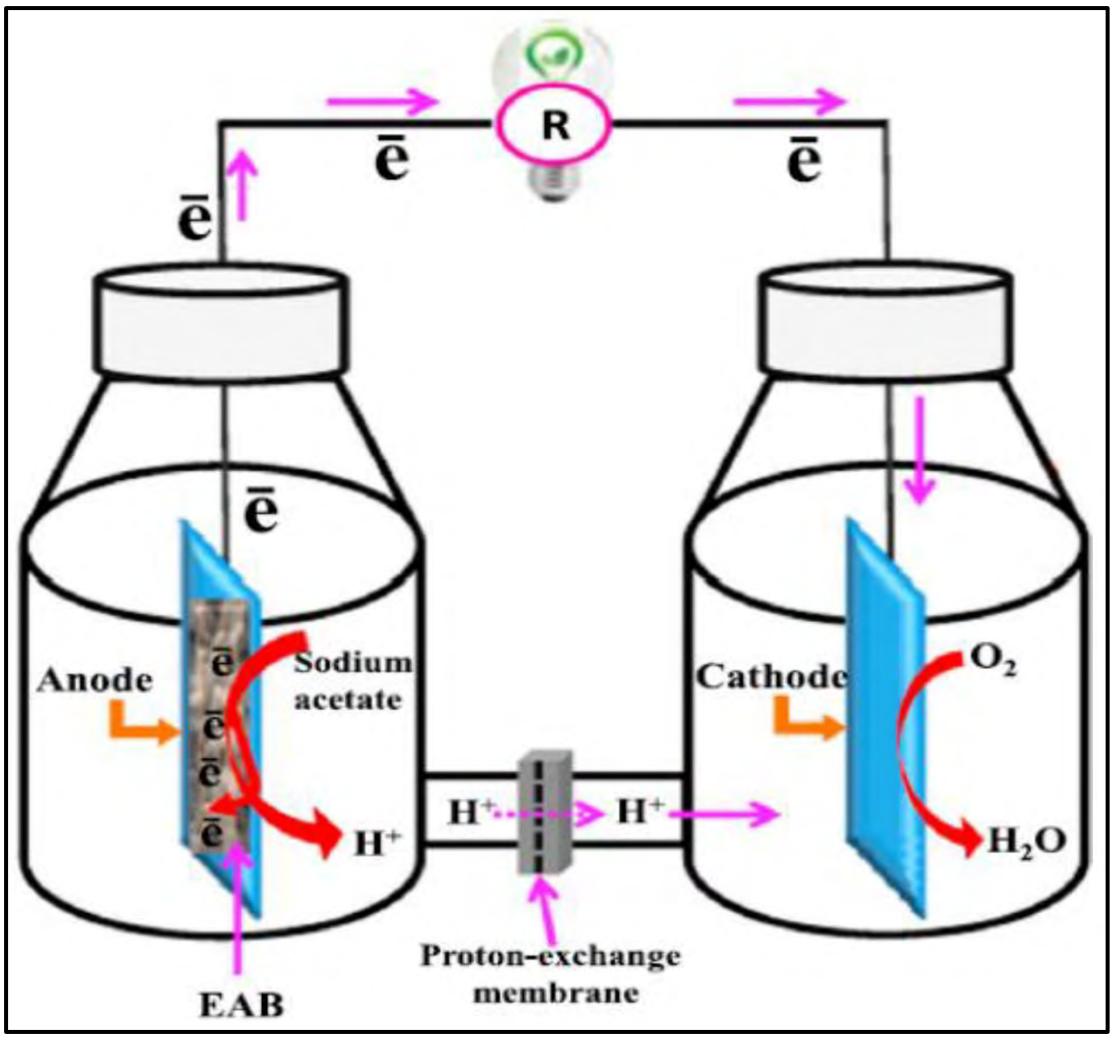

Figure 7: Schematic design of double chamber of double chamber MFC separated by Nafion

There were three MFCs hence we mixed samples and kept textile contaminate soil as a constant in each cell. The anode of cell 'A' (labeled as T) had only 5ml clean soil as an inoculum mixed in 350ml autoclaved media. The anode of cell 'B' (labeled as T+L) had a mixture of landfill and textile soil weighing 2.5g each. Hence anode of third cell 'C' (labeled as T+S) had mixture of textile and sludge weighing 2.5g each. Further anodic chambers had a stirrer to maintain agitation for 3-4 hours every day. Before closing the cells, sparging of N_2 was done in each cell for 30 minutes to create an oxygen free environment, whereas cathodes containing buffer had aerobic environment. This experiment was maintained for 30 days at a temperature of 37°C in an anaerobic incubation chamber (with a CO_2 inlet). In order to obtain a linear growth of the biofilm bacteria, fed batch method was used and the 100ml anodic media was refreshed every 3-5 days whereas the retention time of the catholyte was 5-8 days. The MFCs operated

under open circuit conditions whereas the voltage was provided using potentiostat to enrich the presence of electricigens.

After 30 days of operation, phase 2 of enrichment started for which the previous cell assembly was disarmed. To begin second enrichment, the anodic electrodes were preserved in an autoclaved media in an anaerobic condition. Whereas the cells were disarmed, cleaned, washed with detergent and autoclaved. After disinfection, the cells were reattached as previously mentioned and new cathode electrodes were cut and treated. The Cathodes electrodes were reattached whereas the anodic electrodes (that were preserved) were also reattached in a sterile hood to avoid contamination. Later the media was added to anode chamber and 5ml of previous suspension media were transferred to new anodes as an inoculum along with scraps of biofilm from suspension and biofilm on electrodes surface. Subsequently, cathode was filled with buffer and sparging with N_2 was done for 30 minutes (in anode of each cell) and the cells were incubated under anaerobic conditions at 37°C. This enrichment phase continued for 28days with the aim to increase number of electricigens in the biofilm community.

3.4. Electrochemical analysis

The enrichment of electricigens causes the stability of voltage output as an electrochemical potential establish at anode surface due to biofilm community creating a polarized electrode for electrochemical reaction. These polarized states allow the movement of electrons to create a voltage output which can be measured using a precision multimeter and a potentiostat to do cyclic voltametric analysis.

3.4.1 Voltage measurement

The voltage observed in the anodic chamber is a direct outcome of the electrochemical reactions transpiring within. To measure this voltage, a precision Multimeter (UNI-T; UT61A) was utilized. The measurements were taken for each of the three cells at the initial time point ('0' hour) and subsequently at 24-hour intervals throughout a 30-day period. These sequential readings offer valuable data to monitor the voltage fluctuations over the course of the experiment and to gain a comprehensive understanding of the electrochemical processes unfolding within the anodic chamber during the designated timeframe.

Figure 8: Recording voltage readings using a precision multimeter

3.4.2 Voltage analysis with different resisters

The determination of the internal resistance of the system involved a systematic variation of the external resistor load, ranging from 15Ω to 22KΩ. The point of peak power output was carefully observed, signifying the equilibrium at which the external resistance matched the system's internal resistance. To calculate the current (I), Ohm's law was applied, stating that

$$\mathbf{I = V / R}$$

By utilizing the graph circuit current values (I), current density was calculated (J) dividing Current by total area of the electrode. Whereas voltage multiplied by current density gives power density.

$$\mathbf{J = I / Surface\ area\ of\ the\ electrode}$$

$$Pd = \mathbf{J \times V}$$

3.4.3 Cyclic voltametric analysis

Cyclic voltammetry, a widely employed electrochemical technique, was employed to assess the electrocatalytic behaviour of the anode materials in three distinct microbial electrochemical cells, namely T, T+L, and T+S. The cyclic voltammetry measurements were every conducted every 5 days using a Potentiostat SP-150 instrument, maintaining a scan rate of 20 mV/s. The applied potential range spanned from -2.5V to 2.5V. The experimental setup involved the anode serving as the working electrode, the cathode (composed of carbon felt) acting as the counter electrode, and the reference electrode being Ag/AgCl. By systematically varying the potential within this specified range, valuable insights into the electrocatalytic response of the anode materials in the two microbial fuel cells were obtained.

3.5. Performance of MFCs

The performance evaluation of the Microbial electrochemical Cell (MEC) involved the continuous monitoring of media consumption, signifying the ongoing utilization of the sucrose-based media by biofilm. This metabolic activity led to the degradation of complex components into smaller ones. The initial readings at '0' hour served as a reference, and subsequent readings were taken in conjunction with media renewals throughout the experiment.

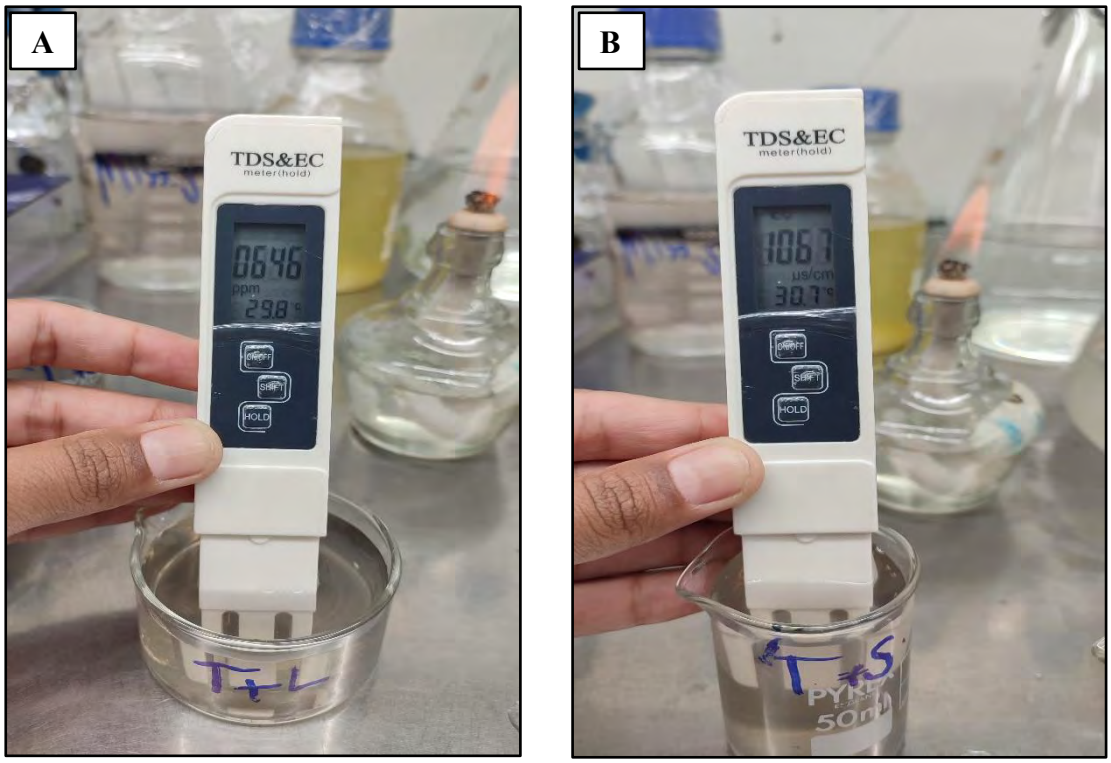

Figure 9: Recording TDS (A) and EC (B) values using TDS & EC meter

3.5.1 TDS

Regarding Total Dissolved Solids (TDS), measurements were obtained within a sterile hood using a TDS meter capable of indicating values in parts per million (ppm). Prior to each use, the TDS meter underwent disinfection with 75% ethanol to maintain cleanliness and accuracy. Observations for TDS were recorded at regular intervals of every 5 days during the initial 30-day phase and the subsequent 28-day phase.

3.5.2 Electric conductivity (EC)

In the context of Electrical Conductivity (EC), readings were acquired through the EC function of the same TDS meter. Similar to the TDS measurements, the TDS meter was disinfected with 75% ethanol before each use. The EC readings were observed at intervals of every 5 days during the first 30-day enrichment phase and the subsequent 28-day enrichment phase.

3.5.3 Fourier-Transform Infrared) spectroscopy FTIR analysis

The FTIR (Fourier-Transform Infrared) spectroscopy analysis was performed on the anodic electrolyte of the MFC. The purpose was to characterize the chemical composition of the anodic solution and identify key functional groups present. The

anodic electrolyte was carefully collected from the MFC after a specific period of operation. The collected electrolyte samples were then stored at 4°C to ensure the stability of the samples during analysis.

FTIR spectra were obtained using a transmission Fourier-transform infrared spectrometer. Prior to the analysis, the spectrometer was calibrated using standard reference materials to ensure accurate wavenumber readings. The spectra were recorded and then analyzed using origin-pro software to identify characteristic absorption peaks corresponding to different functional groups. The peaks in the spectra were compared to reference libraries and published data to assign specific chemical bonds and functional groups present in the anodic electrolyte (Nandiyanto et al., 2019).

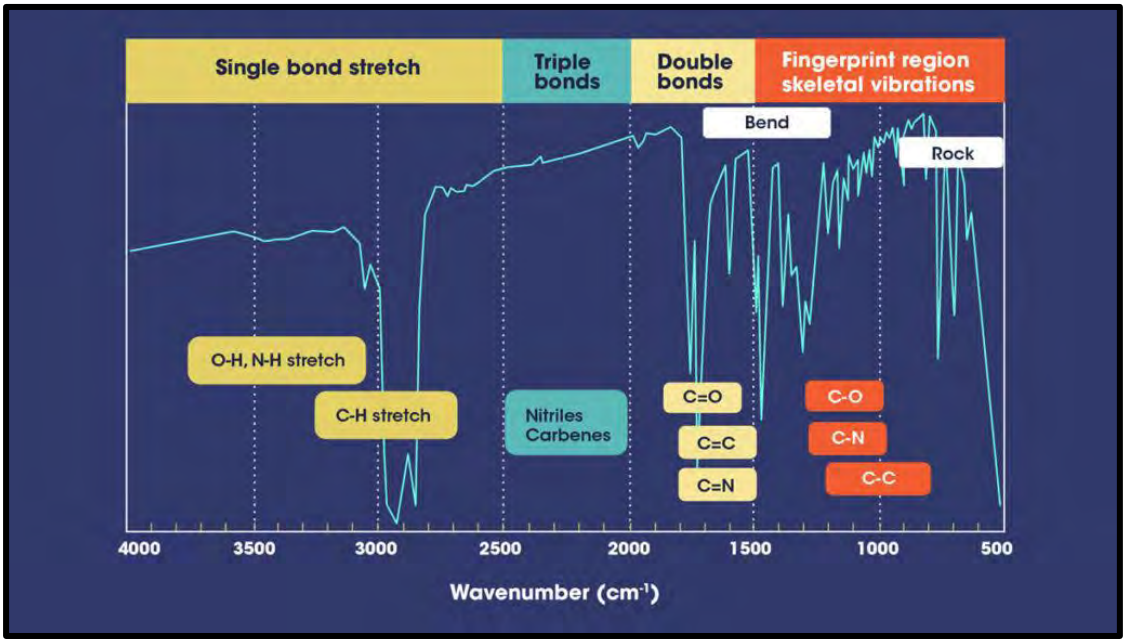

Figure 10: General overview of what FTIR peak depicts

By employing FTIR spectroscopy, valuable insights into the chemical composition of the anodic electrolyte in the MFC were gained, aiding in the understanding of the electrochemical processes and microbial activities within the system.

3.6. Heterotrophic Plate Count and Bacterial Isolation from Anode

The Heterotrophic Plate Count (HPC) and Bacterial Isolation from the anodic biofilm of the Microbial Fuel Cells (MFCs) were conducted in the following manner:

- Sample Collection: Anodic biofilm samples were aseptically collected from the electrodes surface after 25 days of enrichment period.
- Serial Dilution: The collected biofilm samples were then placed in an Eppendorf following with a high-speed vertexing for individual bacterial isolates. Later the suspension was subjected to serial dilution (10^{-2}, 10^{-4}, and 10^{-5}) in sterile distilled water to obtain appropriate dilutions.
- Nutrient Agar (NA) Preparation: NA was prepared according to standard protocols (mentioned on the box), and the petri plates were sterilized before use.
- HPC Analysis: For HPC analysis, 1 mL of the appropriate dilutions was spread evenly onto NA plates using a sterile spreader. The plates were then incubated at the appropriate temperature (e.g., 37°C) for 24-48 hours.
- Colony Counting: After incubation, colonies grown on the NA plates were counted, and the results were expressed as colony-forming units per milliliter (CFU/mL) of the original sample.

  The CFU/ml of biofilm suspension was calculated with the formula:

  CFU / ml = colonies x dilution factor/ Volume plated (mL)
- Bacterial Isolation: Distinct bacterial colonies with different morphologies were selected from the NA plates. Each selected colony was streaked onto fresh NA plates multiple times to obtain pure isolates.
- Storage of Isolates: Selected bacterial isolates were preserved by transferring them to refrigerator at 4°C for short-term storage.

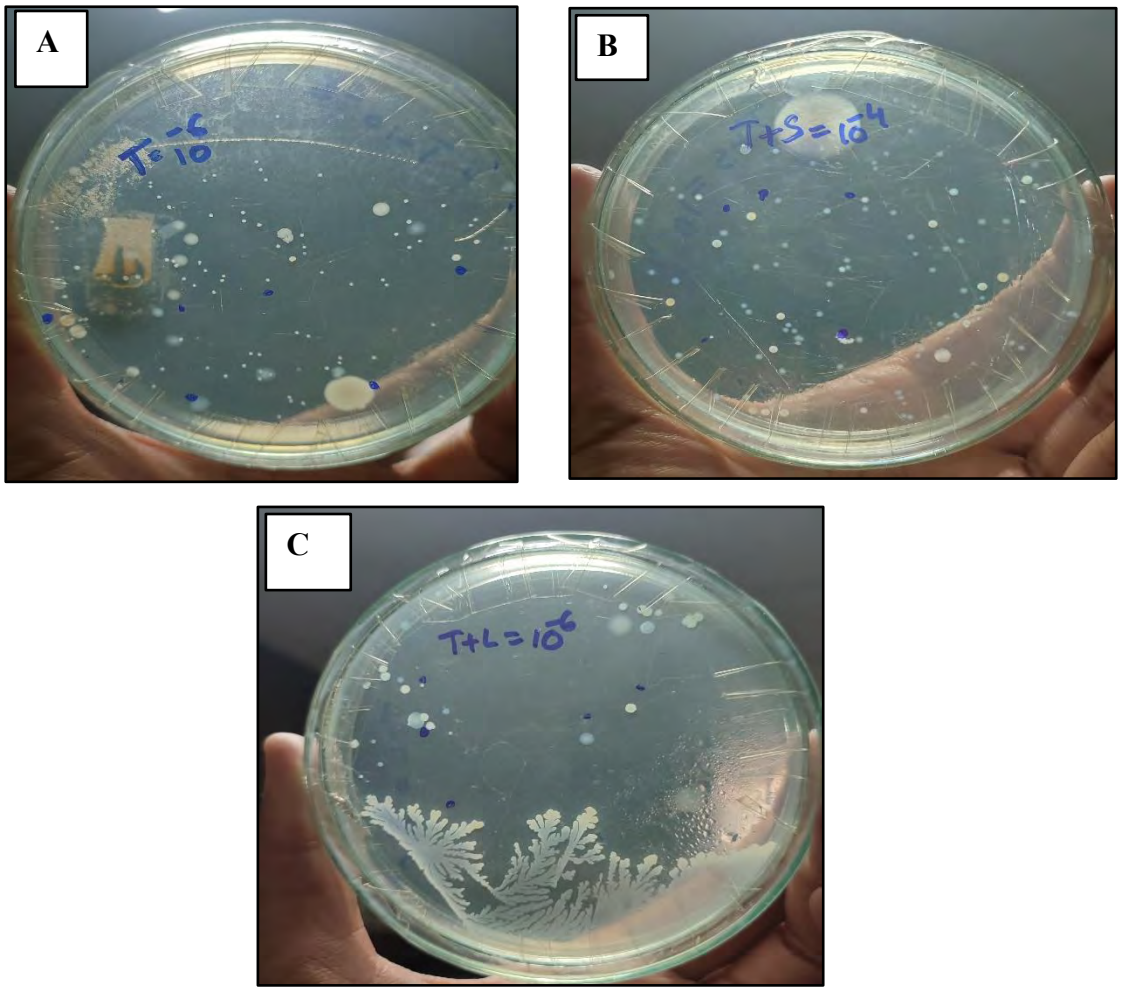

Figure 11: Bacterial colony isolation (A) from textile MFC (B) from T+S MFC (C) from T+L MFC

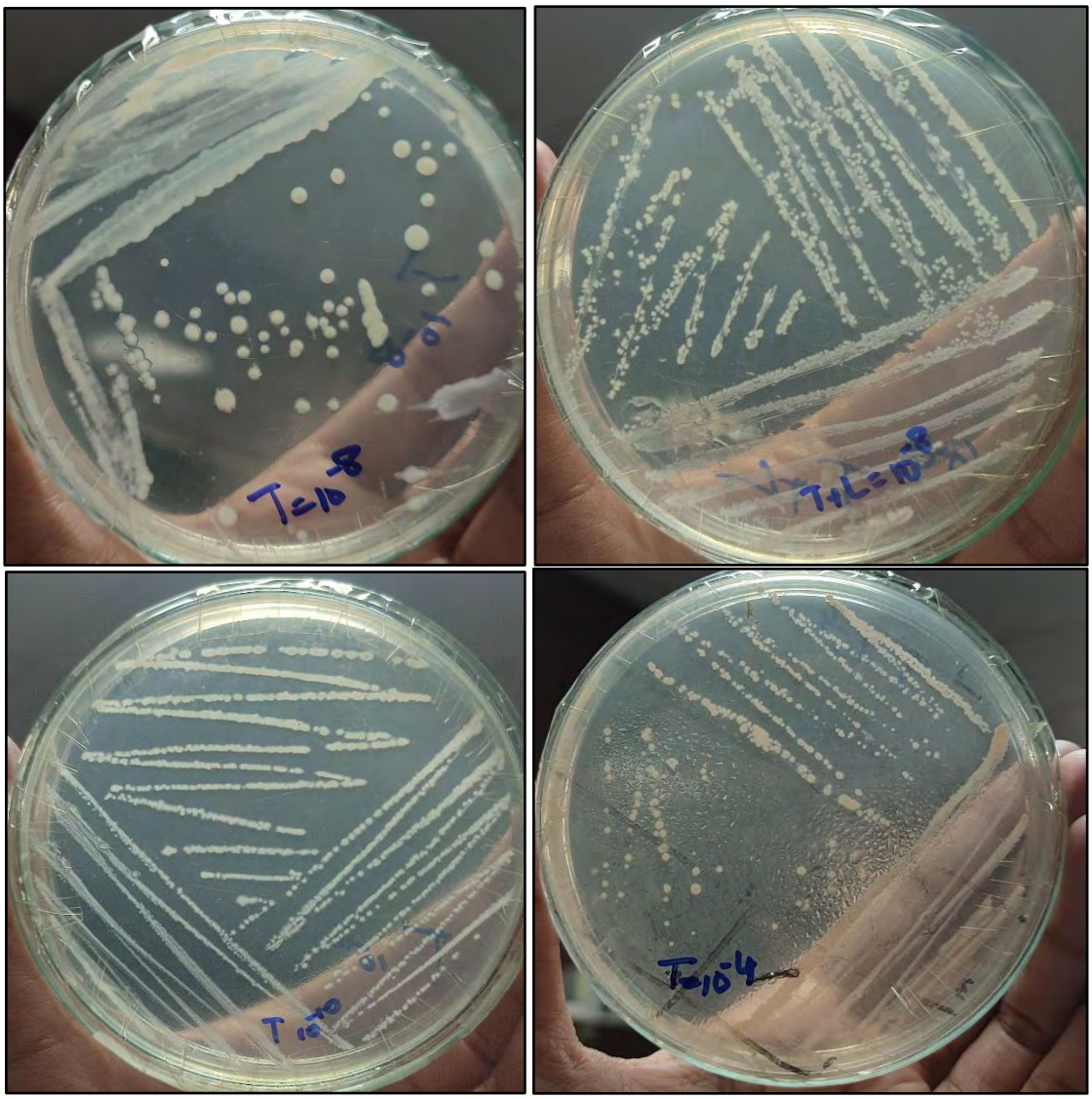

Figure 12: Purified bacterial isolates from the colonies obtained from Biofilm

3.7. Gram staining and light microscopy

In the laboratory setting, Gram staining and light microscopy was conducted to characterize the 28 bacterial strains previously isolated and purified from the enriched biofilm. The purpose was to differentiate the bacterial cells based on their cell wall composition and to gain insight into their morphology.

3.7.1 Gram Staining

a) Aseptically transferred a loopful of each bacterial culture onto separate clean glass slides.

b) Allowed the bacterial smears to air-dry at room temperature.

c) Fixed the bacterial smears by passing them through a Bunsen burner flame several times.
d) Flooded each smear with crystal violet (primary stain) and let it stand for 1 minute.
e) Gently rinsed off the excess crystal violet with distilled water.
f) Then applied Gram's iodine (mordant) to the smears and let it stand for 1 minute. Rinsed the smears with water to remove excess iodine.
g) Decolorized the smears by gently adding ethanol or acetone drop by drop until the runoff is colorless. Rinse with water immediately.
h) Counterstained the smears with safranin (secondary stain) for 1 minute and rinsed the smears with water and blot them dry with filter paper.

3.7.2 Light Microscopy

Freshly prepared bacterial smears on clean glass slides were then subjected to light microscopy. For that the slides were mounted on the stage of a light microscope and started with a low magnification objective (e.g., 10x) to locate the bacterial cells on the slide and then gradually increased the magnification (e.g., 40x, 100x with oil immersion) to observe finer details of bacterial morphology. Adjusted the focus and light intensity for optimal visualization (as required) and recorded observations of bacterial classifications, cell shapes, arrangements, and any notable features. Finally captured images of representative bacterial cells using a mobile camera.

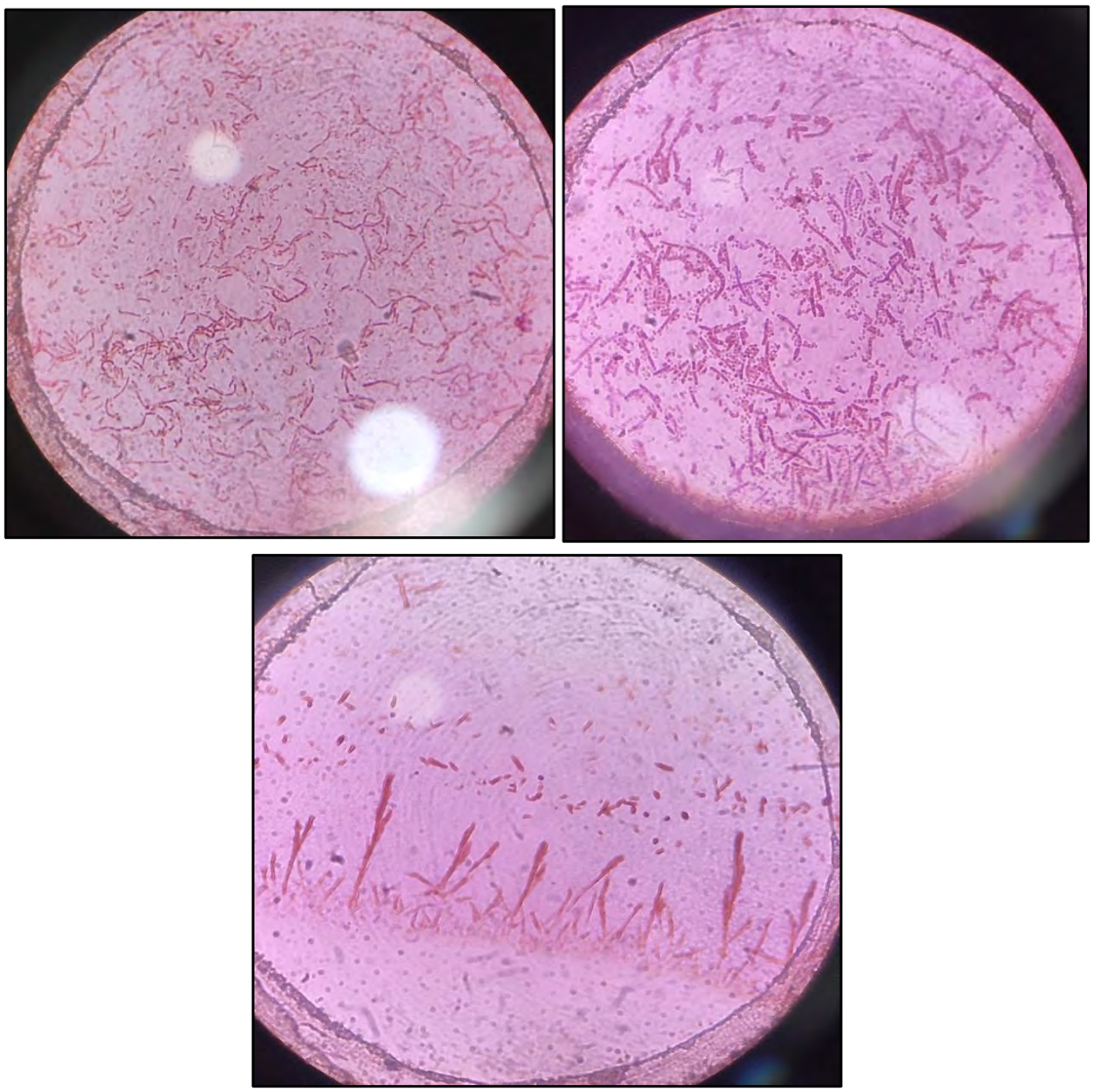

Figure 13: Observation under 100x microscope after Gram staining

3.8. Biochemical Testing

The biochemical tests were performed for identification of the isolated bacterial cultures by following standard laboratory protocols. The experimental test was conducted inside sterile hood and the media were prepared and autoclaved to avoid any contaminations. The specific biochemical tests employed for bacterial identification were as follows:

3.8.1 Catalase Test

A few drops of H_2O_2 solution were placed on a glass slide, and a single colony of the bacterial isolate was transferred onto the slide and mixed. The presence

of bubbles indicated a positive catalase test, while the absence of bubbles indicated a negative result.

3.8.2 Oxidase Test

A few drops of oxidase reagent were applied to a small piece of filter paper, and a single bacterial colony was transferred onto the oxidase reagent spot. A dark blue-purple color appearing within 10-30 seconds indicated a positive result, whereas no color change on the filter paper indicated a negative result.

3.8.3 Urease Test

The entire slant surface of the Simmons citrate medium was streaked with a single colony of the bacterial isolate. After incubating for 24 hours at 37ºC, the slant was observed for a color change. A bright pink color on the slant, possibly extending into the butt, indicated urease production. If the organism was urease negative, no change in the color of the culture medium occurred.

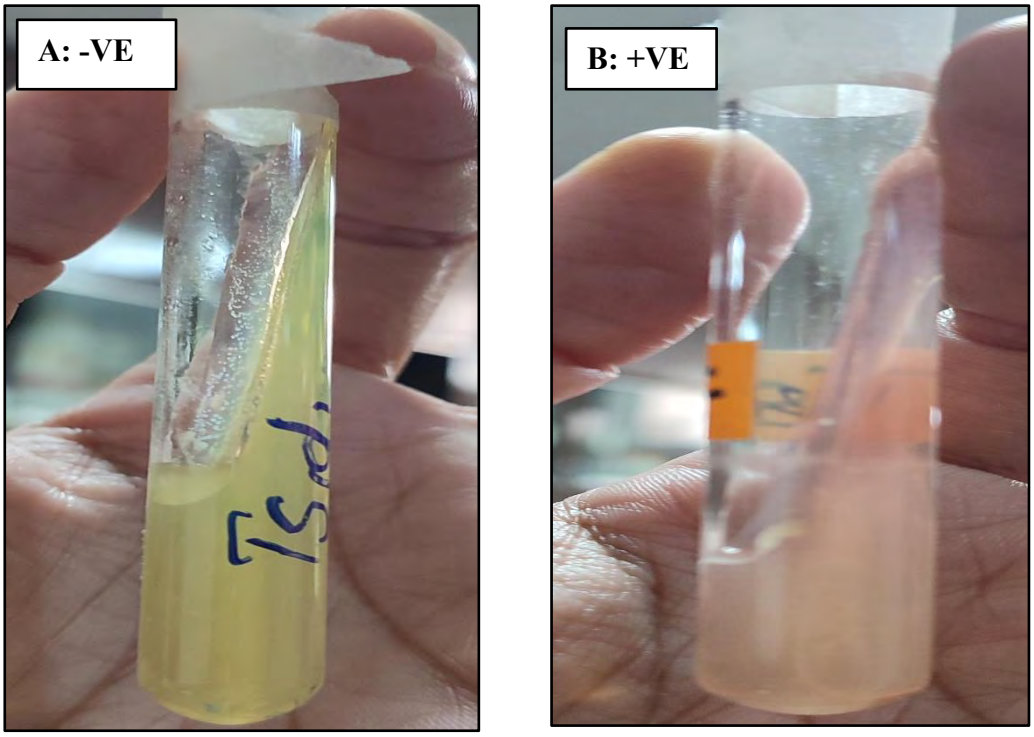

Figure 14: Urease test (A) depicting Negative results (B) depicting positive pinkish slant

3.8.4 Citrate Test

Simmons citrate medium was inoculated with a single colony of bacterial isolates and incubated at 37ºC for 24 hours. After incubation, a change in color

from the original green color to blue was observed. An intense Prussian blue color indicated a positive result, while no color change indicated a negative result.

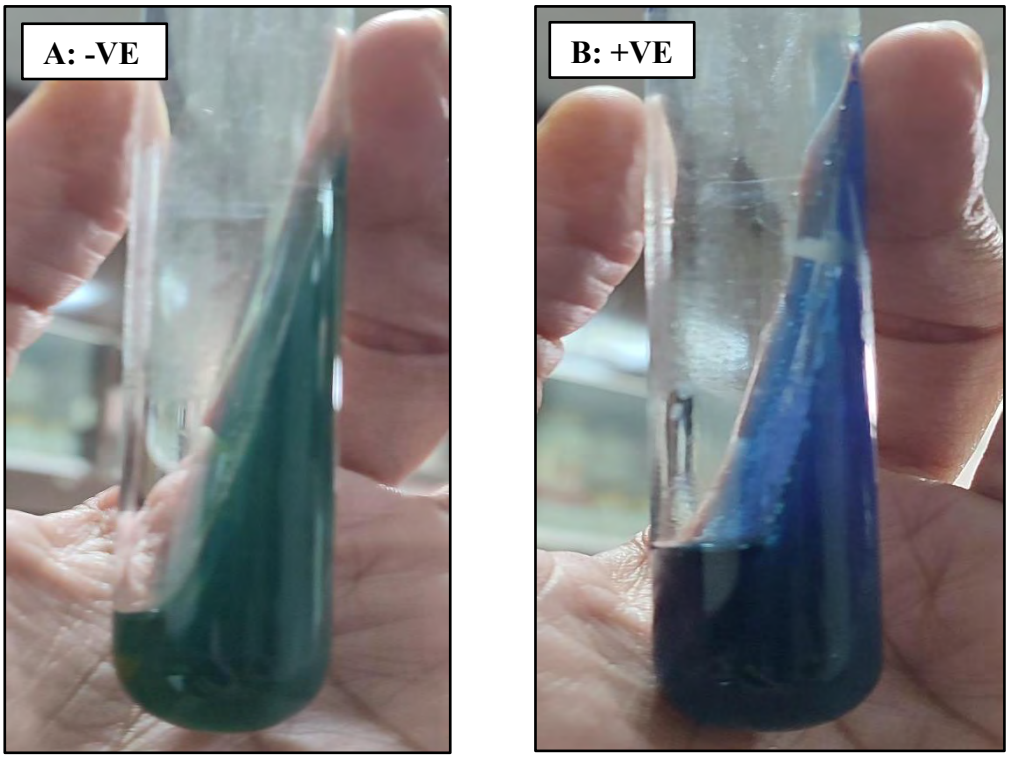

Figure 15: Citrate test (A) indicating negative (B) positive results

3.8.5 TSI Test

A single colony from a 24-hour culture was stabbed through the center of the TSI medium and streaked on the TSI slant using a sterile inoculation needle. The TSI medium was then incubated for 24 hours at 37ºC. After incubation, a yellow color in both the slant and butt indicated fermentation of sugars. A red color in both the slant and butt suggested that neither sugar was fermented. Additionally, blackening of the butt and the presence of cracks or bubbles in the medium indicated gas production.

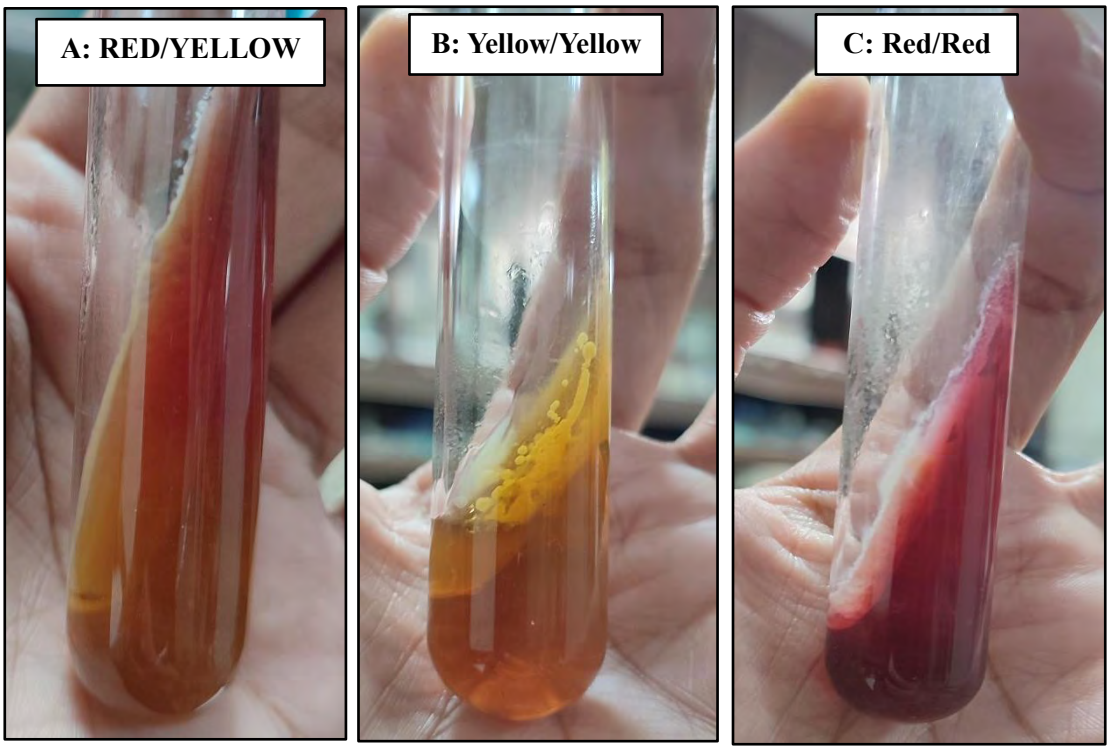

Figure 16: TSI test showing (A) alkaline slant/acidic butt (B) Acidic slant and/acidic butt (C) Alkaline slant and butt

3.8.6 SIM Test

An isolated colony from an 18–24-hour culture was stabbed to a depth of ½ inch through the center of the SIM medium and incubated at 37ºC for 24 hours. Motility and H_2S production in the SIM medium were indicated by a diffused growth zone and blackening of the medium from the line of incubation. After observing motility and H_2S production, a few drops of Kovacs reagent were added, and the development of a pink color on the surface of the medium indicated indole production.

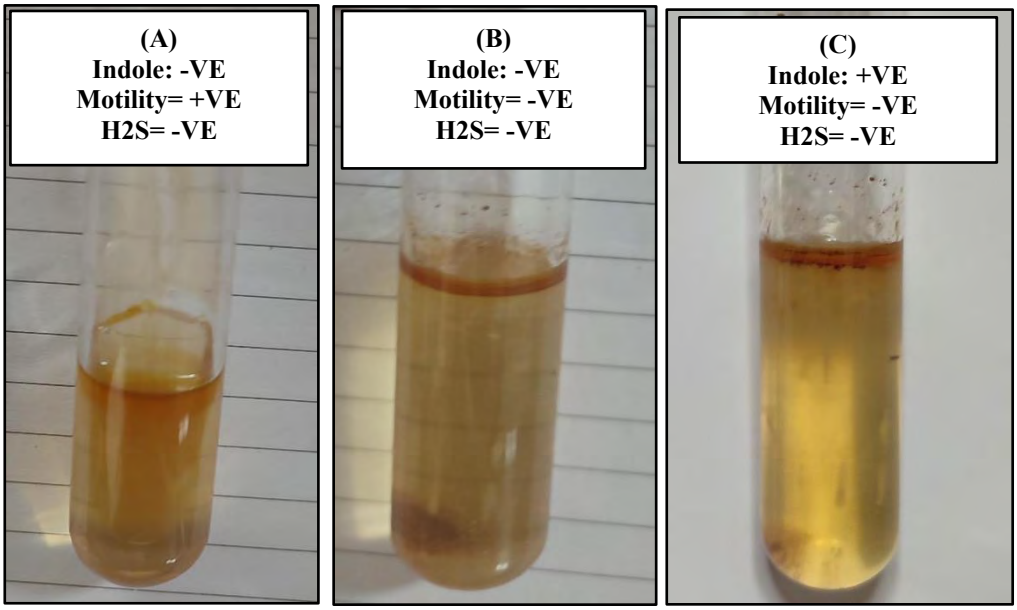

Figure 17: SIM test indicating indole, motility, and H2S production

3.9. DNA Isolation and Running Gel electrophoresis

DNA extraction and gel electrophoresis are fundamental techniques in molecular biology and genetics. They are used to isolate DNA from biological samples and separate DNA fragments based on their size, respectively.

3.9.1 DNA extraction

The DNA extraction was performed using FavorPrep^{TM} Soil DNA Isolation Mini Kit. The protocol to extract DNA was as follows:

1. The liquid sample ~200µl was added into a 2.0 ml Beads Tube and the tube was placed on ice.
2. 600 µl of SDE1 Buffer was added to the sample, and it was vortexed at maximum speed for 5 minutes. The sample was then incubated at 70°C for 10 minutes, and vortexing was performed twice during the incubation. Note that for the isolation of DNA from gram-positive bacteria, additional incubation at 95°C for 5 minutes was required.
3. Afterward, the tube was briefly spun to remove any drops from the inside of the lid. The sample mixture was cooled down, and 200 µl of SDE2 Buffer was added. The mixture was mixed well by vortexing and incubated on ice for 5 minutes.

4. The sample was then centrifuged at full speed (~ 18,000 x g) for 5 minutes. Careful transfer of the clarified supernatant to a 1.5 ml microcentrifuge tube (not provided) was done, and the volume of the supernatant was measured. It was crucial to avoid pipetting any debris and pellet.
5. Next, 1 volume of isopropanol was added to the clarified supernatant and mixed well by vortexing. The sample was then centrifuged at full speed for 10 minutes to pellet the DNA. As an example, if the clarified lysate volume was 450 µl, 450 µl of isopropanol was added to the clarified lysate.
6. After carefully discarding the supernatant, the tube was inverted on a paper towel for 1 minute to remove any residual liquid without disrupting the pellet.
7. Following that, 200 µl of pre-heated Elution Buffer or ddH_2O was added to the tube and vortexed to dissolve the DNA pellet completely.
8. To the sample, 100 µl of SDE3 Buffer was added and mixed well by vortexing. The sample was then incubated at room temperature for 3 minutes. It is important to note that SDE3 Buffer must be completely suspended by vigorously vortexing before each use. Additionally, the end of a 1 ml tip should be cut off to make it easier to pipette the SDE3 Buffer.
9. Finally, the tube was centrifuged at full speed for 2 minutes.
10. The supernatant was carefully transferred to a 1.5 ml microcentrifuge tube, and the volume of the supernatant was measured, ensuring to avoid pipetting any debris and pellet.
11. The tube was briefly spun to remove drops from the inside of the lid.
12. Add 1 volume of SDE4 Buffer and 1 volume of ethanol (96~100%). Mix thoroughly by pulse-vortexing. For example: If the clarified lysate volume is 250 µl, add 250 µl of SDE4 Buffer and 250 µl of ethanol (96~100%) to the sample.
13. A SDE Column was placed into a Collection Tube, and all of the sample mixture was transferred to the SDE Column. The sample was centrifuged at full speed for 1 minute, then the flow-through was discarded, and the SDE Column was placed into a new Collection Tube.
14. 750 µl of Wash Buffer (ethanol added) was added to the SDE Column. The sample was centrifuged at full speed for 1 minute, and then the flow-through was discarded. It was ensured that ethanol (96~100%) had been added to the Wash Buffer when first used.

15. Step 14 was repeated.
16. The SDE column was centrifuged at full speed for an additional 3 minutes to dry it. This step was considered vital as it prevented residual liquid from inhibiting subsequent enzymatic reactions.
17. The SDE Column was placed into the provided Elute Tube. Then, 50~200 µl of preheated Elution Buffer or ddH_2O was added onto the membrane centre of the SDE Column. The SDE Column was allowed to stand for 2 minutes at room temperature. It was emphasized that, for effective elution, it was essential to ensure that the Elution Buffer or ddH2O was dispensed onto the membrane center and was absorbed completely.
18. The sample was centrifuged at full speed for 1 minute to elute DNA.

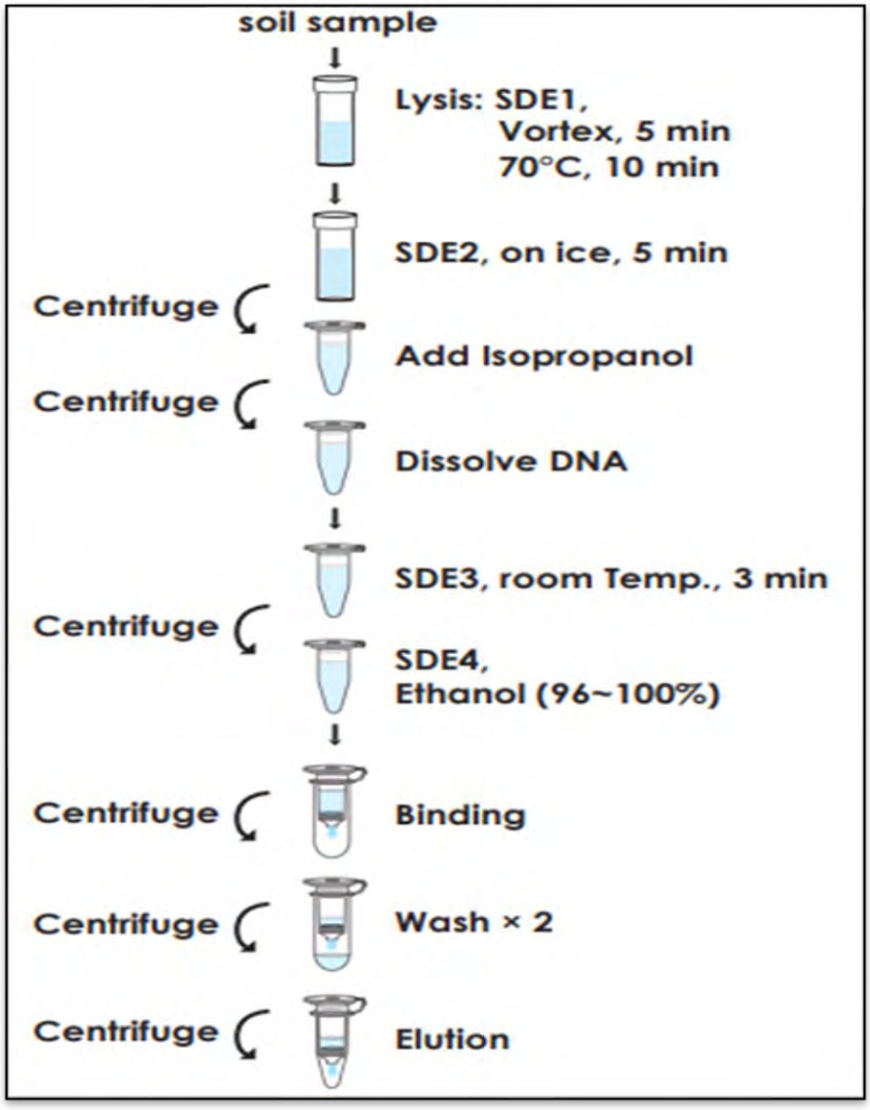

Figure 18: Brief Overview of DNA extraction using extraction kit

3.9.2 Gel Electrophoresis

After DNA extraction gel electrophoresis was performed to see the extraction of biofilm DNA:

- Prepared a 1% agarose gel by weighing 1 g of agarose powder and adding it to 100 ml of 1X TAE buffer in a glass flask. The mixture was heated in a microwave until the agarose was completely dissolved.
- Allowed the agarose-TAE mixture to cool down to approximately 60°C, then added 5 µl of ethidium bromide solution to the gel and mixed it gently by swirling.
- Poured the agarose gel solution into a gel tray with a well comb in place and allowed it to solidify for about 30 minutes at room temperature.
- Prepared the DNA samples by adding 5 µl of loading dye to each sample containing the extracted DNA. The loading dye contained tracking dyes to help monitor the progress of the electrophoresis.
- Loaded the DNA samples and a DNA ladder (1 kb DNA ladder) into separate wells in the gel using a micropipette.
- Connected the gel tray to the electrophoresis apparatus, making sure that the wells were facing the cathode (black electrode) side.
- Poured 1X TAE buffer into the electrophoresis chamber, ensuring that the buffer covered the gel completely.
- Applied an electrical voltage of 100 V across the gel and allowed the electrophoresis to run for approximately 45 minutes. This step allowed the DNA fragments to migrate through the gel based on their size, with the smaller fragments moving faster than the larger ones.
- Monitored the progress of the electrophoresis by observing the migration of the DNA bands under ultraviolet (UV) light. The ethidium bromide-stained DNA bands fluoresced and became visible as bright bands.
- Once the DNA bands had sufficiently separated, turned off the power and carefully removed the gel from the electrophoresis chamber.
- Placed the gel on a UV transilluminator and photographed the gel to document the results.

- Analyzed the gel image to determine the size and quantity of the extracted DNA fragments. The presence of distinct and well-separated bands indicated successful extraction of DNA strands.
- Discarded the agarose gel following proper waste disposal protocols for ethidium bromide-contaminated materials.

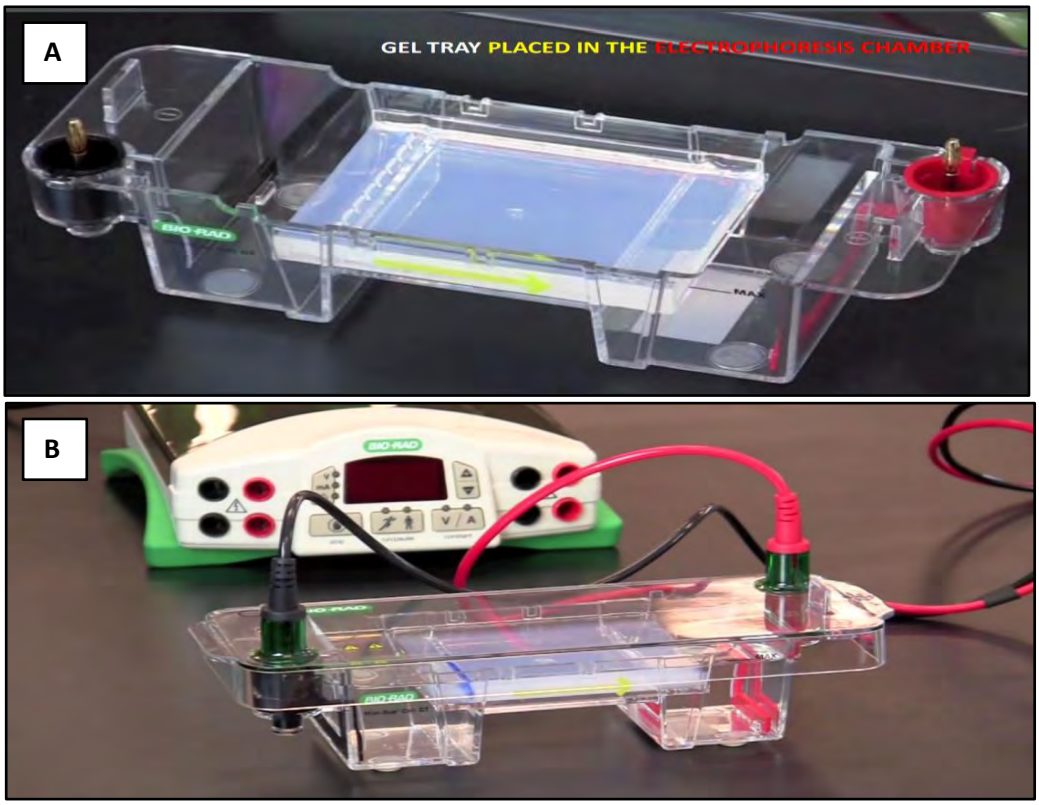

Figure 19: Gel electrophoresis assembly (A) Gel tray with Gel inside (B) Gel tray attached to power supply for voltage

3.10. Molecular phylogeny of Anodic Biofilms

The assessment of purified genomic DNA's quantity and quality was done before preceding for pyrosequencing, with help of gel electrophoresis. Subsequently, the DNA samples were sent to a lab in Thailand for pyrosequencing analysis.

For pyrosequencing, amplicon libraries were constructed using distinct sets of primers, targeting the 16S rRNA genes within the bacterial domain. The targeted genes underwent sequencing on MiSeq, adhering to the manufacturer's guidelines. The pipeline sequence data was subjected to further processing, including the joining of sequences, removal of sequences with barcodes <150bp, and elimination of sequences

containing ambiguous bases. Subsequently, denoising was conducted, and operational taxonomic units (OTUs) were generated, with illusions being subsequently removed.

Operational taxonomic units (OTUs) allowed for comparing community structures without assigning sequences into specific taxonomic ranks. To define operational taxonomic units (OTUs), a collection at 3% divergence (97% similarity) was employed. The final OTUs underwent taxonomic classification using BLAST against a curated database derived from GreenGenes, RDPII, and NCBI.

4. Results

The enrichment of electricigens and anode respiring bacteria (ARBs) was done by utilizing Microbial electrochemical cell concept based MFC. The enrichment had two distinct phases to help growth of electrochemically active bacteria. The phase 1 recorded voltage spikes reaching up to 0.5V in all cells indicting a significant presence of electricigens capable of producing currents without presence of strict dyes. The phase 2 also recorded substantial voltage to support the indication of electricigen purification. Further TDS, EC, and FTIR analysis were done which generated results depicting the breakdown of organic media components. To possibly identify bacteria inside biofilm a series of biochemicals tests were run showing possible presence of electrochemically active facultative anaerobes. To identify bacterial species of biofilm, DNA was extracted and verified by running Gel to make samples ready for 16s rRNA sequencing. Moreover, high resolution microscopic analysis was done using SEM to predominant morphology of anodic biofilm. The detailed results are:

4.1 Electrochemical Performance In MFC

Industrial chemicals and the wastes produced by the human population are causing the contamination of soils and waters. They are serious threat to all life forms; however, these contaminated soils and waters are source of electricigens and ARBs which can serve as the substrate to generate current. The process was conducted in a microbial fuel cell (MFC) to utilize the redox potential of electricigens to produce current and enrich them to increase their efficiencies. The soil and sludge samples were carefully selected and distributed in order to create combinations and diversities of microorganisms capable of forming biofilms to utilize media and generate current.

Three electrochemical cells were assembled based on the inoculum combinations i.e., MFC 1 (T), MFC 2 (T+L), and MFC 3 (T+S). The T cell contains only textile effluent contaminated soil, which is also kept as a constant in every cell, whereas T+L and T+S contains landfill soil and sludge along with textile contaminated soils. The dual chamber cells were separated by proton exchange membrane (Nafion) to help movement of protons. The cells undergone two enrichment phases to extract anaerobic electricigens on anode surface. The details of resulting outputs are following:

4.1.1 Voltage

During Phase 1, the voltage outputs across the three MFCs (T, T+L, and T+S) demonstrated variations that could be attributed to the composition of the inoculum. The initial voltage readings on Day 1 indicated a notable disparity, with MFC T exhibiting the highest voltage output (115 mV), followed by MFC T+S (40 mV), and MFC T+L (26.6 mV). Subsequently, a dynamic shift in voltage outputs was observed across the MFCs.

Figure 20: Voltage measurement for enrichment phase 1

As the enrichment phase progressed, an interesting pattern emerged. MFC T, relying solely on textile-contaminated soil, exhibited a gradual increase in voltage output over the experimental period, reaching a peak of 515 mV on Day 24, followed by a minor decline on Day 25 (498 mV). This consistent increment in voltage output suggested the

development of a stable biofilm community capable of sustaining redox reactions over time.

Conversely, MFCs T+L and T+S, containing additional landfill soil and sludge, displayed more complex trends. Despite fluctuations in their voltage outputs, these MFCs reached relatively higher voltages compared to MFC T. MFC T+L experienced substantial fluctuations until Day 6, where it achieved a remarkable voltage increase from 276 mV to 674 mV. A similar trend was observed in MFC T+S, though with fluctuations and subsequent stabilization. These observations indicated the establishment of dynamic biofilm communities capable of adapting to varying substrates and fostering redox reactions.

During Phase 2, the voltage outputs exhibited distinct trends compared to Phase 1. In this phase, the MFCs exhibited variations in their response to the established biofilm communities. Notably, MFC T+L displayed a consistently high voltage output, reaching 307 mV on Day 18. MFC T+S displayed a more variable behavior, with intermittent spikes and declines in voltage output. MFC T, on the other hand, exhibited a gradual declining voltage output trend, indicating utilize of substrate over period of time.

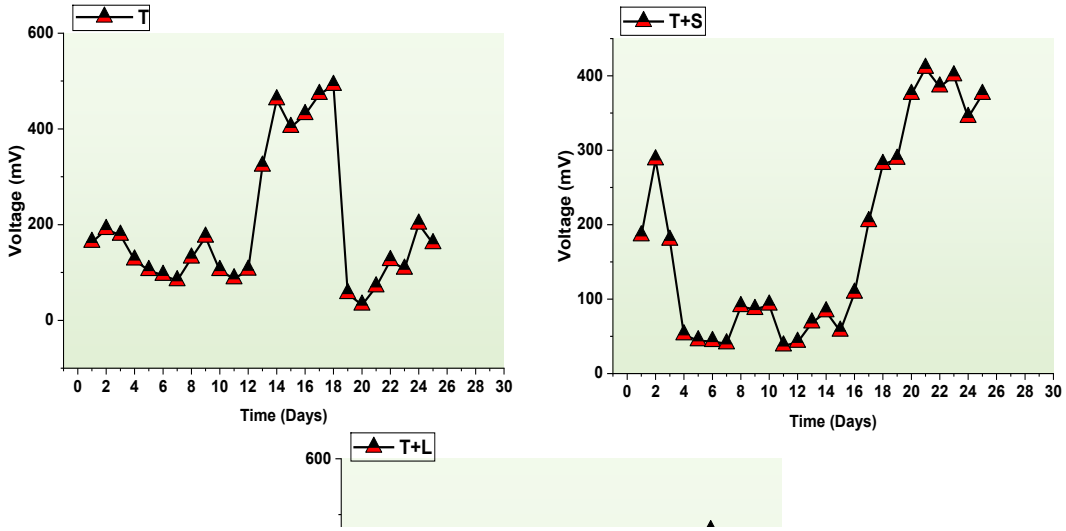

Figure 21: Voltage measurement for enrichment phase 2

The voltage outputs during Phase 2 suggested that the established biofilm communities underwent further adaptation and interaction with the changing environmental conditions. The differences observed among the MFCs underscored the intricate interplay between the composition of the microbial community, the available substrates, and the establishment of redox reactions within the electrochemical cells.

4.1.2 Effect of External Resistance

The performance of microbial electrochemical cells (MFCs) was studied by evaluating the effect of external resistance on voltage output, and subsequently exploring the relationship between voltage, resistance, current density, and power density. Three different MFCs, namely T, T+S, and T+L, were analyzed to understand how the variation in external resistance influenced their electrical characteristics.

The voltage output of the MFCs was measured across a range of external resistances, from 51 ohms to 15,000 ohms. As the external resistance increased, the voltage output generally followed a increasing trend across all three MFCs. This direct relationship

between voltage and resistance and inverse relationship between current and relationship in is a common phenomenon in electrochemical systems, including microbial electrochemical cells and it follows ohms law. The voltage output increased as the external resistance increased, indicating that higher resistance led to reduced electron flow and lower current generation. To gain insights into the performance of the MFCs, current density and power density were calculated for different combinations of external resistance and voltage. Current density is a measure of the flow of electrical current per unit area, while power density represents the rate of energy production per unit area. To obtain current density, current values were obtained by dividing voltage to the surface area of the anode. From these current (I) values, current density was calculated by dividing voltage with resistance whereas, the power density is result of multiplication of voltage and current density.

In the context of current density, the results revealed patterns that aligned with the voltage output. As external resistance increased, current density generally exhibited a decreasing trend. This is in line with the concept of Ohm's Law, which states that current (I) is inversely proportional to resistance (R) at a constant voltage (V). Therefore, higher resistance led to lower current density.

Power density, on the other hand, is a product of voltage and current density. As expected, the power density also showed a trend that correlated with both voltage and current density. Higher voltage and current density values contributed to higher power density. Notably, MFC T+L exhibited the highest power density values across different resistance levels, which could be attributed to the specific combination of soil types and microbial communities in that MFC.

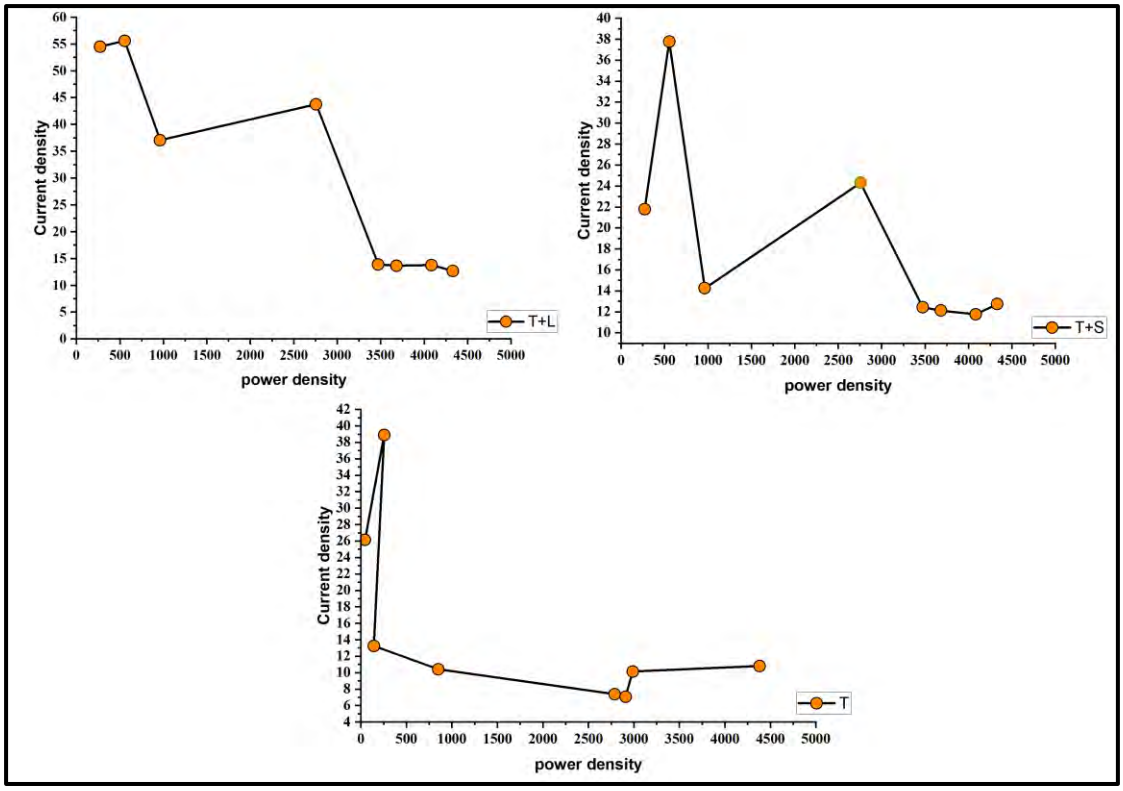

Figure 22: Polarization curve and power density of double chamber MFC at various resisters

The figure 23 shows a direct relation of power with current densities. The cells on average noticed highest current density of 39m A/m^2- 45m A/m^2 at power densities ~500m W/m^2 in the initial days of enrichment which then gradually decreased with the time. Briefly, the effect of external resistance on MFCs was evident in the interplay between voltage output, current density, and power density. Increasing external resistance resulted in lower current output, which subsequently influenced current density and power density. The relationship observed is consistent with fundamental electrochemical principles, highlighting the complex interactions between microbial activity, resistive losses, and energy production in microbial electrochemical cells.

4.1.3 Cyclic voltammetry (CV)

The cyclic voltammogram analysis successfully identified distinct redox signals, thereby facilitating the comprehensive understanding of reduction-oxidation reactions transpiring at the electrode interface (López Zavala et al., 2019). A comprehensive investigation into the electron transfer pathway from the bacterial biofilm to the underlying electrode was conducted through cyclic voltammetry. The orchestrated redox reactions produced by the biocatalytic processes of substrates by bacterial

constituents led to the production of both electrons and protons (H+). These resultant electrons and protons migrated towards the operational electrode (anode), subsequently yielding a discernible voltammogram in response to the applied potential. The potential range for the working electrode encompassed -1.5V to 1.5V, with a scanning rate of 20 mVs^{-1}, performed under open circuit conditions. During each cycle, the potential commenced at the zero point, progressing in the anodic direction to reach 1.5V, followed by a reversal back to the initial potential of -1.5V.

Cyclic voltammetry (CV) analyses were independently conducted for each of the MFCs during both enrichment phases. In Enrichment Phase 1 and Phase 2 of MFC T, distinctive redox loops corresponding to oxidation and reduction processes were clearly determined. The current outputs exhibited higher values during Phase 1, indicative of a greater microbial diversity, while Phase 2 showcased a more specific and defined electricigenic biofilm. Notably, the oxidation and reduction peaks were prominently observed at 1V and -1V during Phase 1, corresponding to current values of 35mA and 30mA, respectively. This manifestation highlights the occurrence of well-defined redox reactions within the cell. In contrast, the voltammograms of Phase 2 displayed a narrower loop at the top, suggesting limited oxidation activity, yet featured two broad reduction peaks at the bottom. A comparative analysis of both phases with the control (taken at time zero) revealed distinctly contrasting voltammogram profiles.

Figure 23: Cyclic voltammograms representing the difference in redox electric current (I) at the scan rate of 20 mV/s in anodic chamber of MFC for enrichment phase-1 for T-cell

Figure 24Cyclic voltammograms representing the difference in redox electric current (I) at the scan rate of 20 mV/s in anodic chamber of MFC for enrichment phase-2 for T-cell

A similar pattern of behaviour was observed in the other two MFCs, T+L and T+S, which closely resembled the tendencies exhibited by MFC-T. The voltammograms of both phases in MFCs T+L and T+S consistently exhibited oxidation and reduction peaks, contrasting with the control (0-hour peak). Phase 1 of T+L and T+S demonstrated peaks at 0.7V and 0.8V, corresponding to currents of 25mA and 24mA, respectively. Phase 2 consistently displayed broader peaks indicative of reduction reactions. The presence of oxidation signals in the CV results suggested substrate oxidation by anodic biofilms. These oxidation and reduction peaks were consistently observed across all MFCs, implying that the measured current was a consequence of the proliferation of electrochemically active bacteria within the MFCs.

Figure 25: Cyclic voltammograms representing the difference in redox electric current (I) at the scan rate of 20 mV/s in anodic chamber of MFC for enrichment phase-1 for T+S-cell

Figure 26: Cyclic voltammograms representing the difference in redox electric current (I) at the scan rate of 20 mV/s in anodic chamber of MFC for enrichment phase-2 for T+S-cell.

Figure 27: Cyclic voltammograms representing the difference in redox electric current (I) at the scan rate of 20 mV/s in anodic chamber of MFC for enrichment phase-1 for T+L-cell

Figure 28: Cyclic voltammograms representing the difference in redox electric current (I) at the scan rate of 20 mV/s in anodic chamber of MFC for enrichment phase-2 for T+L-cell

4.2 Performance of MFC

4.2.1 TDS

Based on the data of TDS values in the microbial electrochemical cells (MFCs) during the two enrichment phases, several observations can be made:

TDS values in each MFC during the first enrichment phase exhibited variations over the course of 25 days. In the T cell, which contained only textile-effluent-contaminated soil, the TDS levels started at 350 and gradually decreased to 540 by day 25. The T+L cell, with additional landfill soil and sludge, showed a similar trend, starting at 410 and

ending at 521. Meanwhile, the T+S cell, containing landfill soil and sludge, began at 310 and concluded at 450 TDS units. These fluctuations in TDS values suggest changes in medium composition due to microbial metabolism, nutrient consumption, and potential biofilm formation. The varying rates of change among the different MFCs might reflect differences in microbial community dynamics, substrate utilization, and biofilm development. During the second enrichment phase, the TDS values continued to provide insights into the ongoing microbial processes. In the T cell, TDS increased from 481 on day 1 to 502 on day 25. In the T+L cell, the values rose from 480 to 528, while in the T+S cell, they increased from 540 to 698.

Figure 29: TDS trends over period of time for enrichment phase 1

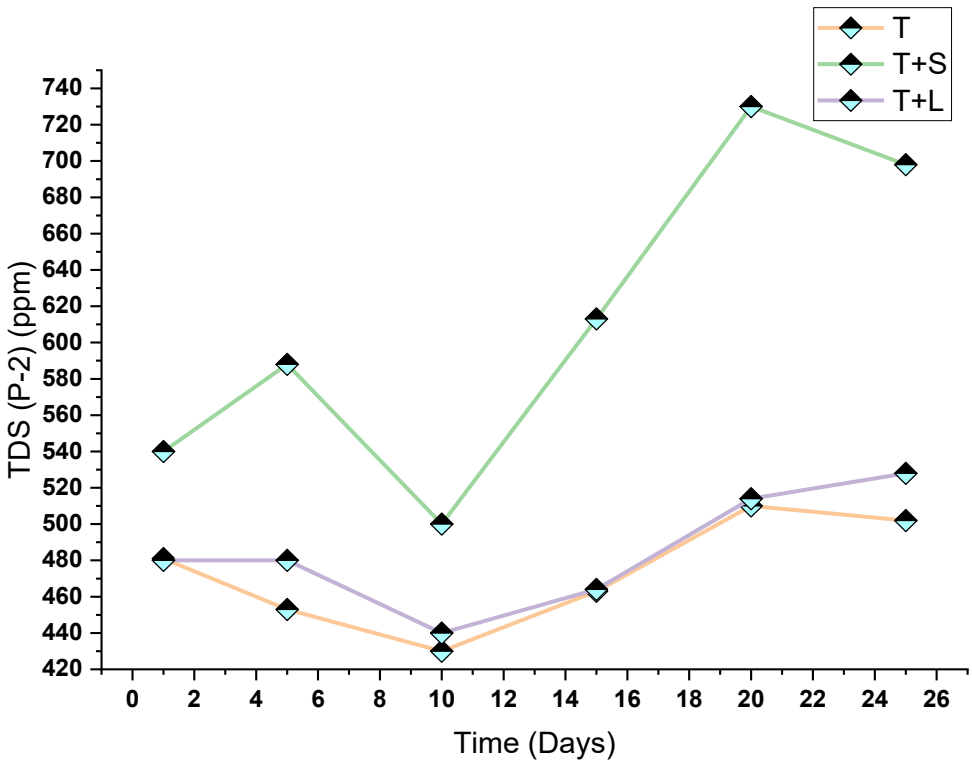

Figure 30: TDS trends over period of time for enrichment phase 2

The initial differences in TDS among the MFCs seem to persist, suggesting that the addition of landfill soil and sludge to the textile-contaminated soil affects the overall composition of the medium, leading to differences in TDS levels. The T+L MFC consistently exhibits higher TDS values compared to the other MFCs in both enrichment phases, indicating a potentially higher concentration of dissolved solids in this combination. The variations in TDS values also reflect changes in the composition of the biofilm forming on the anode electrodes. Differences in biofilm composition could affect the overall performance of the microbial electrochemical cells. The differences in TDS values could be linked to variations in microbial activity and growth in the different MFCs. Higher TDS values are indicative of greater microbial metabolic activity and organic matter consumption.

4.2.2 Electrical Conductivity

The initial EC values for the different MFCs (T, T+S, T+L) vary, likely due to differences in the initial composition of the soil and sludge mixtures. T+S and T+L have higher initial EC values compared to T, suggesting the presence of more ions and dissolved solids in these mixtures. Over the course of the 25 days, the EC values

generally show fluctuations in all MFCs. These fluctuations could be due to changes in the microbial community's metabolic activity and the composition of the medium.

In MFC T, the EC value decreases gradually from day 1 to day 25. This could indicate a reduction in the concentration of dissolved ions and solids in the medium. It's possible that the microbes are metabolizing these compounds and using them as substrates for their growth and energy production. In MFC T+S and MFC T+L, the EC values show fluctuations, with some increase and decrease patterns. This might be indicative of microbial activity that affects the concentration of dissolved ions and solids. The variations could be due to the interplay of various microbial species present in the soil, sludge, and textile-contaminated soil mixtures.

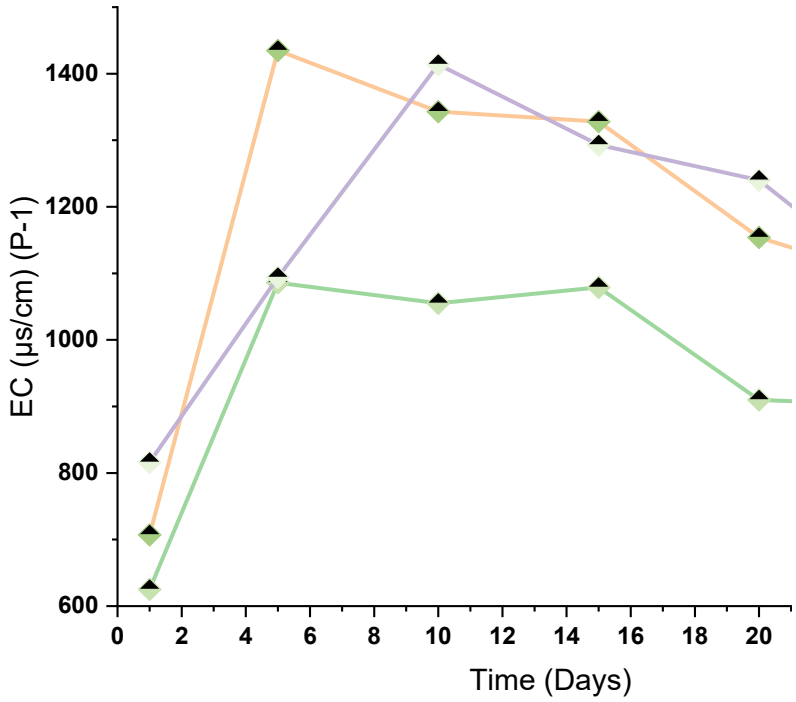

Figure 31: Electrical conductivity trends over period of time for enrichment phase-1

In the second phase, the EC values for all MFCs have changed compared to their initial values. This indicates that the microbial communities have adapted and evolved, leading to alterations in the medium composition. MFC T+S and MFC T+L show different patterns from MFC T. The EC values in MFC T+S and MFC T+L exhibit fluctuations, but these fluctuations are not as pronounced as in the first phase. This might suggest that the microbial communities have become more stable or have reached a different equilibrium in terms of medium composition and metabolic activity.

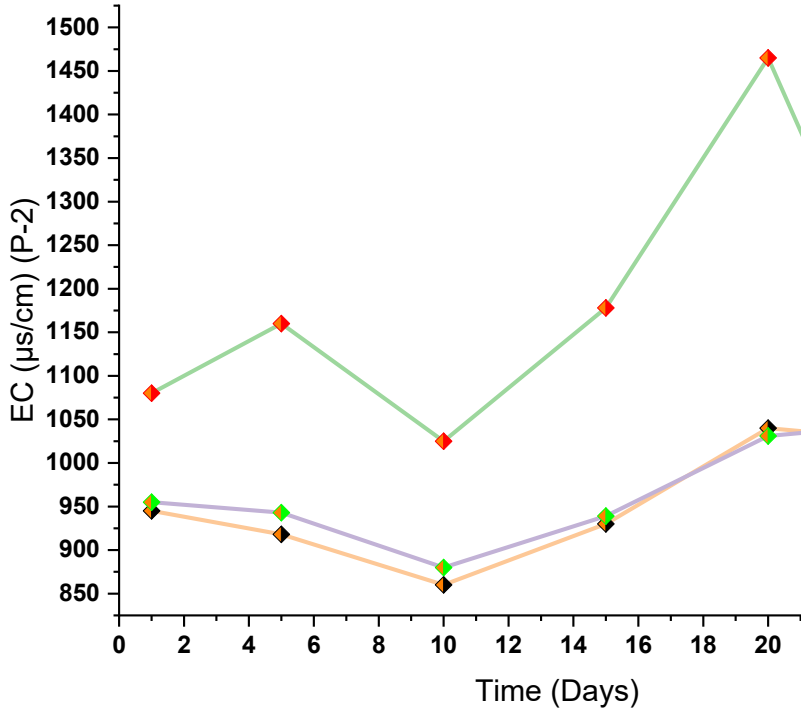

Figure 32: Electrical conductivity trends over period of time for enrichment phase-2

The combination of textile-contaminated soil with landfill soil and sludge (T+S and T+L) appears to enhance the ionic conductivity of the medium. This could be due to the presence of soluble ions from the additional soils or a more diverse microbial community, which might contribute to enhanced biofilm formation and electron transfer. The changes in EC values over time indicate that the microbial communities are adapting to the conditions in the MFCs. The fluctuations could reflect shifts in microbial populations, metabolic pathways, and the utilization of different substrates.

The differences in EC values between the MFCs with varying soil and sludge mixtures suggest that the composition of the medium directly influences the concentration of dissolved ions and solids. This composition affects microbial growth and metabolic activities. The observed fluctuations in EC values could also be related to biofilm formation and electron transfer processes on the anode surface. Biofilm growth and electron transfer efficiency influence the overall performance of microbial electrochemical cells.

4.2.3 FTIR analysis

FTIR analysis allow non-destructive chemical analysis of the sample solutions in the infrared range of wavenumber from 4000cm^{-1} to 400cm^{-1}. The infrared (IR) spectrum is split into three regions based on wavenumbers: far-IR (below 400 cm^-1), mid-IR (400-4000 cm^-1), and near-IR (4000-13000 cm^-1). While the mid-IR range is commonly employed for sample analysis, both far-IR and near-IR regions also offer insights about the samples. This research specifically concentrated on analyzing FTIR within the mid-IR range. The mid-IR spectrum is categorized into four parts:

- Single bond region (2500-4000 cm^{-1})
- Triple bond region (2000-2500 cm^{-1})
- Double bond region (1500-2000 cm^{-1})
- Fingerprint region (600-1500 cm^{-1})

The samples from cell T, T+L, and T+S have shown almost similar peaks indicating the similar behavior of media utilization by electricigen biofilm in all three cells. The bacteria breakdown the larger compounds into simpler ones resulting in the old bond breaking and new bond formations. Following images (of FTIR results for all MFCs) show peaks are concentrated in single bond, double bond, and fingerprint regions. The peaks between 3400-3300cm-1 show stretching of N-H bond and presence of aliphatic primary amines is possible. While the peaks between 1700-1600cm-1 show the presence of double bond and its stretching and the possible compound is alkenes. Lastly the peaks in the fingerprint region (show C-H out of plane bending) below 1000cm-1 and concentrated around 600-500cm-1 show possible presence of alkenes, halo compounds, and aromatic compounds.

Figure 33: FTIR peaks for T-cell control, phase-1 and phase-2

Figure 34: FTIR peaks for T+L-cell control, phase-1 and phase-2

Figure 35: FTIR peaks for T+S-cell control, phase-1 and phase-2

4.3 Culturable Electricigens anodic biofilms

The cultivation of a biofilm within the anodic chamber of the microbial electrochemical cell yielded valuable insights into the composition, characteristics, and potential functionalities of the microbial community involved in electrochemical processes.

A well-developed and cohesive biofilm was successfully cultured on the anode surface over the course of 25 days. The biofilm exhibited a distinctive three-dimensional architecture, with observable layers of microbial cells tightly adhering to the electrode. This adherence indicated a robust interaction between the microbial consortia and the electrode surface, facilitating efficient electron transfer. The analysis of the cultured biofilm demonstrated a diverse community of culturable bacteria. Through isolation and purification, 28 individual colonies were obtained, representing multiple bacterial species. Subsequent characterization through techniques such as gram staining and biochemical tests revealed a range of bacterial strains, highlighting the presence of electricigens and anaerobic anode-respiring bacteria.

4.3.1 Plate count

Plate counting analysis was conducted to assess the culturable microbial populations within the anodic chambers of three distinct microbial electrochemical cells: T, T+L, and T+S. The results provide insights into the abundance and distribution of viable microbial communities within these cells. The CFU was calculated utilizing following formula:

CFU / ml = no. of colonies/ Volume plated (mL) x dilution factor

Cell T (Textile Effluent-Contaminated Soil): The plate count analysis of cell T revealed a total of 98×10^6 colony-forming units (CFUs) per milliliter. The culturable microbial density in this cell indicated the presence of a viable and active microbial community associated with the textile effluent-contaminated soil.

Cell T+L (Landfill Soil + Textile-Contaminated Soil): In cell T+L, the plate counting yielded 31×10^6 CFUs per milliliter. The incorporation of landfill soil along with textile-contaminated soil appeared to influence the microbial density within the anodic chamber, indicating a dynamic microbial population responding to the mixed substrate composition.

Cell T+S (Sludge + Textile-Contaminated Soil): The analysis of cell T+S displayed 83×10^4 CFUs per milliliter. The presence of sludge and textile-contaminated soil in the substrate blend contributed to a distinct microbial density within the anodic chamber, suggesting a unique microbial community composition and response to this combination of substrates.

The comparative plate count results among the three cells revealed variations in culturable microbial densities. These differences may be attributed to the diverse substrates used in each cell configuration, reflecting the impact of substrate composition on microbial colonization and proliferation. The plate count data collectively emphasize the importance of substrate selection and composition in shaping the microbial populations within the anodic chambers of microbial electrochemical cells. Understanding these variations in microbial density provides valuable insights into the interactions between different microbial groups and their potential contributions to electrochemical processes.

4.3.2 Purification

The purification process was done to isolate each unique colony obtained from biofilm isolates of all three cells. The T+L cell provides 10 distinct colonies whereas T+S and T had 9 morphologically distinct colonies. These colonies were streaked on petri plates containing 20ml of nutrient agar (NA). After 48-hours, 28 plates had purified strains ready for further analysis. The purified colonies represented a diverse range of microbial species. The morphological variations observed among the colonies suggested differences in cell size, shape, and pigmentation. This diversity indicated the presence of multiple bacterial genera within the biofilm community.

4.3.3 Gram staining

The Gram staining technique was employed to categorize the bacterial isolates obtained from the cultured biofilm based on their cell wall characteristics. The results of the Gram staining procedure revealed a diverse array of Gram-positive and Gram-negative

The Gram staining technique provides a preliminary means of classifying bacterial isolates based on their cell wall composition, aiding in the initial identification.

Staining Result	**Bacterial Type**	**Cell Wall Characteristics**
Violet-Purple	Gram-Positive Bacteria	Thick peptidoglycan layer
Pink, Red	Gram-Negative Bacteria	Thinner peptidoglycan layer

The morphological characteristics were observed and recorded for each colony on plate and under microscope. The summary of identifications is as follows:

Table 3: Gram staining and colony characteristics

Characteristics	**Observations**
Gram reaction	Gram positive, Gram negative
Shape	Cocci, Bacilli, Spiral
Arrangement	Single, Pair, Chain, Cluster, Irregular
Size	Pinpoint, Small, Moderate, Large
Colour	White, Grey, Yellow, etc.
Form	Punctiform, Circular, Irregular, Rhizoid
Opacity	Opaque, Transparent, Translucent
Margin	Entire, Lobate, Undulate, Serrate, Filamentous
Elevation	Flat, Raised, Convex
Consistency	Buttery, Viscid, Brittle, Mucoid
Surface	Smooth, Glistening, Rough, Dull

4.3.4 Biochemical testing

A series of biochemical tests was conducted to delve deeper into the metabolic traits and functionalities of the isolated bacterial colonies from the cultured biofilm.

Catalase Test: The catalase test revealed intriguing outcomes among the tested bacterial colonies. A vigorous effervescence was observed in colonies that tested positive for catalase activity. The effervescence was attributed to the rapid breakdown of hydrogen peroxide into water and oxygen by the catalase enzyme. The active production of oxygen bubbles highlighted the metabolic vigor of these colonies, suggesting their capacity to thrive in oxygen-rich environments.

Oxidase Test: The oxidase test uncovered the presence of colonies with a distinct blue-purple color change upon exposure to the oxidase reagent. This color transformation indicated positive oxidase activity, indicating the potential involvement of these bacteria in redox reactions. The observed enzymatic activity signified their ability to transfer electrons to oxygen, reinforcing their significance in various oxidative processes.

Urease Test**:** The urease test showcased colonies that exhibited a striking color shift to pink upon exposure to the urease medium. This color transition was indicative of a positive urease activity, signifying the hydrolysis of urea into ammonia and carbon

dioxide. The production of ammonia by these colonies suggested their potential role in nitrogen cycling and their capacity to adapt to nitrogen-rich environments.

Simmon Citrate Test: The Simmon citrate test yielded colonies that demonstrated differential color changes in the citrate agar slant. Colonies that turned from green to blue were indicative of positive citrate utilization. This ability to metabolize citrate as a sole carbon source hinted at the versatility of these bacteria in exploiting diverse substrates for energy and growth.

TSI (Triple Sugar Iron) Test: The TSI test solved an intriguing contrast among the tested colonies. Some displayed a remarkable color shift from red to yellow throughout the medium, while others exhibited no color change. These diverse outcomes reflected variations in sugar fermentation patterns and gas production. The distinct metabolic profiles showcased the multifaceted nature of the bacterial community and its potential contributions to fermentation processes.

***SIM (Sulfur Indole Motility) Test*:** The SIM test showcased a spectrum of behaviors exhibited by the colonies. Some colonies displayed a dense black precipitate, indicating positive sulfur reduction. Others showed evidence of indole production, as indicated by a red layer after Kovac's reagent addition. Furthermore, the presence or absence of motility was observed through diffuse growth radiating from the stab line. These diverse responses underscored the adaptability and complexity of the microbial population.

Morphologically, the bacteria isolated from biofilms samples were rods and cocci. Furthers detailed biochemical characterization of isolated bacterial strains are shown in below table:

Results

Table 4: Identification of isolated bacterial strain through biochemical test. Here, MAC= MacConkey agar, EMB= Eosin methylene blue, TSI= Triple sugar iron, SIM= Sulfur indole motility, LF= Lactose fermenters, NLF= Non-lactose fermenters, Y/Y= yellow/yellow (slant & butt alkaline), R/R= Red/Red (slant & butt acidic), Y/R= Yellow/red (slant alkaline and butt acidic), M= Motility, I= Indole, (+) = Growth, (-) = No growth

Colony ID	Gram staining	EMB & MAC	Oxidase	Catalase	Urease	SIM	Citrate	TSI	Possible Identity
C1	G+ cocci	EMB: - MAC: -	-	-	-	1. H2S: - 2. Motility: - 3. Indole: +	-	Y/Y	*Escherichia coli*
C2	G- cocci in long chains	EMB: + MAC: +	-	+	+	1. H2S: - 2. Motility: + 3. Indole: +	-	Y/Y	*Enterococcus feacalis*
C3	G+ cocci in groups	EMB: - MAC: -	-	+	+	1. H2S: - 2. Motility: + 3. Indole: -	-	R/Y	*Bacillus subtilis*
C4	G- Rods	EMB: + (LF) MAC: + (LF)	-	-	+	1. H2S: - 2. Motility: - 3. Indole: +	-	R/Y	*Enterobacter cloacea*
C5	G+ cocci	EMB: - MAC: -	-	+	-	1. H2S: - 2. Motility: - 3. Indole: -	-	Y/Y	*Staphylococcus aureus*
C6	G+ Cocci in clusters	EMB: - MAC: -	-	+	+	1. H2S: - 2. Motility: + 3. Indole: -	-	Y/Y	*Staphylococcus saprophyticus*
C7	G- small Cocci	EMB: + (NL) MAC: +	-	+	-	1. H2S: - 2. Motility: - 3. Indole: +	-	Y/Y	*Klebsiella pneumoniae*
C8	G+ cocci	EMB: - MAC: -	-	-	-	1. H2S: - 2. Motility: - 3. Indole: -	-	R/Y	*Micrococcus spp.*

Results

C9	G- cocci in groups	EMB: + MAC: +	-	-	-	1. H2S: - 2. Motility: - 3. Indole: -	-	R/Y	*Staphylococcus epidermidis*
C10	G+ rods in chains	EMB: - MAC: -	-	+	+	1. H2S: - 2. Motility: - 3. Indole: +	+	R/Y	*Bacillus cereus*
C11	G+ cocci clusters	EMB: - MAC: -	-	-	-	1. H2S: - 2. Motility: - 3. Indole: +	-	Y/Y	*Streptococcus spp.*
C12	G+ rods in chains	EMB: - MAC: -	+	+	-	1. H2S: + 2. Motility: - 3. Indole: -	-	Y/Y	*Clostridium spp.*
C13	G- cocci chains	EMB: + MAC: +	-	+	-	1. H2S: - 2. Motility: - 3. Indole: -	-	Y/Y	*Enterobacter cloacae*
C14	G+ cocci clusters	EMB: - MAC: -	-	+	+	1. H2S: - 2. Motility: + 3. Indole: +	-	R/Y	*Micrococcus luteus*
C15	G- cocci chains	EMB: + MAC: +	-	+	+	1. H2S: - 2. Motility: - 3. Indole: +	-	R/Y	*Enterobacter aerogenes*
C16	G+ elongated cocci chains	EMB: - MAC: -	+	-	-	1. H2S: - 2. Motility: + 3. Indole: +	-	R/Y	*Streptococcus agalactiae*
C17	G+ rods	EMB: - MAC: -	-	-	-	1. H2S: - 2. Motility: + 3. Indole: +	-	R/Y	*Geobacter sulferreducens*
C18	G+ cocci	EMB: - MAC: -	-	-	+	1. H2S: - 2. Motility: - 3. Indole: -	-	Y/Y	*Desulfovivrio spp.*
C19	G+ cocci	EMB: - MAC: -	-	-	-	1. H2S: - 2. Motility: - 3. Indole: -	-	Y/Y	*Aerococcus spp.*
C20	G- Rods	EMB: + (LF)	+	-	+	1. H2S: -	-	R/Y	*Klebsiella penumoniae*

Results

		MAC: +				2. Motility: - 3. Indole: -			
C21	G- cocci chains	EMB: + MAC: +	-	-	+	1. H2S: - 2. Motility: - 3. Indole: +	-	Y/Y	*Pseudomonas aureginosa*
C22	G- cocci chains	EMB: + (LF) MAC: + (LF)	-	-	-	1. H2S: - 2. Motility: + 3. Indole: +	-	R/Y	*Citrobacter spp.*
C23	G- Rods chain	EMB: + MAC: +	+	+	+	1. H2S: - 2. Motility: + 3. Indole: +	-	R/Y	*Citrobacter freundii*
C24	G- Rods	EMB: + (NL) MAC: + (NL)	+	+	-	1. H2S: - 2. Motility: + 3. Indole: +	-	R/Y	*Shewanella spp.*
C25	G+ Rods	EMB: - MAC: -	-	+	+	1. H2S: - 2. Motility: - 3. Indole: +	-	R/Y	*Clostridium perfringens*
C26	G- Rods	EMB: + (NL) MAC: + (NL)	+	-	+	1. H2S: - 2. Motility: + 3. Indole: +	-	R/Y	*Shewanella oneidensis*
C27	G+ cocci	EMB: - MAC: -	+	-	-	1. H2S: - 2. Motility: - 3. Indole: +	-	Y/Y	*Geobacter spp.*
C28	G+ cocci clusters	EMB: - MAC: -	+	-	+	1. H2S: - 2. Motility: + 3. Indole: +	+	R/R	*Corynebacterium spp.*

4.4. DNA extraction and Gel Electrophoresis

4.4.1 DNA extraction

The DNA extraction process using the FavorPrepTM Soil DNA Isolation Mini Kit was successful in obtaining DNA from the biofilm samples labeled as T, T+L, and T+S. The extracted DNA was collected in Eppendorf and stored.

The successful extraction of DNA from the biofilm samples is a crucial step towards understanding the molecular basis of the species present within the biofilm. Biofilms are complex microbial communities that form on electrode surfaces, often composed of various species of bacteria, archaea, fungi, and other microorganisms. Extracting DNA from these biofilms allows us to explore the genetic information of these microorganisms, providing insights into their identities and potential functions.

DNA extraction was a fundamental step in studying microbial communities because it provided the genetic material necessary for downstream analysis. In enrichment case, the goal was to identify the microbes present in the biofilm using pyrosequencing. Pyrosequencing is a high-throughput sequencing method that allows to determine the order of nucleotides in DNA fragments, effectively providing a snapshot of the genetic makeup of the microbial community.

By analyzing the DNA extracted from the biofilm samples, following objectives are achieved:

- **Microbial Diversity:** Pyrosequencing will allow you to identify the various species of microorganisms present in the biofilm samples. This information will provide insights into the diversity and composition of the microbial community.
- **Taxonomic Classification:** The sequences obtained from pyrosequencing can be compared against databases of known microbial DNA sequences to determine the taxonomic classification of the identified microorganisms. This will help in identifying the specific genera and species within the biofilm.
- **Functional Potential**: In addition to taxonomic identification, some sequencing methods can also provide information about the functional potential of the microbial community. By analyzing specific gene markers or functional genes potential metabolic capabilities of the microorganisms can be assessed.
- **Community Dynamics:** Comparative analysis of DNA sequences from different samples (e.g., T, T+L, T+S) can reveal how the microbial community

composition changes under different conditions. This can help in understanding how microbes interact from various sample sources in the biofilm community structure.

4.4.2 Gel electrophoresis

Gel electrophoresis was performed on the extracted DNA samples labeled as T, T+L, and T+S. The gel visualization revealed distinct and well-separated DNA bands for each sample.

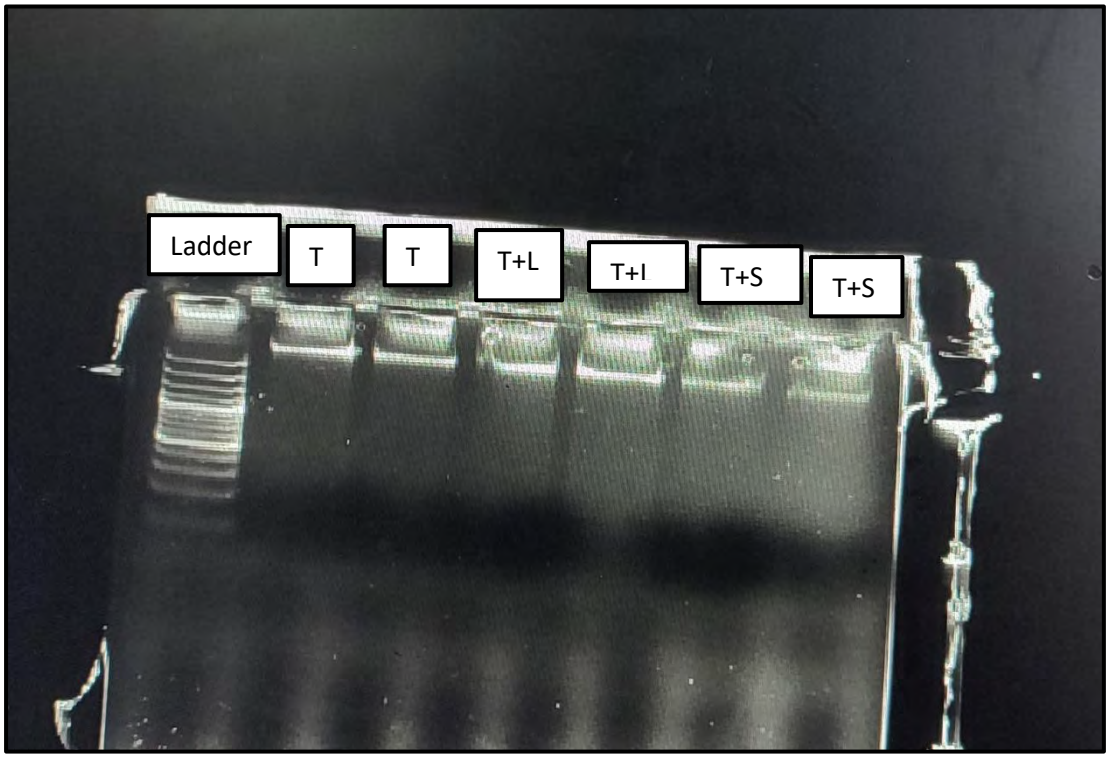

Figure 36: DNA fragment bands after successful DNA extraction and gel electrophoresis run

Gel electrophoresis is a fundamental technique used to visualize and analyze DNA fragments based on their size. Performing gel electrophoresis after DNA extraction was a critical step to assess the quality and integrity of the extracted DNA before proceeding to pyrosequencing. The successful visualization of DNA bands confirms the success of DNA extraction process and ensures that the extracted DNA is suitable for further molecular analysis, such as pyrosequencing.

Here's how gel electrophoresis ensured the success of DNA extraction and prepared the samples for pyrosequencing:

- **DNA Fragment Size:** The distinct and well-separated DNA bands observed on the gel correspond to different sizes of DNA fragments. The presence of these bands indicated that DNA was successfully extracted from the biofilm samples and that the DNA strands were not significantly degraded during the extraction process.
- **Quality Control:** The clear separation of DNA bands suggests that the extracted DNA is of high quality. Smear-like or smudged bands could indicate DNA degradation, which might affect the accuracy of downstream analysis.
- **Quantity Assessment:** The intensity of the DNA bands provided a rough estimation of DNA quantity. However, for accurate quantification, a DNA ladder with known fragment sizes was used as a reference. This estimation helped to ensure sufficient DNA for pyrosequencing.
- **Sample Comparison:** Running all three samples (T, T+L, and T+S) on the same gel allowed to visually compare the DNA band patterns. Any noticeable differences indicated variations in DNA content or quality between the samples.

4.5 Molecular phylogeny of Anodic Biofilms (pyrosequencing)

Pyrosequencing, also referred to as 454 sequencing, produces informative outcomes elucidating the genetic composition and diversity within both DNA samples (control 1, 2, & 3) and raw samples (raw sludge, RL soil, and RTEC soil). Illustrated in Figure 38 is the taxonomic distribution observed in both raw and DNA samples. The raw samples exhibit a higher percentage of genera and species that are uncategorizable, while the DNA samples reveal the presence of *Rhodococcus, Stenotrophomonas, Acetoacyeriodes, Sporomusa, Azospira, Enterobacteriaceae,* and *Ochrobactrum.*

These phylogenetic trees, serving as rooted representations of taxonomy, establish evolutionary connections through their branches. The distance of branches from the node in both raw and DNA (control) samples signifies the elapsed time since their divergence (Xiao et al., 2015a; Z. Yang et al., 2022).

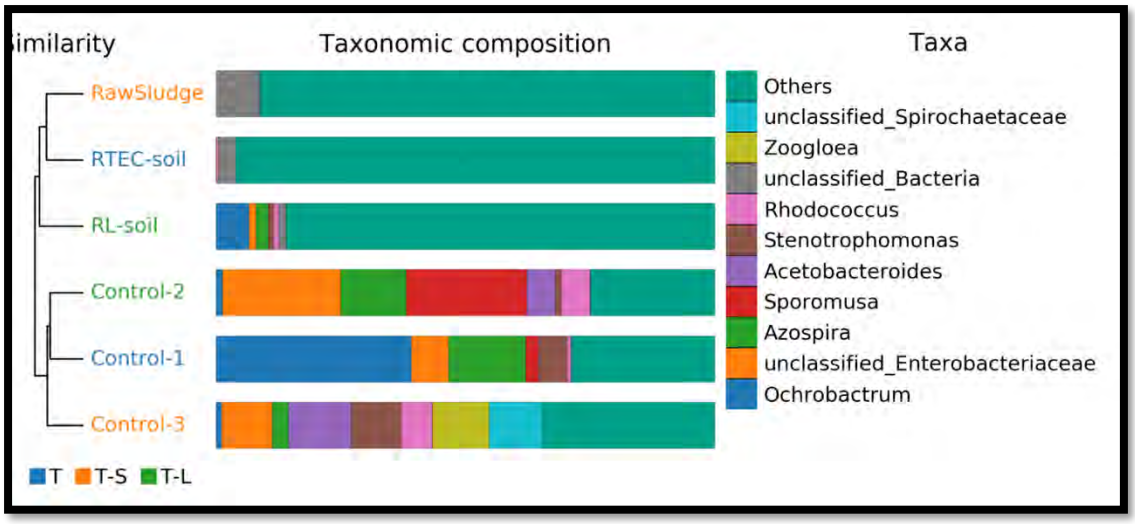

Figure 37: Taxonomic composition of RAW and Isolated bacteria strains using Pyrosequencing

Pyrosequencing contributes to the analysis of biodiversity within communities by generating rank abundance plots. These plots aid in uncovering the richness and evenness of species within the communities, providing a straightforward yet effective means to comprehend abundance distribution among different species. The key components of a rank abundance plot include the X-axis, which ranks species from the most abundant (rank 1) to the least abundant, and the Y-axis, representing the relative abundance of each species, often displayed logarithmically.

Species ranked below 500 indicate low species evenness, where a few species dominate the community, while the majority are rare. Shallow slopes between 1000-2000 on the x-axis suggest an even distribution of species, indicating that no single species dominates the community, and most species have similar abundance levels (Z. Yang et al., 2022).

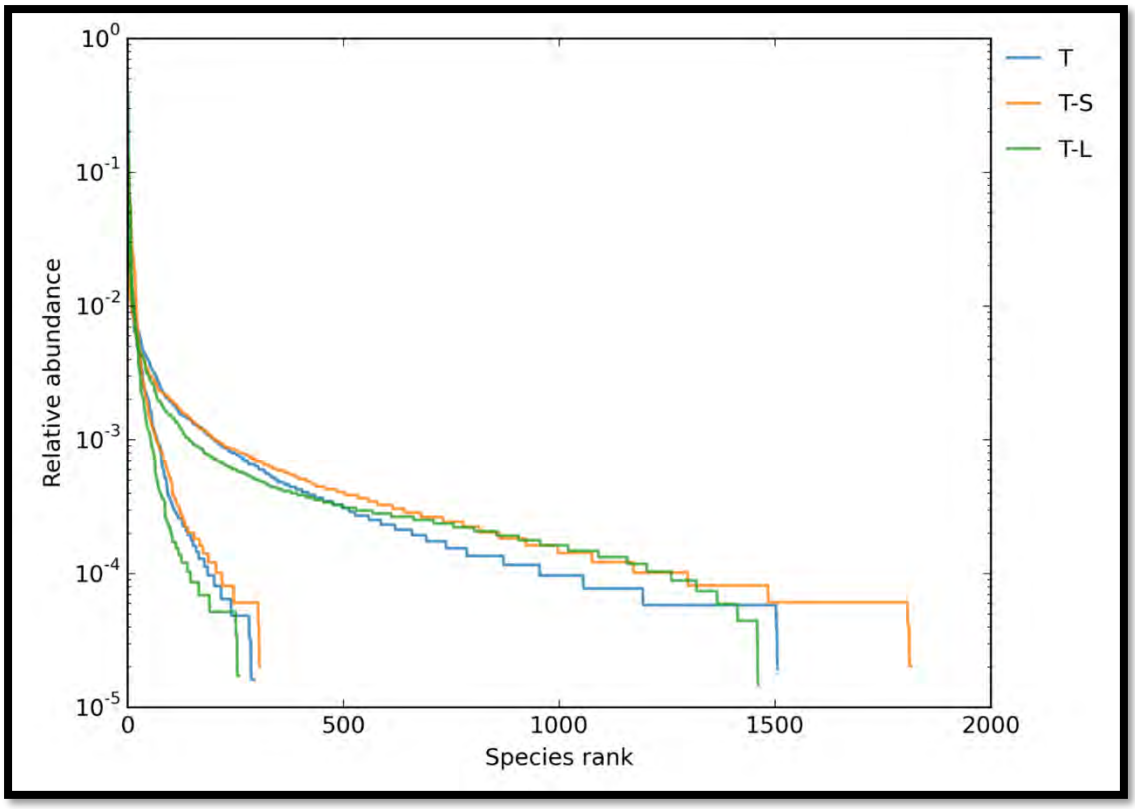

Figure 38: Rank abundance plot

Venn diagrams serve as effective visual aids for depicting relationships among sets of species, offering clarity on both shared characteristics and distinctions. These diagrams encompass fundamental components:

- Circles: Each circle signifies a set of species with shared characteristics, and can be appropriately labeled.
- Overlapping areas: The regions where circles intersect denote items that belong to both sets, showcasing shared characteristics.
- Non-overlapping areas: Sections where circles do not overlap represent items unique to each set, highlighting distinct characteristics.
- Numbers or labels within circles: These annotations may indicate the quantity of items or specific elements within each set and at their intersections.

The particular Venn diagram generated through pyrosequencing illustrates the distinct number of species in each sample and the common number of species shared between each sample, as well as collectively among the three samples (Xiao et al., 2015a). Notably, this specific Venn diagram reveals the presence of 57 species that are shared among samples T, T+L, and T+S.

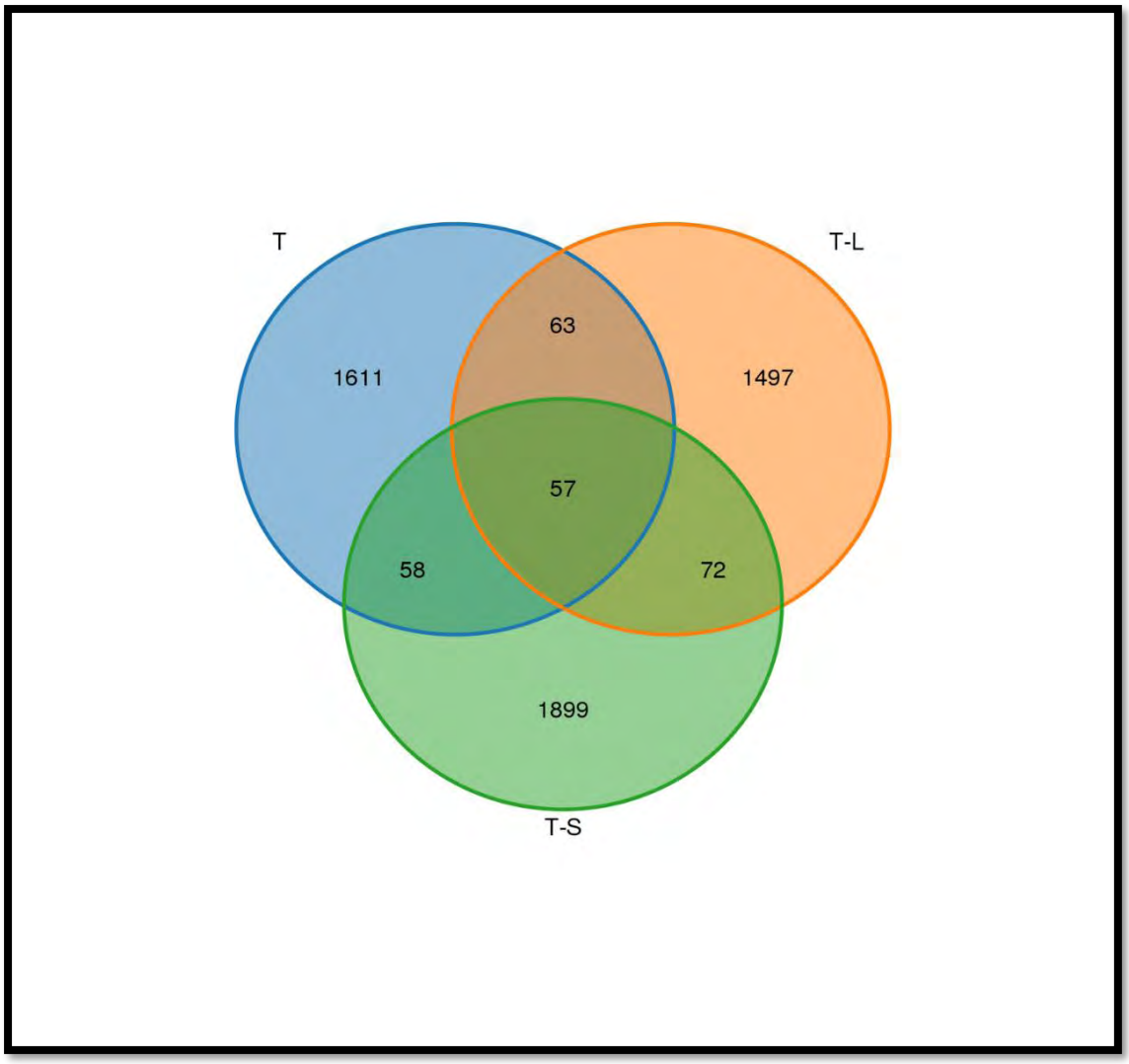

Figure 39: Venn diagram: Showing diverse distribution of species across samples

5. Discussion

The current global landscape necessitates alternative energy resources that not only safeguard the environment but also combat the proliferation of contaminants within natural components (Parthasarathy & Chellaram, 2014). Microbial Fuel Cells (MFCs) emerge as a dual-purpose solution, offering the dual benefits of energy generation through the enrichment of electrochemically active bacteria and the simultaneous degradation of hazardous pollutants (Kurniawan et al., 2022; Yaqoob, Khatoon, et al., 2020). Within the MFC framework, the anode's three-dimensional porous design facilitates the adhesion of bacteria, enabling their engagement in electrochemical processes (He et al., 2021; Mahmoud & El-Khatib, 2020). These bacteria, recognized as anode-respiring bacteria (ARBs), exhibit a remarkable capacity to respire and transfer electrons from organic substrates to solid electrodes (Banerjee et al., 2019; Huong Le et al., 2017). Electricigens, stemming from diverse sources such as textile soil, landfill soil, and anaerobic digester sludge, exhibit proficiency in organic matter degradation while yielding electric current (Leicester et al., 2023). To explore this potential, a trio of dual-chamber MFC reactors with bio-anodes were orchestrated, combining soil and sludge samples based on inoculum availability. To sustain robust biofilm development and consistent current flow, a synthetic medium was periodically introduced every 5 days. The experimental design included two successive enrichment stages, terminating in the cultivation of a biofilm harboring concentrated assembly of electricigens (Miceli et al., 2012).

This experiment to enrich a biofilm with the presence of electricigens was a success as a current greater than 1.5A/m^2 was observed in all cells with pure textile and mixed inocula (Moradian et al., 2021; Yee et al., 2020). Previously various experiments were conducted by using acetate and glucose as the carbon donors; hence this experiment was based on acetate as carbon donor and anode with voltage supply of -0.3V against reference electrode Ag/AgCl (Cao et al., 2019; Katuri et al., 2020a; Miceli et al., 2012). The inoculum was collected from a textile industry where its toxic dye effluents were contaminating the soil (Anuar et al., 2013a). Hence the bacteria present in the specific area were not extensively studied and have the potential to be studied further. These bacteria are capable of living under stress and anaerobic/facultative conditions by degrading the toxic dye effluent. Certainly, many organisms possess the ability to perform anode respiration (Pierra et al., 2015). This is a common way they conserve

energy, especially when dealing with metal oxide respiration in natural settings. In such environments, these metal oxides are often present as solid substances, like electrodes (Weber et al., 2006).

The overall electrochemical performance of the cells was great and the open circuit voltage (OCV) of all cells was approx.110mV within few hours of inoculum addition (Nguyen et al., 2019). This increase in voltage is indicative for the presence of electricigens and average maximum was 550mv in all cells during phase 1. The observation of the voltage in phase-2 was almost similar to the phase-1 showing the presence of electrogenic ARBs. The voltage output was stability in last 15days of enrichment in both phases, depicting a stabilized formation of ARB biofilm. The voltage showed an increasing trend after each media feed because of the renewing of available substrate to biofilm (Anuar et al., 2013b; Nguyen et al., 2019). Voltage happens to drop which indicted the consumption of carbon-based media and hence the fast-growing biofilm needed more substrate every few days (Oh & Logan, 2007). The nitrogen sparging every few days was used to prevent the aerobic digestion of substrate.

The resistance appears to have a direct relationship with the voltage; however, it has inverse relationship with the current, hence the current density decreases with the increase in resistance (JM et al., 2017). Similar pattern was observed in this experiment where with the increase of resistance the voltage output was also increased. The highest current densities in the biggening of enrichment of all cells were between 36m A/m^2 to 38m A/ m^2 which as the biofilm become old, gradually dropped to 10m A/m^2. After reaching 10A/m^2 the current and power density showed a linear behavior (Digitalcommons@uri et al., 2021; Lang et al., 2017; Mousavi Karimi & Davis, 2023). At the resistance between 390Ω-1100Ω a highest power density was observed. The cyclic voltammogram of cells showed the redox reaction taking place between ARBs and electrode (Boas et al., 2022; Fricke et al., 2008). The oxidation and reduction peaks during both enrichment phases increased with the increase of the biofilm stability and its ability to make donate electrons and utilize the substrate. However, as the biofilm became old the as slight decrease in the oxidation and reduction peaks can be observed on the last day of reactor reaction. The phase-2 of enrichment exhibited a rather narrow oxidation peaks and broad reduction peaks, indicating a more active reduction potential. These redox reactions depicted the biofilm contains bacteria that are electrochemically

active and have a greater potential to generate current output (Boas et al., 2022; Fricke et al., 2008).

The TDS and EC values were noted every five days and it showed an amazing trend collaborating with voltage and CV patterns. The phase-1 show a gradual increase in the TDS and EC until 6^{th}-8^{th} day where they hit their maximum values between 550-700ppm and 1000-1400µs/cm (Al-saned et al., 2021; Sikder & Rahman, 2023). After that a slight decrease was observed, indicating a normal substrate utilization pattern by bacteria (Bhatti et al., 2022; Lertngim et al., 2017). However, in the phase-2 of enrichment, as the biofilm was already matured and lack of inoculum, have indicative lower values as compared to phase-1. During the phase-1 the biofilm was actively forming, and metabolism rate was high, resulting in more utilization and degradation of substrate (Stefanova & Nikolova, 2018; Zhang et al., 2011). The patterns were confirmed by performing FTIR spectroscopy on the electrolyte samples indicating stretching and bending of various single, double, and triple bonds along with a peak in fingerprint area. The possible peaks between 3400-330cm^{-1} had C-C, C-H, N-H stretching, changing into alcohols, amines and carboxylic acids (Nandiyanto et al., 2019). Whereas the peaks around 1600 cm^{-1} have double bond alkenes and conjugated alkenes forming as functional compound. The fingerprint area shows the formation of alkenes, aromatic, and halo compounds (Munajad et al., 2018). The overall peaks are lower than the control peaks indicating bacterial degradation (Nandiyanto et al., 2019). All this data has conceded with the fact that carbon-based substrate was utilized, and various resulting compounds were formed (Nandiyanto et al., 2019).

Although biochemical test doesn't prove that any specific genus or specie identification, however, by considering the site of sample, the morphology, growth conditions and parameters, it can estimate the type of microbes living in sample. Hence the biochemical test provides with a possible identification (Muzzamal et al., 2012; Sujana et al., 2013). Majority of the dye and waste degrading microbes were Gram positive while testing the cell wall characteristics using gram staining. These bacteria were facultative in nature because they were able to grow under non-strict anaerobic conditions. Furthermore, out of 28 different isolated colonies only 5-6 were able to grow on MAC and EMB agar, which are selective and differential media for gram negatives and lactose fermenters. Some identified bacteria like *Geobacter sulferreducens, Desulfovivrio spp. Aerococcus spp. Klebsiella penumoniae, Shewanella*

spp., E. coli, Bacillus subtilis and *cereus* are some examples that are facultative, electrochemically active and live in places like soil and sludge (Ali et al., 2017; Inoue et al., 2011a; Niu et al., 2020).

Pyrosequencing identified both Gram-positive and Gram-negative bacterial genera within the anodic biofilm, confirming a higher prevalence of Gram-positive bacteria compared to conventional culturing methods, as reported in previous studies (Xiao et al., 2015b). The pyrosequencing results indicated presence of few families and genus that are commonly present in every biofilm (which was generated from different sample sources) i.e., *Enterobacteriaceae, Ochrobactrum, Azospira, Strentophomonas,* and *Rhodococcus*. Species of genus *Ochrobactrum* like *O. anthropi* and *O. intermedium* have shown promising performance in microbial fuel cells (MFCs) due to their ability to degrade various organic compounds and transfer electrons to the anode. Whereas species of genus *Azospira* are known for their ability to fix nitrogen and utilize various organic substrates and several *Rhodococcus* species, like *R. opacus* and *R. ruber,* are known for their versatility in degrading complex organic compounds and can generate current in MFCs (P. Cheng et al., 2018). Their ability to adapt to diverse environments and utilize various substrates makes them attractive for Bioelectrochemical applications.

6. Conclusion

In conclusion, this study successfully achieved enrichment of anode-respiring bacteria from soil contaminated with textile effluent using a Microbial Fuel Cell (MFC). Through meticulous experimentation and analysis, valuable insights were gained into the potential of these bacteria to play a crucial role in harnessing energy from pollutants in contaminated environments. The findings underscore the importance of understanding microbial interactions within MFCs, highlighting their potential applications in both environmental remediation and sustainable energy production.

- All the MFC were operated successfully with a significant voltage output and a cyclic voltammogram depicted the redox potential of electricigens.
- TDS, EC, and FTIR analysis confirmed that the carbon-based substrate was broken down and utilized by the metabolically and electrochemically active biofilm.
- The biochemical analysis also identified potential electricigens like *Geobacter sulferreducens* and *Desulfovivrio spp.* The biofilm contains majority of gram positive and limited gram-negative species.
- Identification of genus like *Azospira, Rhodococuss,* and *Ochrobactrum* through pyrosequencing indicted the presence of electrochemically active microorganisms capable of degrading organic compounds and generating voltage.

7. References

Ali, N., Anam, M., Yousaf, S., Maleeha, S., & Bangash, Z. (2017). Characterization of the Electric Current Generation Potential of the Pseudomonas aeruginosa Using Glucose, Fructose, and Sucrose in Double Chamber Microbial Fuel Cell. *Iranian Journal of Biotechnology*, *15*(4), 216–223. https://doi.org/10.15171/IJB.1608

Al-saned, A. J. O., Kitafa, B. A., & Badday, A. S. (2021). Microbial fuel cells (MFC) in the treatment of dairy wastewater. *IOP Conference Series: Materials Science and Engineering*, *1067*(1), 012073. https://doi.org/10.1088/1757-899x/1067/1/012073

Anam, M., Yousaf, S., Sharafat, I., Zafar, Z., Ayaz, K., & Ali, N. (2017). Comparing natural and artificially designed bacterial consortia as biosensing elements for rapid non- specific detection of organic pollutant through microbial fuel cell. *International Journal of Electrochemical Science*, *12*(4), 2836–2851. https://doi.org/10.20964/2017.04.49

Anuar, N., Suja, F., Syazana, N., Hisham, N., Md Zain, S., Jusoh, S., Ismail, A., Ezlin, N., & Basri, A. (2013a). Microbial fuel cells using different types of wastewater for electricity generation and simultaneously removed pollutant. In *CITATIONS Journal of Engineering Science and Technology* (Vol. 8, Issue 3). https://www.researchgate.net/publication/289559252

Anuar, N., Suja, F., Syazana, N., Hisham, N., Md Zain, S., Jusoh, S., Ismail, A., Ezlin, N., & Basri, A. (2013b). Microbial fuel cells using different types of wastewater for electricity generation and simultaneously removed pollutant. In *CITATIONS Journal of Engineering Science and Technology* (Vol. 8, Issue 3). https://www.researchgate.net/publication/289559252

Baicha, Z., Salar-García, M. J., Ortiz-Martínez, V. M., Hernández-Fernández, F. J., de los Ríos, A. P., Labjar, N., Lotfi, E., & Elmahi, M. (2016). A critical review on microalgae as an alternative source for bioenergy production: A promising low cost substrate for microbial fuel cells. *Fuel Processing Technology*, *154*, 104–116. https://doi.org/10.1016/J.FUPROC.2016.08.017

Banerjee, R., Bevilacqua, N., Mohseninia, A., Wiedemann, B., Wilhelm, F., Scholta, J., & Zeis, R. (2019). Carbon felt electrodes for redox flow battery: Impact of

compression on transport properties. *Journal of Energy Storage*, *26*. https://doi.org/10.1016/j.est.2019.100997

Bazina, N., Ahmed, T. G., Almdaaf, M., Jibia, S., & Sarker, M. (2023). Power generation from wastewater using microbial fuel cells: A review. *Journal of Biotechnology*, *374*, 17–30. https://doi.org/10.1016/J.JBIOTEC.2023.07.006

Bhargavi, G., Venu, V., & Renganathan, S. (2018). Microbial fuel cells: Recent developments in design and materials. *IOP Conference Series: Materials Science and Engineering*, *330*(1). https://doi.org/10.1088/1757-899X/330/1/012034

Bhatti, Z. A., Syed, M., Maqbool, F., Zhao, Y. G., Ying, X., Siddiqui, M. F., & Mahmood, Q. (2022). Potential of molasses substrate for bioelectricity production in microbial fuel cell with the help of active microbial community. *International Journal of Energy Research*, *46*(8), 11185–11199. https://doi.org/10.1002/er.7919

Boas, J. V., Peixoto, L., Oliveira, V. B., Simões, M., & Pinto, A. M. F. R. (2022). Cyclic voltammetry study of a yeast-based microbial fuel cell. *Bioresource Technology Reports*, *17*. https://doi.org/10.1016/j.biteb.2022.100974

Busalmen, J. P., Esteve-Nuñez, A., & Feliu, J. M. (2008). Whole cell electrochemistry of electricity-producing microorganisms evidence an adaptation for optimal exocellular electron transport. *Environmental Science and Technology*, *42*(7), 2445–2450. https://doi.org/10.1021/es702569y

Cabrera, J., Dai, Y., Irfan, M., Li, Y., Gallo, F., Zhang, P., Zong, Y., & Liu, X. (2022). Novel continuous up-flow MFC for treatment of produced water: Flow rate effect, microbial community, and flow simulation. *Chemosphere*, *289*. https://doi.org/10.1016/j.chemosphere.2021.133186

Cao, Y., Mu, H., Liu, W., Zhang, R., Guo, J., Xian, M., & Liu, H. (2019). Electricigens in the anode of microbial fuel cells: Pure cultures versus mixed communities. In *Microbial Cell Factories* (Vol. 18, Issue 1). BioMed Central Ltd. https://doi.org/10.1186/s12934-019-1087-z

Carmona-Martínez, A. A., Harnisch, F., Kuhlicke, U., Neu, T. R., & Schröder, U. (2013a). Electron transfer and biofilm formation of Shewanella putrefaciens as

function of anode potential. *Bioelectrochemistry*, *93*, 23–29. https://doi.org/10.1016/j.bioelechem.2012.05.002

Carmona-Martínez, A. A., Harnisch, F., Kuhlicke, U., Neu, T. R., & Schröder, U. (2013b). Electron transfer and biofilm formation of Shewanella putrefaciens as function of anode potential. *Bioelectrochemistry*, *93*, 23–29. https://doi.org/10.1016/j.bioelechem.2012.05.002

Chae, K. J., Choi, M. J., Lee, J. W., Kim, K. Y., & Kim, I. S. (2009a). Effect of different substrates on the performance, bacterial diversity, and bacterial viability in microbial fuel cells. *Bioresource Technology*, *100*(14), 3518–3525. https://doi.org/10.1016/j.biortech.2009.02.065

Chae, K. J., Choi, M. J., Lee, J. W., Kim, K. Y., & Kim, I. S. (2009b). Effect of different substrates on the performance, bacterial diversity, and bacterial viability in microbial fuel cells. *Bioresource Technology*, *100*(14), 3518–3525. https://doi.org/10.1016/j.biortech.2009.02.065

Chatterjee, P., Dessì, P., Kokko, M., Lakaniemi, A.-M., & Lens, P. (2019). *Selective enrichment of biocatalysts for bioelectrochemical systems: A critical review*. https://www.sciencedirect.com/science/article/pii/S1364032119302242

Chaturvedi, V., & Verma, P. (2016). Microbial fuel cell: a green approach for the utilization of waste for the generation of bioelectricity. *Bioprocess*, *3*, 38. https://doi.org/10.1186/s40643-016-0116-6

Chen, L., Zhang, P., Shang, W., Zhang, H., Li, Y., Zhang, W., Zhang, Z., & Liu, F. (2018). Enrichment culture of electroactive microorganisms with high magnetic susceptibility enhances the performance of microbial fuel cells. *Bioelectrochemistry*, *121*, 65–73. https://doi.org/10.1016/j.bioelechem.2018.01.005

Cheng, P., Shan, R., Yuan, H. R., Deng, L. fang, & Chen, Y. (2018). Enhanced Rhodococcus pyridinivorans HR-1 anode performance by adding trehalose lipid in microbial fuel cell. *Bioresource Technology*, *267*, 774–777. https://doi.org/10.1016/J.BIORTECH.2018.08.006

References

Cheng, S., Xing, D., & Logan, B. E. (2011). Electricity generation of single-chamber microbial fuel cells at low temperatures. *Biosensors and Bioelectronics*, *26*, 1913–1917. https://doi.org/10.1016/j.bios.2010.05.016

De Schamphelaire, L., Van Den Bossche, L., Hai, S. D., Höfte, M., Boon, N., Rabaey, K., & Verstraete, W. (2008). Microbial fuel cells generating electricity from rhizodeposits of rice plants. *Environmental Science and Technology*, *42*(8), 3053–3058. https://doi.org/10.1021/es071938w

Dessì, P., Porca, E., Haavisto, J., Lakaniemi, A. M., Collins, G., & Lens, P. N. L. (2018). Composition and role of the attached and planktonic microbial communities in mesophilic and thermophilic xylose-fed microbial fuel cells. *RSC Advances*, *8*(6), 3069–3080. https://doi.org/10.1039/c7ra12316g

Digitalcommons@uri, D., Müller, G., & Coyne, R. (2021). *5. Electric current and current density. Resistivity, resistance, and 15. Electric current and current density. Resistivity, resistance, and resistor resistor*. https://digitalcommons.uri.edu/phy204-lecturenotes/15

El-Khatib, K. M., Mohamed Hazaa, M., Hassan, R. Y., Khater, D., El-khatib, K., Hazaa, M., & A Hassan, R. Y. (2015). Activated Sludge-based Microbial Fuel Cell for Bio-electricity Generation. *Journal of Basic and Environmental Sciences*, *2*, 63–73. https://www.researchgate.net/publication/303913568

Fakhirruddin, F., Amid, A., Wan Salim, W. W. A., & Azmi, A. S. (2018a). Electricity Generation in Microbial Fuel Cell (MFC) by Bacterium Isolated from Rice Paddy Field Soil. *E3S Web of Conferences*, *34*. https://doi.org/10.1051/e3sconf/20183402036

Fakhirruddin, F., Amid, A., Wan Salim, W. W. A., & Azmi, A. S. (2018b). Electricity Generation in Microbial Fuel Cell (MFC) by Bacterium Isolated from Rice Paddy Field Soil. *E3S Web of Conferences*, *34*. https://doi.org/10.1051/e3sconf/20183402036

Fan, L., & Xue, S. (2016). Overview on Electricigens for Microbial Fuel Cell. *The Open Biotechnology Journal*, *10*(1), 398–406. https://doi.org/10.2174/1874070701610010398

References

Flimban, S. G. A., Ismail, I. M. I., Kim, T., & Oh, S. E. (2019). Overview of recent advancements in the microbial fuel cell from fundamentals to applications: Design, major elements, and scalability. In *Energies* (Vol. 12, Issue 17). MDPI AG. https://doi.org/10.3390/en12173390

Fricke, K., Harnisch, F., & Schröder, U. (2008). On the use of cyclic voltammetry for the study of anodic electron transfer in microbial fuel cells. *Energy and Environmental Science*, *1*(1), 144–147. https://doi.org/10.1039/b802363h

Haavisto, J. M., Lakaniemi, A. M., & Puhakka, J. A. (2019). Storing of exoelectrogenic anolyte for efficient microbial fuel cell recovery. *Environmental Technology (United Kingdom)*, *40*(11), 1467–1475. https://doi.org/10.1080/09593330.2017.1423395

Haddadi, S., Nabi-Bidhendi, G. R., & Mehrdadi, N. (2014). Evaluation of inoculation method and limiting conditions on bacterial activity in microbial electrochemical cells. *Journal of Environmental Chemical Engineering*, *2*(1), 612–618. https://doi.org/10.1016/j.jece.2013.10.018

Hassan, S. H. A., Kim, Y. S., & Oh, S. E. (2012). Power generation from cellulose using mixed and pure cultures of cellulose-degrading bacteria in a microbial fuel cell. *Enzyme and Microbial Technology*, *51*(5), 269–273. https://doi.org/10.1016/j.enzmictec.2012.07.008

He, Y., Yang, J., Fu, Q., Li, J., Zhang, L., Zhu, X., & Liao, Q. (2021). Structure design of 3D hierarchical porous anode for high performance microbial fuel cells: From macro-to micro-scale. *Journal of Power Sources*, *516*. https://doi.org/10.1016/j.jpowsour.2021.230687

Heidrich, E. S., Dolfing, J., Wade, M. J., Sloan, W. T., Quince, C., & Curtis, T. P. (2018). Temperature, inocula and substrate: Contrasting electroactive consortia, diversity and performance in microbial fuel cells. *Bioelectrochemistry*, *119*, 43–50. https://doi.org/10.1016/j.bioelechem.2017.07.006

Hidayat, A. R. P., Widyanto, A. R., Asranudin, A., Ediati, R., Sulistiono, D. O., Putro, H. S., Sugiarso, D., Prasetyoko, D., Purnomo, A. S., Bahruji, H., Ali, B. T. I., & Caralin, I. S. (2022). Recent development of double chamber microbial fuel cell for hexavalent chromium waste removal. In *Journal of Environmental Chemical*

Engineering (Vol. 10, Issue 3). Elsevier Ltd. https://doi.org/10.1016/j.jece.2022.107505

Holmes, D. E., Bond, D. R., O'Neil, R. A., Reimers, C. E., Tender, L. R., & Lovley, D. R. (2004). Microbial communities associated with electrodes harvesting electricity from a variety of aquatic sediments. *Microbial Ecology*, *48*(2), 178–190. https://doi.org/10.1007/s00248-003-0004-4

Huong Le, T. X., Bechelany, M., & Cretin, M. (2017). Carbon felt based-electrodes for energy and environmental applications: A review. In *Carbon* (Vol. 122, pp. 564–591). Elsevier Ltd. https://doi.org/10.1016/j.carbon.2017.06.078

Imran, M., Prakash, O., Pushkar, P., Mungray, A., Kailasa, S. K., Chongdar, S., & Mungray, A. K. (2019). Performance enhancement of benthic microbial fuel cell by cerium coated electrodes. *Electrochimica Acta*, *295*, 58–66. https://doi.org/10.1016/j.electacta.2018.08.158

Inoue, K., Leang, C., Franks, A. E., Woodard, T. L., Nevin, K. P., & Lovley, D. R. (2011a). Specific localization of the c-type cytochrome OmcZ at the anode surface in current-producing biofilms of Geobacter sulfurreducens. *Environmental Microbiology Reports*, *3*(2), 211–217. https://doi.org/10.1111/j.1758-2229.2010.00210.x

Inoue, K., Leang, C., Franks, A. E., Woodard, T. L., Nevin, K. P., & Lovley, D. R. (2011b). Specific localization of the c-type cytochrome OmcZ at the anode surface in current-producing biofilms of Geobacter sulfurreducens. *Environmental Microbiology Reports*, *3*(2), 211–217. https://doi.org/10.1111/J.1758-2229.2010.00210.X

Jana, A., Sarathi, P., & Madhao, M. (2018). *Title Comparison of performance of an earthen plate and nafion as membrane separators in dual chamber microbial fuel cells*. http://hdl.handle.net/10379/14973

Javed, M. M., Nisar, M. A., Ahmad, M. U., Yasmeen, N., & Zahoor, S. (2018). Microbial fuel cells as an alternative energy source: current status. *Biotechnology & Genetic Engineering Reviews*, *34*(2), 216–242. https://doi.org/10.1080/02648725.2018.1482108

References

Jeremiasse, A. W., Hamelers, H. V. M., Croese, E., & Buisman, C. J. N. (2012). Acetate enhances startup of a H 2-producing microbial biocathode. *Biotechnology and Bioengineering*, *109*(3), 657–664. https://doi.org/10.1002/bit.24338

Jiang, Y. J., Hui, S., Tian, S., Chen, Z., Chai, Y., Jiang, L. P., Zhang, J. R., & Zhu, J. J. (2022). Enhanced transmembrane electron transfer in Shewanella oneidensis MR-1 using gold nanoparticles for high-performance microbial fuel cells. *Nanoscale Advances*, *5*(1), 124–132. https://doi.org/10.1039/d2na00638c

Jiang, Y., Xu, Y., Yang, Q., Chen, Y., Zhu, S., & Shen, S. (2014). Power generation using polyaniline/multi-walled carbon nanotubes as an alternative cathode catalyst in microbial fuel cells. *International Journal of Energy Research*, *38*(11), 1416–1423. https://doi.org/10.1002/er.3155

JM, K., DN, M., JM, M., FB, M., & GN, K. (2017). Microbial Fuel Cells: Influence of External Resistors on Power, Current and Power Density. *Journal of Thermodynamics & Catalysis*, *08*(01). https://doi.org/10.4172/2157-7544.1000182

Jothinathan, D., & Wilson, R. T. (2017). Comparative analysis of power production of pure, coculture, and mixed culture in a microbial fuel cell. *Energy Sources, Part A: Recovery, Utilization and Environmental Effects*, *39*(5), 520–527. https://doi.org/10.1080/15567036.2016.1233306

Katuri, K. P., Kamireddy, S., Kavanagh, P., Muhammad, A., Conghaile, P., Kumar, A., Saikaly, P. E., & Leech, D. (2020a). Electroactive biofilms on surface functionalized anodes: The anode respiring behavior of a novel electroactive bacterium, Desulfuromonas acetexigens. *Water Research*, *185*. https://doi.org/10.1016/j.watres.2020.116284

Katuri, K. P., Kamireddy, S., Kavanagh, P., Muhammad, A., Conghaile, P., Kumar, A., Saikaly, P. E., & Leech, D. (2020b). Electroactive biofilms on surface functionalized anodes: The anode respiring behavior of a novel electroactive bacterium, Desulfuromonas acetexigens. *Water Research*, *185*. https://doi.org/10.1016/j.watres.2020.116284

Khater, D. Z., El-Khatib, K. M., & Hassan, H. M. (2017a). Microbial diversity structure in acetate single chamber microbial fuel cell for electricity generation. *Journal of*

References

Genetic Engineering and Biotechnology, *15*(1), 127–137. https://doi.org/10.1016/j.jgeb.2017.01.008

Khater, D. Z., El-Khatib, K. M., & Hassan, H. M. (2017b). Microbial diversity structure in acetate single chamber microbial fuel cell for electricity generation. *Journal of Genetic Engineering and Biotechnology*, *15*(1), 127–137. https://doi.org/10.1016/j.jgeb.2017.01.008

Kim, G. T., Webster, G., Wimpenny, J. W. T., Kim, B. H., Kim, H. J., & Weightman, A. J. (2006a). Bacterial community structure, compartmentalization and activity in a microbial fuel cell. *Journal of Applied Microbiology*, *101*(3), 698–710. https://doi.org/10.1111/j.1365-2672.2006.02923.x

Kim, G. T., Webster, G., Wimpenny, J. W. T., Kim, B. H., Kim, H. J., & Weightman, A. J. (2006b). Bacterial community structure, compartmentalization and activity in a microbial fuel cell. *Journal of Applied Microbiology*, *101*(3), 698–710. https://doi.org/10.1111/j.1365-2672.2006.02923.x

Kim, J. R., Jung, S. H., Regan, J. M., & Logan, B. E. (2007). Electricity generation and microbial community analysis of alcohol powered microbial fuel cells. *Bioresource Technology*, *98*(13), 2568–2577. https://doi.org/10.1016/j.biortech.2006.09.036

Kumar, R., Singh, L., & Zularisam, A. W. (2017). Microbial fuel cells: Types and applications. In *Waste Biomass Management - A Holistic Approach* (pp. 367–384). Springer International Publishing. https://doi.org/10.1007/978-3-319-49595-8_16

Kurniawan, T. A., Othman, M. H. D., Liang, X., Ayub, M., Goh, H. H., Kusworo, T. D., Mohyuddin, A., & Chew, K. W. (2022). Microbial Fuel Cells (MFC): A Potential Game-Changer in Renewable Energy Development. In *Sustainability (Switzerland)* (Vol. 14, Issue 24). MDPI. https://doi.org/10.3390/su142416847

Lahiri, D., Nag, M., Ghosh, S., Dey, A., & Ray, R. R. (2022). Electroactive biofilm and electron transfer in MES. *Scaling Up of Microbial Electrochemical Systems: From Reality to Scalability*, 87–101. https://doi.org/10.1016/B978-0-323-90765-1.00006-X

References

Lang, M., Bohn, C., Henke, M., Schiller, G., Willich, C., & Hauler, F. (2017). Understanding the Current-Voltage Behavior of High Temperature Solid Oxide Fuel Cell Stacks. *Journal of The Electrochemical Society*, *164*(13), F1460–F1470. https://doi.org/10.1149/2.1541713jes

Lee, J., Phung, N. T., Chang, I. S., Kim, B. H., & Sung, H. C. (2003a). Use of acetate for enrichment of electrochemically active microorganisms and their 16S rDNA analyses. *FEMS Microbiology Letters*, *223*(2), 185–191. https://doi.org/10.1016/S0378-1097(03)00356-2

Lee, J., Phung, N. T., Chang, I. S., Kim, B. H., & Sung, H. C. (2003b). Use of acetate for enrichment of electrochemically active microorganisms and their 16S rDNA analyses. *FEMS Microbiology Letters*, *223*(2), 185–191. https://doi.org/10.1016/S0378-1097(03)00356-2

Leicester, D. D., Settle, S., McCann, C. M., & Heidrich, E. S. (2023). Investigating Variability in Microbial Fuel Cells. *Applied and Environmental Microbiology*, *89*(3). https://doi.org/10.1128/aem.02181-22

Lertngim, A., Phiriyawirut, M., Wootthikanokkhan, J., Yuwawech, K., Sangkhun, W., Kumnorkaew, P., & Muangnapoh, T. (2017). Preparation of surlyn films reinforced with cellulose nanofibres and feasibility of applying the transparent composite films for organic photovoltaic encapsulation. *Royal Society Open Science*, *4*(10). https://doi.org/10.1098/rsos.170792

Li, X., Chen, S., Angelidaki, I., & Zhang, Y. (2018). Bio-electro-Fenton processes for wastewater treatment: Advances and prospects. In *Chemical Engineering Journal* (Vol. 354, pp. 492–506). Elsevier B.V. https://doi.org/10.1016/j.cej.2018.08.052

Liu, G., Yates, M. D., Cheng, S., Call, D. F., Sun, D., & Logan, B. E. (2011). Examination of microbial fuel cell start-up times with domestic wastewater and additional amendments. *Bioresource Technology*, *102*(15), 7301–7306. https://doi.org/10.1016/j.biortech.2011.04.087

Liu, L., Tsyganova, O., Lee, D. J., Chang, J. S., Wang, A., & Ren, N. (2013). Double-chamber microbial fuel cells started up under room and low temperatures. *International Journal of Hydrogen Energy*, *38*(35), 15574–15579. https://doi.org/10.1016/j.ijhydene.2013.02.090

References

Liu, L., Tsyganova, O., Lee, D. J., Su, A., Chang, J. S., Wang, A., & Ren, N. (2012). Anodic biofilm in single-chamber microbial fuel cells cultivated under different temperatures. *International Journal of Hydrogen Energy*, *37*(20), 15792–15800. https://doi.org/10.1016/J.IJHYDENE.2012.03.084

Liu, Y., Harnisch, F., Fricke, K., Sietmann, R., & Schröder, U. (2008). Improvement of the anodic bioelectrocatalytic activity of mixed culture biofilms by a simple consecutive electrochemical selection procedure. *Biosensors and Bioelectronics*, *24*(4), 1006–1011. https://doi.org/10.1016/j.bios.2008.08.001

López Zavala, M. Á., Peña, O. I. G., Ruelas, H. C., Mena, C. D., & Guizani, M. (2019). Use of cyclic voltammetry to describe the electrochemical behavior of a dual-chamber microbial fuel cell. *Energies*, *12*(18). https://doi.org/10.3390/en12183532

Madjarov, J., Prokhorova, A., Messinger, T., Gescher, J., & Kerzenmacher, S. (2016). The performance of microbial anodes in municipal wastewater: Pre-grown multispecies biofilm vs. natural inocula. *Bioresource Technology*, *221*, 165–171. https://doi.org/10.1016/j.biortech.2016.09.004

Mahmoud, M., & El-Khatib, K. M. (2020). Three-dimensional graphitic mesoporous carbon-doped carbon felt bioanodes enables high electric current production in microbial fuel cells. *International Journal of Hydrogen Energy*, *45*(56), 32413–32422. https://doi.org/10.1016/j.ijhydene.2020.08.207

Malik, S., Kishore, S., Dhasmana, A., Kumari, P., Mitra, T., Chaudhary, V., Kumari, R., Bora, J., Ranjan, A., Minkina, T., & Rajput, V. D. (2023). A Perspective Review on Microbial Fuel Cells in Treatment and Product Recovery from Wastewater. In *Water (Switzerland)* (Vol. 15, Issue 2). MDPI. https://doi.org/10.3390/w15020316

Miceli, J. F., Parameswaran, P., Kang, D. W., Krajmalnik-Brown, R., & Torres, C. I. (2012). Enrichment and analysis of anode-respiring bacteria from diverse anaerobic inocula. *Environmental Science and Technology*, *46*(18), 10349–10355. https://doi.org/10.1021/es301902h

Michie, I. S., Kim, J. R., Dinsdale, R. M., Guwy, A. J., & Premier, G. C. (2013). Factors affecting microbial fuel cell acclimation and operation in temperate climates.

References

Water Science and Technology, *67*(11), 2568–2575. https://doi.org/10.2166/WST.2013.159

Min O, B. A., & Benito Román Irini Angelidaki, scar A. (2008). *Importance of temperature and anodic medium composition on microbial fuel cell (MFC) performance*. https://doi.org/10.1007/s10529-008-9687-4

Mohd Yusoff, M. Z., Hu, A., Feng, C., Maeda, T., Shirai, Y., Hassan, M. A., & Yu, C. P. (2013a). Influence of pretreated activated sludge for electricity generation in microbial fuel cell application. *Bioresource Technology*, *145*, 90–96. https://doi.org/10.1016/j.biortech.2013.03.003

Mohd Yusoff, M. Z., Hu, A., Feng, C., Maeda, T., Shirai, Y., Hassan, M. A., & Yu, C. P. (2013b). Influence of pretreated activated sludge for electricity generation in microbial fuel cell application. *Bioresource Technology*, *145*, 90–96. https://doi.org/10.1016/j.biortech.2013.03.003

Moqsud, M. A., Omine, K., Yasufuku, N., Hyodo, M., & Nakata, Y. (2013). *Microbial fuel cell (MFC) for bioelectricity generation from organic wastes*. https://doi.org/10.1016/j.wasman.2013.07.026

Moradian, J. M., Fang, Z., & Yong, Y. C. (2021). Recent advances on biomass-fueled microbial fuel cell. In *Bioresources and Bioprocessing* (Vol. 8, Issue 1). Springer Science and Business Media Deutschland GmbH. https://doi.org/10.1186/s40643-021-00365-7

Mousavi Karimi, Z., & Davis, J. A. (2023). *Current Density-Voltage (J-V) Characterization of Monolithic Nanolaminate Capacitors*. 54. https://doi.org/10.3390/iocn2023-14590

Munajad, A., Subroto, C., & Suwarno. (2018). Fourier transform infrared (FTIR) spectroscopy analysis of transformer paper in mineral oil-paper composite insulation under accelerated thermal aging. *Energies*, *11*(2). https://doi.org/10.3390/en11020364

Muzzamal, H., Sarwar, R., Sajid, I., & Hasnain, S. (2012). Isolation, Identification and Screening of Endophytic Bacteria Antagonistic to Biofilm Formers. In *Pakistan J. Zool* (Vol. 44, Issue 1). http://www.ncbi.nlm.nih.gov

References

Naik, S., & Jujjavarappu, S. E. (2020). Simultaneous bioelectricity generation from cost-effective MFC and water treatment using various wastewater samples. *Environmental Science and Pollution Research*, *27*(22), 27383–27393. https://doi.org/10.1007/S11356-019-06221-8/FIGURES/5

Nandiyanto, A. B. D., Oktiani, R., & Ragadhita, R. (2019). How to read and interpret ftir spectroscope of organic material. *Indonesian Journal of Science and Technology*, *4*(1), 97–118. https://doi.org/10.17509/ijost.v4i1.15806

Naseer, M. N., Zaidi, A. A., Khan, H., Kumar, S., Owais, M. T. bin, Jaafar, J., Suhaimin, N. S., Wahab, Y. A., Dutta, K., Asif, M., Hatta, S. F. W. M., & Uzair, M. (2021). Mapping the field of microbial fuel cell: A quantitative literature review (1970–2020). *Energy Reports*, *7*, 4126–4138. https://doi.org/10.1016/j.egyr.2021.06.082

Nasrabadi, A. M., & Moghimi, M. (2022). 4E analysis of stacked microbial fuel cell as a component in power plants for power generation and water treatment; with a cost-benefit perspective. *Sustainable Energy Technologies and Assessments*, *53*. https://doi.org/10.1016/j.seta.2022.102742

Nevin, K. P., Richter, H., Covalla, S. F., Johnson, J. P., Woodard, T. L., Orloff, A. L., Jia, H., Zhang, M., & Lovley, D. R. (2008). Power output and columbic efficiencies from biofilms of Geobacter sulfurreducens comparable to mixed community microbial fuel cells. *Environmental Microbiology*, *10*(10), 2505–2514. https://doi.org/10.1111/j.1462-2920.2008.01675.x

Nguyen, C. L., Tartakovsky, B., & Woodward, L. (2019). Harvesting Energy from Multiple Microbial Fuel Cells with a High-Conversion Efficiency Power Management System. *ACS Omega*, *4*(21), 18978–18986. https://doi.org/10.1021/acsomega.9b01854

Niu, Y., Yuan, L., Wang, R., Meng, Y., & Liu, M. (2020). Mechanism of electricigenic respiration mediated by electron transfer mediator of Klebsiella oxytoca d7. *Electrochimica Acta*, *353*. https://doi.org/10.1016/j.electacta.2020.136571

Obileke, K. C., Onyeaka, H., Meyer, E. L., & Nwokolo, N. (2021). Microbial fuel cells, a renewable energy technology for bio-electricity generation: A mini-review. *Electrochemistry Communications*, *125*, 107003. https://doi.org/10.1016/J.ELECOM.2021.107003

References

Obileke, K., Onyeaka, H., Meyer, E. L., & Nwokolo, N. (2021). NC-ND license Mini Review Microbial fuel cells, a renewable energy technology for bio-electricity generation: A mini-review. *Electrochemistry Communications*, *125*, 107003. https://doi.org/10.1016/j.elecom.2021.107003

Oh, S. E., & Logan, B. E. (2007). Voltage reversal during microbial fuel cell stack operation. *Journal of Power Sources*, *167*(1), 11–17. https://doi.org/10.1016/j.jpowsour.2007.02.016

Oliveira, V. B., Simões, M., Melo, L. F., & Pinto, A. M. F. R. (2013). Overview on the developments of microbial fuel cells. In *Biochemical Engineering Journal* (Vol. 73, pp. 53–64). https://doi.org/10.1016/j.bej.2013.01.012

Parthasarathy, V., & Chellaram, C. (2014). Microbial fuel cells as an alternate strategy for sustainable energy generation. *Biosciences Biotechnology Research Asia*, *11*(1), 249–252. https://doi.org/10.13005/bbra/1262

Patil, S. A., Harnisch, F., Kapadnis, B., & Schröder, U. (2010). Electroactive mixed culture biofilms in microbial bioelectrochemical systems: The role of temperature for biofilm formation and performance. *Biosensors and Bioelectronics*, *26*(2), 803–808. https://doi.org/10.1016/j.bios.2010.06.019

Phung, N. T., Lee, J., Kang, K. H., Chang, I. S., Gadd, G. M., & Kim, B. H. (2004). Analysis of microbial diversity in oligotrophic microbial fuel cells using 16S rDNA sequences. *FEMS Microbiology Letters*, *233*(1), 77–82. https://doi.org/10.1016/j.femsle.2004.01.041

Pierra, M., Carmona-Martínez, A. A., Trably, E., Godon, J. J., & Bernet, N. (2015). Microbial characterization of anode-respiring bacteria within biofilms developed from cultures previously enriched in dissimilatory metal-reducing bacteria. *Bioresource Technology*, *195*, 283–287. https://doi.org/10.1016/j.biortech.2015.07.010

Rabaey, K., Boon, N., Siciliano, S. D., Verhaege, M., & Verstraete, W. (2004a). Biofuel cells select for microbial consortia that self-mediate electron transfer. *Applied and Environmental Microbiology*, *70*(9), 5373–5382. https://doi.org/10.1128/AEM.70.9.5373-5382.2004

References

Rabaey, K., Boon, N., Siciliano, S. D., Verhaege, M., & Verstraete, W. (2004b). Biofuel cells select for microbial consortia that self-mediate electron transfer. *Applied and Environmental Microbiology*, *70*(9), 5373–5382. https://doi.org/10.1128/AEM.70.9.5373-5382.2004

Rajesh, S., & Kumawat, A. S. (2023). Opportunities for microbial fuel cells to utilize post-harvest agricultural residues. *Ionics*. https://doi.org/10.1007/s11581-023-05175-9

Ramirez-Nava, J., Martínez-Castrejón, M., García-Mesino, R. L., López-Díaz, J. A., Talavera-Mendoza, O., Sarmiento-Villagrana, A., Rojano, F., & Hernández-Flores, G. (2021). The implications of membranes used as separators in microbial fuel cells. In *Membranes* (Vol. 11, Issue 10). MDPI. https://doi.org/10.3390/membranes11100738

Ren, Y., Chen, J., Li, X., Yang, N., & Wang, X. (2017). *Enhanced bioelectricity generation of air-cathode buffer-free microbial fuel cells through short-term anolyte pH adjustment*. https://doi.org/10.1016/j.bioelechem.2017.12.007

Ren, Y., Chen, J., Li, X., Yang, N., & Wang, X. (2018). Enhanced bioelectricity generation of air-cathode buffer-free microbial fuel cells through short-term anolyte pH adjustment. *Bioelectrochemistry*, *120*, 145–149. https://doi.org/10.1016/j.bioelechem.2017.12.007

Roy, H., Rahman, T. U., Tasnim, N., Arju, J., Rafid, M. M., Islam, M. R., Pervez, M. N., Cai, Y., Naddeo, V., & Islam, M. S. (2023). Microbial Fuel Cell Construction Features and Application for Sustainable Wastewater Treatment. *Membranes*, *13*(5). https://doi.org/10.3390/MEMBRANES13050490/S1

Samuel, A. A. (n.d.). □□□□□□□□□□ □□□□ □□□□□□□□ □□□□□ □□□□□□□□ □□□□□□□ □□□□□ □□□□□ □□□□□□□□ □□ □□□□□□□□□ □□□□ □□□□□□□□□ □□□ □ □ □-□□□□□ □□□□ □□□□ □□□□ □□ *Energy Models for* □□□□ □□□□ □□□□ □□□□ □□□□ □□□□□ *.Renewable Energy Utilization and To Replace fossil fuels*

Santoro, C., Arbizzani, C., Erable, B., & Ieropoulos, I. (2017). Microbial fuel cells: From fundamentals to applications. A review. *Journal of Power Sources*, *356*, 225–244. https://doi.org/10.1016/j.jpowsour.2017.03.109

References

Santoro, C., Kodali, M., Herrera, S., Serov, A., Ieropoulos, I., & Atanassov, P. (2018). Power generation in microbial fuel cells using platinum group metal-free cathode catalyst: Effect of the catalyst loading on performance and costs. *Journal of Power Sources*, *378*, 169–175. https://doi.org/10.1016/j.jpowsour.2017.12.017

Sato, C., Paucar, N. E., Chiu, S., Mahmud, M. Z. I. M., & Dudgeon, J. (2021). Single-chamber microbial fuel cell with multiple plates of bamboo charcoal anode: Performance evaluation. *Processes*, *9*(12). https://doi.org/10.3390/pr9122194

Shrestha, N., Chilkoor, G., Vemuri, B., Rathinam, N., Sani, R. K., & Gadhamshetty, V. (2018). Extremophiles for microbial-electrochemistry applications: A critical review. *Bioresource Technology*, *255*, 318–330. https://doi.org/10.1016/J.BIORTECH.2018.01.151

Sikder, S., & Rahman, M. M. (2023). Efficiency of microbial fuel cell in wastewater (municipal, textile and tannery) treatment and bioelectricity production. *Case Studies in Chemical and Environmental Engineering*, *8*. https://doi.org/10.1016/j.cscee.2023.100421

Singh, S., Bairagi, P. K., & Verma, N. (2018). Candle soot-derived carbon nanoparticles: An inexpensive and efficient electrode for microbial fuel cells. *Electrochimica Acta*, *264*, 119–127. https://doi.org/10.1016/j.electacta.2018.01.110

Stefanova, A., & Nikolova, K. (2018). INFLUENCE OF ELECTRICAL CONDUCTIVITY AND TEMPERATURE IN A MICROBIAL FUEL CELL FOR TREATMENT OF MINING WASTE WATER. In *Assoc. Prof., PhD, University of Mining and Geology*. https://www.utgjiu.ro/rev_ing/pdf/2018-3/02_A.STEFANOVA%20-INFLUENCE%20OF%20ELECTRICAL%20CONDUCTIVITY%20AND%20TEMPERATURE%20IN%20A%20MICROBIAL%20FUEL%20CELL%20FOR%20TREATMENT%20OF%20MINING%20WASTE%20WATER.pdf

Sujana, K., Abraham, K. P., Mikkili, I., Kodali, A., & Prabhakar, V. (2013). BIOCHEMICAL AND MOLECULAR CHARACTERIZATION OF BIOFILM PRODUCING BACTERIA. *International Journal of Pharma and Bio Sciences*, *4*(1), 702–712. www.ijpbs.net

References

Sun, W., Lin, Z., Yu, Q., Cheng, S., & Gao, H. (2021). Promoting Extracellular Electron Transfer of Shewanella oneidensis MR-1 by Optimizing the Periplasmic Cytochrome c Network. *Frontiers in Microbiology*, *12*. https://doi.org/10.3389/fmicb.2021.727709

Toczyłowska-Mamińska, R., Szymona, K., Król, P., Gliniewicz, K., Pielech-Przybylska, K., Kloch, M., & Logan, B. E. (2018). Evolving microbial communities in cellulose-fed microbial fuel cell. *Energies*, *11*(1). https://doi.org/10.3390/en11010124

Torres, C. I., Krajmalnik-Brown, R., Parameswaran, P., Marcus, A. K., Wanger, G., Gorby, Y. A., & Rittmann, B. E. (2009a). Selecting anode-respiring bacteria based on anode potential: Phylogenetic, electrochemical, and microscopic characterization. *Environmental Science and Technology*, *43*(24), 9519–9524. https://doi.org/10.1021/es902165y

Torres, C. I., Krajmalnik-Brown, R., Parameswaran, P., Marcus, A. K., Wanger, G., Gorby, Y. A., & Rittmann, B. E. (2009b). Selecting anode-respiring bacteria based on anode potential: Phylogenetic, electrochemical, and microscopic characterization. *Environmental Science and Technology*, *43*(24), 9519–9524. https://doi.org/10.1021/es902165y

Uria, N., Ferrera, I., & Mas, J. (2017). Electrochemical performance and microbial community profiles in microbial fuel cells in relation to electron transfer mechanisms. *BMC Microbiology*, *17*(1). https://doi.org/10.1186/s12866-017-1115-2

Vishwanathan, A. S. (2021). Microbial fuel cells: a comprehensive review for beginners. In *3 Biotech* (Vol. 11, Issue 5). Springer Science and Business Media Deutschland GmbH. https://doi.org/10.1007/s13205-021-02802-y

Weber, K. A., Achenbach, L. A., & Coates, J. D. (2006). Microorganisms pumping iron: anaerobic microbial iron oxidation and reduction. *Nature Reviews Microbiology 2006 4:10*, *4*(10), 752–764. https://doi.org/10.1038/nrmicro1490

Weerasinghe Mohottige, T. N., Ginige, M. P., Kaksonen, A. H., Sarukkalige, R., & Cheng, K. Y. (2017). *Rapid start-up of a bioelectrochemical system under alkaline*

and saline conditions for efficient oxalate removal. https://doi.org/10.1016/j.biortech.2017.11.009

Wei, J., Liang, P., Cao, X., & Huang, X. (2010). A new insight into potential regulation on growth and power generation of geobacter sulfurreducens in microbial fuel cells based on energy viewpoint. *Environmental Science and Technology*, *44*(8), 3187–3191. https://doi.org/10.1021/es903758m

Wu, X., Ren, X., Owens, G., Brunetti, G., Zhou, J., Yong, X., Wei, P., & Jia, H. (2018). A facultative electroactive chromium(VI)-reducing bacterium aerobically isolated from a biocathode microbial fuel cell. *Frontiers in Microbiology*, *9*(NOV). https://doi.org/10.3389/fmicb.2018.02883

Xiao, Y., Zheng, Y., Wu, S., Zhang, E. H., Chen, Z., Liang, P., Huang, X., Yang, Z. H., Ng, I. S., Chen, B. Y., & Zhao, F. (2015a). Pyrosequencing Reveals a Core Community of Anodic Bacterial Biofilms in Bioelectrochemical Systems from China. *Frontiers in Microbiology*, *6*(DEC), 1410. https://doi.org/10.3389/FMICB.2015.01410

Xiao, Y., Zheng, Y., Wu, S., Zhang, E. H., Chen, Z., Liang, P., Huang, X., Yang, Z. H., Ng, I. S., Chen, B. Y., & Zhao, F. (2015b). Pyrosequencing reveals a core community of anodic bacterial biofilms in bioelectrochemical systems from China. *Frontiers in Microbiology*, *6*(DEC), 167264. https://doi.org/10.3389/FMICB.2015.01410/BIBTEX

Yang, N., Zhan, G., Li, D., Wang, X., He, X., & Liu, H. (2019). Complete nitrogen removal and electricity production in Thauera-dominated air-cathode single chambered microbial fuel cell. *Chemical Engineering Journal*, *356*, 506–515. https://doi.org/10.1016/j.cej.2018.08.161

Yang, Z., Li, H., Li, N., Sardar, M. F., Song, T., Zhu, H., Xing, X., & Zhu, C. (2022). Dynamics of a Bacterial Community in the Anode and Cathode of Microbial Fuel Cells under Sulfadiazine Pressure. *International Journal of Environmental Research and Public Health*, *19*(10). https://doi.org/10.3390/IJERPH19106253/S1

References

Yaqoob, A. A., Ibrahim, M. N. M., Rafatullah, M., Chua, Y. S., Ahmad, A., & Umar, K. (2020). Recent advances in anodes for microbial fuel cells: An overview. In *Materials* (Vol. 13, Issue 9). MDPI AG. https://doi.org/10.3390/ma13092078

Yaqoob, A. A., Khatoon, A., Setapar, S. H. M., Umar, K., Parveen, T., Ibrahim, M. N. M., Ahmad, A., & Rafatullah, M. (2020). Outlook on the Role of Microbial Fuel Cells in Remediation of Environmental Pollutants with Electricity Generation. *Catalysts 2020, Vol. 10, Page 819*, *10*(8), 819. https://doi.org/10.3390/CATAL10080819

Yee, M. O., Deutzmann, J., Spormann, A., & Rotaru, A. E. (2020). Cultivating electroactive microbes-from field to bench. *Nanotechnology*, *31*(17). https://doi.org/10.1088/1361-6528/ab6ab5

Yi, T., & Harper, W. F. (2012). Energy Production in Mediator-Less Microbial Fuel Cells with High Internal Resistance: The Effects of Nitrate and Sulfate. *Proceedings of the Water Environment Federation*, *2009*(17), 542–555. https://doi.org/10.2175/193864709793955816

Yousaf, S., Anam, M., Saeed, S., & Ali, N. (2017). Electricigens: source, enrichment and limitations. In *Environmental Technology Reviews* (Vol. 6, Issue 1, pp. 117–134). Taylor and Francis Ltd. https://doi.org/10.1080/21622515.2017.1318182

Yu, B., Feng, L., He, Y., Yang, L., & Xun, Y. (2020). *Effects of anode materials on the performance and anode microbial community of soil microbial fuel cell*. https://doi.org/10.1016/j.jhazmat.2020.123394

Zafar, Z., Ayaz, K., Nasir, M. H., Yousaf, S., Sharafat, I., & Ali, N. (2019). Electrochemical performance of biocathode microbial fuel cells using petroleum-contaminated soil and hot water spring. *International Journal of Environmental Science and Technology*, *16*(3), 1487–1500. https://doi.org/10.1007/s13762-018-1757-0

Zhang, L., Ding, L., Li, C., Xu, K., & Ren, H. (2011). Effects of electrolyte total dissolved solids (TDS) on performance and anodic microbes of microbial fuel cells. *African Journal of Biotechnology*, *10*(74), 16909–16914. https://doi.org/10.5897/AJB11.1993

References

Zheng, T., Li, J., Ji, Y., Zhang, W., Fang, Y., Xin, F., Dong, W., Wei, P., Ma, J., & Jiang, M. (2020). Progress and Prospects of Bioelectrochemical Systems: Electron Transfer and Its Applications in the Microbial Metabolism. In *Frontiers in Bioengineering and Biotechnology* (Vol. 8). Frontiers Media S.A. https://doi.org/10.3389/fbioe.2020.00010

Zhou, H., Mei, X., Liu, B., Xie, G., & Xing, D. (2019). Magnet anode enhances extracellular electron transfer and enrichment of exoelectrogenic bacteria in bioelectrochemical systems. *Biotechnology for Biofuels*, *12*(1). https://doi.org/10.1186/s13068-019-1477-9